2024

Utilising Plutonium Isotopes to Evaluate Soil Erosion in Tropical East African Agri-systems

Dowell, Sophia Marie

COPYRIGHT STATEMENT

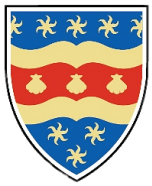

UNIVERSITY OF
PLYMOUTH

Utilising Plutonium Isotopes to Evaluate Soil Erosion in Tropical East African Agri-systems

By
Sophia Marie Dowell, BSc

A thesis submitted to the University of Plymouth
in partial fulfilment for the degree of

DOCTOR OF PHILOSOPHY

School of Geography, Earth, and Environmental Sciences

[In collaboration with
the British Geological Survey]

November 2023

Acknowledgements

First and foremost, I would like to thank my supervisory team, Dr. Michael Watts, Prof. William Blake, and Prof. Odipo Osano for their support throughout the project. Thank you for giving me the opportunity to work on this project, providing valuable guidance and feedback, and challenging me to grow as a scientist. Special thanks to Michael Watts for his support throughout my academic career from taking me on as a placement student at BGS to pushing me to take on my PhD. I am grateful for the opportunities and life experience it has given me.

Thanks to the ARIES DTP and BUFI teams for funding this research and providing invaluable support networks and training opportunities. I would also like to thank the support provided from the British Academy in improving my writing skills and to the Society for Environmental Geochemistry and Health network who provided opportunities throughout my PhD through the early career network.

At the British Geological Survey, I would like to thank all of the Inorganic Geochemistry team for their help and support with the study. First of all, I would like to thank Olivier Humphrey for his encouragement across the entire research project. I would also like to thank Simon Chenery, Thomas Barlow, and Charlie Gowing for their assistance with analysis and Charles Brettle for assistance with sample preparation. Additionally, Andy Tye for support with soil erosion sampling and Andy Marriott, Amanda Gardner, Andrea Mills, Lorraine Field, and David King for always lending a listening ear.

This work wouldn't have been possible without the support from Kenyan counterparts at the University of Eldoret. Special thanks to both Odipo Osano and Job Isaboke, whom without, fieldwork wouldn't have been possible. Their in-depth knowledge of the local area and dedication to the research project have been invaluable.

Last but and most definitely not least, I would like to express my deepest appreciation to the support of my family and friends who have been the backbone of this PhD; pushing me to believe in myself and my abilities. In particular, my amazing parents and Alex who have given me unconditional love and always put my wellbeing first; this endeavour would not have been possible without them. Finally, I would like to thank all my pets for all the entertainment and emotional support, especially during the difficult times during the COVID pandemic.

Author's declaration

At no time during the registration for the degree of Doctor of Philosophy has the author been registered for any other University award without prior agreement of the Doctoral College Quality Sub-Committee.

Work submitted for this research degree at the University of Plymouth has not formed part of any other degree either at the University of Plymouth or at another establishment.

This study was financed by the ARIES doctoral programme in partnership with the University of Plymouth (NE/S007334/1) and the BGS University Funding Initiative (BUFI) (GA/19S/017) with additional support from BGS-NERC grant NE/R000069/1 entitled 'Geoscience for Sustainable Futures' and BGS Centre for Environmental Geochemistry programmes, the NERC National Capability International Geoscience programme entitled 'Geoscience to tackle global environmental challenges' (NE/X006255/1). Additionally, financial support from The Royal Society international collaboration awards 2019 (grant ICA/R1/191077) entitled 'Dynamics of environmental geochemistry and health in a lake wide basin', alongside support provided from the British Academy Early Career Researchers Writing Skills Workshop (WW21100104).

A programme of advanced study was undertaken, which included intensive training in relevant sampling methodologies, laboratory protocols, data analysis, and other research skills.

The following external institutions were visited for data collection and laboratory analysis purposes:

- The British Geological Survey, Inorganic Geochemistry, Nottingham, UK.
- The University of Eldoret, School of Environmental Sciences, Eldoret, Kenya.
- Kenyan Marine Fisheries Research Institution (KMFRI), Kisumu, Kenya.

Parts of this thesis are published or submitted to peer-reviewed scientific journals:

- Chapter 2: **Dowell, S.M**., Humphrey, O.S., Blake, W.H., Osano, O., Chenery, S., Watts, MJ. 2023. Ultra-Trace Analysis of Fallout Plutonium Isotopes in Soil: Emerging Trends and Future Perspectives. Chemistry Africa. https://doi.org/10.1007/s42250-023-00659-7.

- Chapter 3: **Dowell, S.M.,** Barlow, T.S., Chenery, S.R., Humphrey, O.S., Isaboke, J., Blake, W.H., Osano, O., Watts, M.J. 2023. Optimisation of plutonium separations using TEVA cartridges and ICP-MS/MS analysis for applicability to large-scale studies in tropical soils. Anal. Methods. https://doi.org/10.1039/D3AY01030A.

- Chapter 4: **Dowell, S.M**., Humphrey, O.S., Gowing, J.B., Barlow, T.S., Chenery, S.R., Isaboke, J., Blake, W.H., Osano, O., Watts, M.J. 2023. Suitability of $^{210}Pb_{ex}$, ^{137}Cs and $^{239+240}Pu$ as soil erosion tracers in western Kenya. J. Environ. Radioact. https://doi.org/10.1016/j.jenvrad.2023.107327

- Chapter 5: **Dowell, S.M**., Humphrey, O.S., Isaboke, J., Blake, W.H., Osano, O., Watts, M.J. 2023. Plutonium isotopes can be used to model soil erosion in Kenya. Environmental Geochemistry and Health (submitted 19th March 2024).

Additional publications are listed in section A0 of the appendices.

Multiple scientific conferences were attended for disseminating results:

- **Dowell, S.M.,** Marriott. A.L., Blake, W.H., Osano, O., Watts, M.J. (2021) Fallout Radionuclides as Soil Erosion Tracers in East Africa. Society for Environmental Geochemistry and Health Live 2. Online. (Presentation)

- **Dowell, S.M.,** Humphrey, O.S., Marriott. A.L., Blake, W.H., Osano, O., Watts, M.J. (2021) Fallout Radionuclides as Soil Erosion Tracers in Kenya. BGS University Funding Initiative festival. Online. (Poster)

- **Dowell, S.M.,** Barlow, T.S., Chenery, S.R., Humphrey, O.S., Hamilton, E., Watts, M.J. (2021) Determining baseline plutonium in environmental Soil samples. Nuclear mass spec group annual meeting. Online. (Presentation)

- **Dowell, S.M.,** Barlow, T.S., Chenery, S.R., Humphrey, O.S., Marriott, A.L., Blake, W.H., Osano, O., Watts, M.J. (2021) Determining baseline plutonium in

environmental Soil samples. Conference on Applied Radiation Metrology. Online. (Presentation)

- **Dowell, S.M.,** Barlow, T.S., Chenery, S.R., Humphrey, O.S., Marriott, A.L., Blake, W.H., Osano, O., Watts, M.J. (2022) Determining baseline plutonium in environmental Soil samples. Society for Environmental Geochemistry and Health International Conference on Environmental Geochemistry and Health. Eldoret, Kenya. (Presentation) - ***SEGH Early Career Researcher Award – 1st Prize***

- **Dowell, S.M.,** Barlow, T.S., Chenery, S.R., Humphrey, O.S., Isaboke, J., Blake, W.H., Osano, O., Watts, M.J. (2023) Plutonium: A novel soil erosion tracer in Eastern Africa. Society for Environmental Geochemistry and Health International Conference on Environmental Geochemistry and Health. Athens, Greece. (Presentation)

Word count of main body of thesis: 34,107

Signed: 

Dated: 16th November 2023

Sophia Dowell

Utilising Plutonium Isotopes to Evaluate Soil Erosion in Tropical East African Agri-systems

Abstract

In the beautiful landscapes of Tropical East Africa, agriculture serves as the lifeblood of both people and ecosystems. The delicate balance between agriculture and soil preservation forms a complex web of factors that significantly impact soil and plant health in the region. The use of plutonium (Pu) isotopes is a potential strategy for unravelling the history of soil erosion in this ecologically varied and agriculturally crucial area. This thesis investigates a novel method using Pu isotopes to study small-scale soil redistribution patterns across various land use histories and management practices in the Rift Valley region of the Winam Gulf catchment of Lake Victoria in western Kenya.

The study aims to develop a method for measuring Pu isotopes in African soils to provide measurements of soil redistribution patterns, to better understand the factors that drive erosion processes. Analysing tropical soils poses specific challenges, and so the first objective was the optimisation of analytical methodology to enhance sensitivity. The developed separation procedure used TEVA resin to effectively reduce UH^+ interference while improving the selectivity of analysis for Pu. The application of O_2 gas in ICP-MS/MS mode for the analysis of samples facilitated the mass shifting of Pu isotopes away from interfering UH_n^+ ions, resulting in a straightforward, robust, and cost-effective method suitable to detect ultra-trace fallout $^{239+240}Pu$ in African soils with detection limits of 0.18 pg kg^{-1}.

The second objective was to understand the usability of $^{239+240}Pu$ as a soil erosion tracer in western Kenya compared against conventional isotopes $^{210}Pb_{ex}$ and ^{137}Cs. The lowest coefficient of variation and greatest peak-to-detection limit ratio was found for $^{239+240}Pu$ showing the greatest potential as a tropical soil erosion tracer. Additionally, $^{239+240}Pu$ met

the 'allowable error' criteria, establishing its applicability to large-scale studies in Western Kenya, where the selection of appropriate reference sites is a significant challenge. Consequently, $^{239+240}$Pu stands as a robust tracer for assessing soil erosion pattern estimates in western Kenya.

Finally, soil erosion patterns were modelled using the MODERN model at sites with distinct land use and clearance scales to gain insights into small-scale erosion processes and the influence of differing management practices. This research highlights the importance of community-led participation in the effective management of land degradation processes and highlights the pivotal role that vegetation cover plays in limiting soil erosion. This innovative application of fallout Pu as a tracer can improve our understanding of how soil erosion processes respond to land management practices, thereby supporting the implementation of effective mitigation strategies. Additionally, Pu is presented as a robust soil erosion tracer applicable to large-scale studies in tropical Africa. Data derived from Pu activities will facilitate the validation of predictive models, paving the way for community-designed solutions to combat land degradation and inform future related policy.

List of Contents

List of Figures

Chapter 6

List of Tables

Chapter 1

Chapter 2

Chapter 3

Chapter 4

Chapter 5

List of Appendices

List of Abbreviations and Acronyms

α-spectroscopy	Alpha spectroscopy
$^{210}Pb_{ex}$	Unsupported Lead 210
AE	Allowable Error
AMS	Accelerator Mass Spectrometry
Bq	Becquerel
CO2	Carbon Dioxide
CPS	Counts Per Second
CRC	Collision Reaction Cell
CRM	Certified Reference Material
Cs	Caesium
CV	Coefficients of Variation
DDM	Diffusion and Migration model
DI	Deionised
DRC	Dynamic Reaction Cell
ESA	Electrostatic energy Analyser
FAO	Food and Agriculture Organization of the United Nations
FRN	Fallout Radionuclide
g	Gram
GIS	Geographic Information System
ha	Hectare
HCl	Hydrochloric acid
HNO_3	Nitric acid
HP Ge	High Purity Germanium detector
IAEA	International Atomic Energy Agency
ICP-MS	Inductively Coupled Plasma Mass Spectrometry

ICP-MS/MS	Tandem Inductively Coupled Plasma Mass Spectrometry
INEEL	Idaho National Engineering and Environmental Laboratory
k'	Retention factor
Kg	kilogram
LEK	Local Environmental Knowledge
LOD	Limit Of Detection
LSC	Liquid Scintillation Counting
m	Meter
m/z	Mass-to-charge ratio
MBM	Mass Balance Model
MC/ICP-MS	Multi-Collector Inductively Coupled Plasma Mass Spectrometry
MDA	Minimum Detectable Activity
Mg	Megagram
mg	Milligram
min	Minute
ml	Millilitre
MODERN	Modelling Deposition and Erosion Rates with Radionuclides
$NaNO_2$	Sodium nitrite
NH_3	Ammonia
O_2	Oxygen
ºC	Degrees Celsius
Pb	Lead
PDM	Profile Distribution Model
pg	Picogram
pH	Potential of Hydrogen
PM	Proportional Model

PTFE	Polytetrafluoroethylene
Pu	Plutonium
Pu (III)	Plutonium oxidation state +3
Pu (IV)	Plutonium oxidation state +4
Pu (VI)	Plutonium oxidation state +6
PuO^+	Plutonium Oxide
QA	Quality Assurance
QQQ	Triple Quadrupole
RIMS	Resonance Ionization Mass Spectrometry
RPM	Repetitions Per Minute
RSD	Relative Standard Deviation
RUSLE	The Revised Universal Soil Loss Equation
σ	Standard Deviation
SF/ICP-MS	Sector-Field Inductively Coupled Plasma Mass Spectrometry
TEVA	Trialkyl methylammonium nitrate
TIMS	Thermal Ionization Mass Spectrometry
TOF	Time Of Flight
TRU	Octylphenyl-N,N-di-isobutyl carbamoylphosphine oxide
U	Uranium
UH^+	Uranium Hydride
USLE	The Universal Soil Loss Equation
UTEVA	Dipentyl pentylphosphonate
yr	Year
µg	Microgram

Chapter 1 - Introduction

Soil erosion is a critical environmental concern that affects agriculture, ecosystems, and water quality. The accurate measurement of soil erosion is essential for understanding its causes and effects and for developing effective mitigation strategies (Alewell et al., 2017; Batista et al., 2019; Labriére et al., 2015). Fertile soil is an essential resource; however, a large proportion of the world's soils are degraded to some extent, with soil erosion presenting the greatest risk to land degradation worldwide (Lal, 2001; Lorenz et al., 2019; Pimentel, 2006; Whitlow, 1988b). Even in the most developed countries, the soil erosion rate has been reported to exceed that of soil formation (Alewell et al., 2015; Montgomery, 2007; Pimentel & Burgess, 2013). This concern is notably greater within African countries and tropical environments which can experience extreme wet/dry weather patterns, driving rain and wind driven soil erosion (Farnsworth et al., 2011; Sultan & Gaetani, 2016). This represents a major problem concerning the sustainable intensification of agriculture; particularly in the developing world, where both land and water resources can be limited (Borrelli et al., 2017, 2020; Lal., 1983). Food production and quality can be compromised as a result of soil erosion, with soil nutrient shortages in tropical soils being of major concern for the future (Hossain et al., 2020). Food security, which can be defined as "improved health through food sufficiency, quality and safety", is key to Kenya's economic and social development; yet approximately 10 million people in Kenya currently suffer from some kind of food insecurity (Lokuruka., 2021; Mutie et al., 2020).

As a regionally important source of food from both land and water, the Winam Gulf catchment of Lake Victoria in Kenya is an exemplar of these processes. This research is important owing to the rapid development and environmental pressures faced by the Winam Gulf of Lake Victoria (Fusilli et al., 2014; Marriott et al., 2023). This is

compounded by poor coordination of environmental data (land-to-lake) to guide regulatory bodies (Kelly et al., 2020). Developing countries have experienced large expansions in agriculture since the colonial period, sometimes onto marginal land in response to rapid increases in population as well as the limited availability of land suitable for agriculture (Collier & Dercon, 2014; Laurance et al., 2014). This urbanisation and the rapid conversion of natural environments for agricultural use, within the Winam Gulf catchment of Lake Victoria, exacerbate the degradation caused by soil erosion and with limited water exchange in the Gulf, the aquaculture industry is threatened with diminishing water quality and sediment influx (Marriott et al., 2023; Nassali et al., 2020; Odada et al., 2003).

Eroded sediment can act as a vector for the transportation of agrochemicals used on land, as well as naturally enriched elements into water bodies. This results in a loss of storage capacity due to siltation as well as eutrophication due to nutrient enrichment (Nassali et al., 2020; Njagi et al., 2022). Some of the main drivers of soil erosion include topography, land cover, soil texture, precipitation, and land-use management practices (Boardman, 2006; Joint FAO/IAEA, 2014; Lal, 2001). Current rates of erosion are not sustainable and with changes in both precipitation and land cover on the rise, these rates could increase significantly (Montgomery, 2007; Pimentel, 2006). As a result, soil nutrient shortages in tropical soils is a major concern for the future and effects both crop yields and protection of crops against disease, which could dramatically increase the likelihood of food shortages worldwide; impacting nutrition for both humans and farmed animals (Pimentel & Burgess, 2013).

A large proportion of this degradation is a direct result of poor land management practices and vegetation clearance (Abdulkareem et al., 2019; Wynants et al., 2019). To plan

mitigation strategies for sustainable soil conservation measures, there is a need for reliable quantitative data detailing rates of soil erosion and sedimentation. This data can also aid in the validation of prediction models, that allow a better understanding of factors which can influence the processes involved (Joint FAO/IAEA, 2014).

Traditional techniques such as sediment yield monitoring and erosion pins have been used for many years in Africa, however, these methods can lack representativeness at scale as well as spatial resolution (Elwell, 1978; Whitlow, 1988a) (*Table 1*). Furthermore, they involve expensive long-term monitoring and cannot be used to provide information on long term rates of soil erosion (Zapata, 2003). Other methods which are used to quantify soil redistribution processes include satellite imagery, GIS models, and sediment fingerprinting, however, these methods are beyond the scope of this research (Seutloali et al., 2018; Smith & Blake, 2014).

Increasing soil erosion and deposition across many tropical soils within sub-Saharan Africa raises growing concerns regarding food security. Reliable empirical data on soil erosion rates is essential to inform the design of targeted erosion mitigation strategies in developing countries (Ruecker et al., 2008; Pimentel, 2006). Recent attention has focused on the use of fallout radionuclides (FRN) as tracing tools to quantify soil erosion and sedimentation rates within a landscape (Alewell et al., 2017; Loba et al., 2022; Mabit et al., 2014). The data produced from these methods, can be used to validate soil erosion prediction models and to provide a foundation on which to develop new land use policies for environmental protection (Walling et al., 2011; Gharbi et al., 2020; Hoo et al., 2011; Joint FAO/IAEA, 2014; Parwada et al., 2023). Therefore, the aim of this chapter is to compare, and contrast FRN methods utilised for the assessment of soil erosion and subsequent deposition in tropical soils.

Table 1 - Descriptions of the different methods of erosion measurement used.

Methods of erosion measurement	**Description**
Sediment Yield Monitoring	Involves the monitoring of sediment yield in rivers and water bodies downstream of erosion-prone areas. This method provides valuable data but lacks spatial resolution
Erosion Pins and Flags	Is used to measure soil surface loss directly. These simple, low-cost devices are valuable for small-scale studies but may not capture all erosion processes
Aerial Photography and Satellite Imagery	Using satellite imagery has become indispensable for large-scale soil erosion studies. They provide spatial and temporal information
GIS-Based Erosion Models	Allows the integration of various data sources to model and predict erosion rates across landscapes, providing valuable insights into erosion patterns
Use of Radioactive Tracers	Tracers such as ^{137}Cs, $^{210}Pb_{ex}$ and $^{239+240}Pu$ have been employed to trace the movement of soil particles and estimate erosion rates
Sediment Source Fingerprinting	Involves analysing sediment samples for unique characteristics, such as grain size distribution or mineral composition, to identify their source areas and estimate erosion contributions from specific locations
Rainfall Simulation Experiments	Use's controlled rainfall simulations to replicate erosive events to assess the effectiveness of various erosion control and mitigation measures
Soil Erosion Models	Numerical models, like the Universal Soil Loss Equation (USLE) and the Revised Universal Soil Loss Equation (RUSLE), are widely used to estimate soil loss potential based on factors such as rainfall, soil type, land cover, and slope
Soil Erosion Monitoring Stations	Monitoring stations are established to collect continuous data on soil erosion, rainfall, and other relevant variables. Long-term data from these stations are crucial for understanding erosion trends

Use of fallout radionuclides to evaluate soil redistribution patterns

Fallout radionuclides (FRN) offer an alternative way to quantify soil erosion, without the need for expensive long-term monitoring techniques. The FRN method, in contrast to traditional methods, can be performed within a single sampling campaign and can assess for both erosion and deposition rates (Alewell et al., 2014; Joint FAO/IAEA, 2014; Parwada et al., 2023). Furthermore, by using the FRN method, the resultant erosional rates are representative of all processes which lead to redistribution of soil (Mabit et al., 2014). Analysis of FRN deposited into the environment globally through precipitation has proven to be an effective tool for quantifying the redistribution of soil for the past 60 years and these techniques have been utilised to increase knowledge on the resilience and status of agro-ecosystems around the world (Alewell et al., 2017; Mabit et al., 2012; Zapata, 2003). This success can be attributed to the adsorption of FRN onto the surface of soil and sediment particles both rapidly and irreversibly (Ashraf et al., 2014; Kersting, 2013; Missana et al., 2004).

The use of FRN for assessment of soil erosion began in the early 1960s with the initial use of ^{90}Sr and ^{137}Cs (Ritchie et al., 1974; Zapata, 2003). Since then > 4000 papers have detailed the use of similar methods for quantifying soil erosion (Ritchie & Ritchie, 2005). Some FRN such as ^{137}Cs and $^{239+240}$Pu can be associated with negative connotations due to their anthropogenic origin, radiogenic threats, and high toxicity, but owing to their ability to bind strongly and irreversibly to soils they are ideal elements to be utilised as soil erosion tracers (Alewell et al., 2017; Zapata, 2003). In addition to ^{137}Cs and $^{239+240}$Pu, some naturally occurring FRN such as ^{210}Pb and ^{7}Be which can be found in soils as a result of atmospheric processes can also be used owing to their global distribution in soils as a result of atmospheric processes (Kassab et al., 2021; Mabit et al., 2014). A short-term tracer which has been used successfully around the world is ^{7}Be, which due to its

short half-life of only 53 days can quantify erosion which has occurred within a particular erosional event (Mabit & Blake, 2019). As this chapter focuses on methods used for long term erosion processes ^{7}Be as a tracer is beyond the scope of this research.

General concept

FRN methods are based on the comparison between the inventory (Bq per unit area) of a representative undisturbed reference site and the inventory at a given sampling site (Joint FAO/IAEA, 2014). By using the assumption that the loss of radionuclide at a particular reference site is only due to radioactive decay, soil erosion can be calculated from the loss of radionuclide at the site which is under investigation (Loba et al., 2022; Mabit et al., 2014). Documenting the subsequent redistribution of the FRN in the soil, can then provide an effective way to trace rates and patterns of erosion within a landscape (*Figure 2*). Erosion is indicated by a lower FRN inventory, than the reference inventory, while deposition is indicated by higher FRN inventories (Joint FAO/IAEA, 2014).

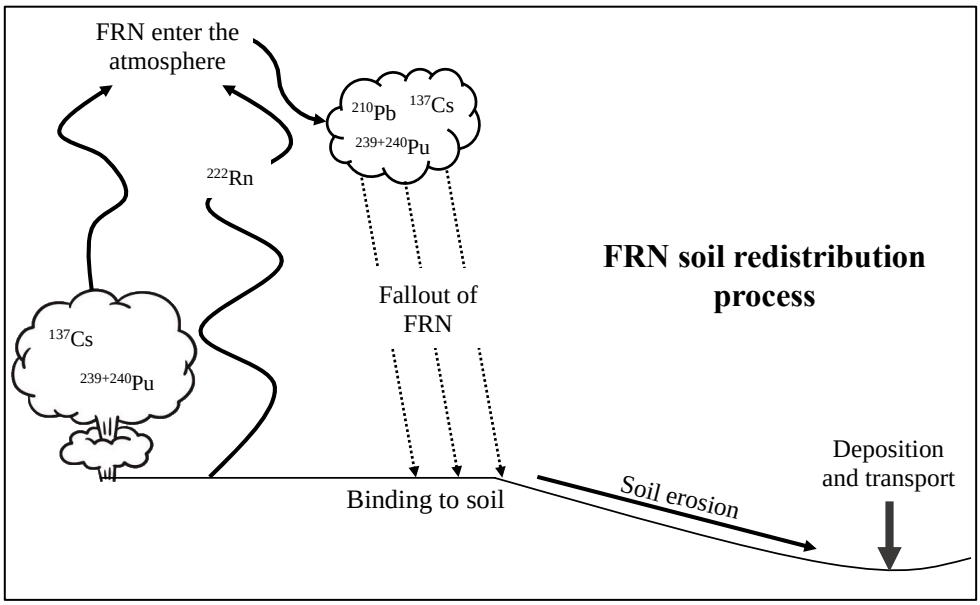

Figure 1 - Redistribution process of fallout radionuclides in the environment (Adapted from Walling et al., 2003)

For a FRN to be considered as a possible tracer for soil erosion, it is an important requirement that when it is deposited, it binds strongly and irreversibly to the soil, resulting in low mobility within the landscape. This allows for the assumption that any subsequent redistribution of the radionuclide in the soil is a direct result of soil redistribution processes only (Alewell et al., 2017). Another key requirement for using the FRN method is the assignment of a suitable reference site for the area of interest. A typical reference site will be a flat, well vegetated, and unploughed area, to limit any possible soil redistribution at that site. In addition, as the FRN inventory at the reference site is assumed to represent the baseline fallout, it is important that the fallout of that radionuclide has been spatially uniform across the study site (Joint FAO/IAEA, 2014). Sutherland, (1996) suggested that the number of samples representing the reference inventory should be increased until an allowable error is reached whereby if the coefficient of variation at a reference site exceeds 30% it can be deemed unsuitable and sample numbers should be increased accordingly.

To calculate soil erosion and deposition rates from calculated changes in inventory, conversion models can be used. These conversion models mathematically define the relationship between an increase or decrease in the FRN inventory to return average soil redistribution rates in terms of tonnes per hectare per year (t ha^{-1} yr^{-1}) (Walling et al., 2011; Gharbi et al., 2020; He & Walling, 1997; Soto & Navas, 2008). These models differ in complexity with simple models such as the proportional model having only a few input parameters, while more complex models such as Mass Balance model consider many more (Walling et al., 2011; Gharbi et al., 2020; He and Walling, 1997; Soto and Navas, 2008). The FRNs can be used to assess soil erosion rates over different time periods as dictated by its year of deposition, distribution globally and half-life (*Table 2*).

Table 2 - Properties of radionuclides used in soil erosion/deposition rate studies.

Radionuclide	Origin	Fallout occurrence	Energy of emission	Half life (Yr)	Erosion time span
^{137}Cs	Anthropogenic (nuclear weapon tests fallout and NPP accident release)	Worldwide with higher deposit in northern hemisphere	662.66[a]	30.17	50 years
^{210}Pb	Natural (decay of ^{226}Ra)	Worldwide	46.5[a]	22.26	100 years
$^{239+240}$Pu	Anthropogenic (nuclear weapon tests fallout)	Worldwide with higher deposit in northern hemisphere	239 - 5.16[b] 240 - 5.17[b]	239 - 24110 240 - 6561	50 years

[a] KeV
[b] MeV

A suitable reference site can be defined according to Joint FAO/IAEA, 2014:

- having experienced neither soil loss nor deposition so that the inventory can be assumed to only reflect atmospheric inputs of the radionuclide and its decay through time;
- having been under continuous vegetation cover for the period since deposition of began in the early 1950s;
- located as close as possible to the disturbed sites that are to be sampled;
- having an inventory which can be compared to any available national or global-level radionuclide-deposition data.

A typical reference site tends to be level and from an area which has not received any flow from upslope sites. The most common suitable reference sites tend to be parks and ceremonial areas as these are likely to have been under continuous vegetation cover for a long period of time, however, when sampling at these locations cultural sensitivity must be considered (Sutherland, 1996). In terms of land cover, areas with little cover such as

perennial grasses tend to be most suitable as reference sites due to the higher spatial variation of fallout radionuclides in forest areas. This spatial variation is a result of interception of fallout, soil-to-plant transfers, and bioturbation (Joint FAO/IAEA, 2014; Wilken et al., 2020). Multiple reference sites are required within each study area to determine the spatial variation of the inventory (Sutherland, 1996).

^{137}Caesium

The most mature radionuclide technique commonly utilised in soil erosion studies is Caesium (Cs), with over 4000 research papers employing the radionuclide as a tracer of soil erosion (Ritchie & Ritchie, 2005). This is owing to its low solubility and capacity to adsorb rapidly onto the soil upon deposition. This rapid adsorption can be attributed to Cs binding strongly and irreversibly to the soil and is predominantly associated with fine clay minerals (Chibowski et al., 1999; Schimmack et al., 2001; Suchara et al., 2016). The element Cs is an alkali metal with the atomic number 55 which has many isotopes; of which only one is a stable isotope (^{133}Cs). The isotope which is utilised as a tracer of soil erosion is 137 and this is a gamma emitter (662.66 KeV) with a half-life of 30.17 years (Russell et al., 2015). Upon deposition, ^{137}Cs has been shown to adsorb to the cation exchange sites of clay and organic particles within the soil (Chibowski et al., 1999; Schimmack et al., 2001; Suchara et al., 2016). Any ^{137}Cs which has been intercepted on fallout or taken up by plants can be considered negligible as it is released to the soil upon the vegetation dying and decaying (Alewell et al., 2017).

In the environment ^{137}Cs is not found naturally and is only present as a result of nuclear fission. As ^{137}Cs is an anthropogenic radionuclide, its global presence in the environment is a direct result of nuclear weapons testing; with the main fallout period between 1953

and 1964 (Prăvălie, 2014). Global variation in the radionuclide's distribution, is determined from both the test location of weapons and the patterns in annual precipitation (Pálsson et al., 2006; Thiessen et al., 1999). Due to this, fallout in the northern hemisphere has been significantly higher than in the southern hemisphere (Joint FAO/IAEA, 2014). This poses a challenge in regard to the use of ^{137}Cs in tropical soils where often activity in the soil is below gamma spectroscopy detection limits (deGraffenried & Shepherd, 2009; Hoo et al., 2011). Additionally, there are further inputs of ^{137}Cs into soils due to nuclear power plant accidents such as Chernobyl, although more locally dispersed with a high spatial variability (Khodadadi et al., 2021.; Schimmack et al., 2001). There have been several research papers employing the ^{137}Cs method in the tropical soils of sub-Saharan Africa in countries including Kenya, Uganda, and Zambia (Collins et al., 2001; deGraffenried & Shepherd, 2009; Ruecker et al., 2008) (*Table 3*).

Table 3 - Previous soil erosion studies utilising ^{137}Cs within sub-Saharan Africa.

Reference	Study location	^{137}Cs reference inventory (Bq m^{-2})	Average erosion rate (t ha^{-1} yr^{-1})
(Rabesiranana et al., 2016)	Madagascar	216	7.4
(Junge et al., 2010)	Nigeria	568	14.4
(Ruecker et al., 2008)	Uganda	416	12.8
(Collins et al., 2001)	Zambia	192	2.5
(Pennock, 2000)	Ghana	925	N/A
(Chappell et al., 1998)	Niger	3788	15.9
(Quine et al., 1993)	Zimbabwe	300	23

The Erosional behaviour of ^{137}Cs, allows for the assumption that it is only redistributed within the soil, because of physical processes and can therefore be used as a tracer (Joint FAO/IAEA, 2014). The depth profile of ^{137}Cs at a reference site typically follows an exponential pattern, with sharp declines in activity as the depth increases (Ruecker, 2008; Sutherland, 1996). In most cases more than 75% of the total inventory for Cs is found

within the first 15cm of the depth profile. This evidence suggests that there is minimal vertical translocation of Cs in the soil (Walling & Quine, 1992; Poreba, 2006). However, the vertical distribution is dependent on a wide range of physical, chemical, and biological processes and so must be identified within each study area (Alewell et al., 2014; Arata, et al., 2016a; Joint FAO/IAEA, 2014). At sites which have been cultivated, it can be expected that ^{137}Cs will be distributed uniformly within the plough layer due to the mixing which occurs. It is typical for total inventories to be lower on convex slopes which are eroded and higher in depressions where the soil may deposit (Poreba, 2006).

The ^{137}Cs method has some limitations in comparison to other FRN methods. First, because of its half-life being only 30.17 years, more than 70% of the originally deposited ^{137}Cs has now decayed (Evrard et al., 2020; Mabit et al., 2014). As a consequence of this, much of the remaining ^{137}Cs will also disappear in the years to come, creating challenges in using it as a tracer of soil erosion; especially in the southern hemisphere where only one third of that in the northern hemisphere was originally deposited (Alewell et al., 2017; Hoo et al., 2011). As the activity diminishes, the accurate measurement of ^{137}Cs in the soil becomes a challenge especially for the deep soil (> 15 cm), where the sensitivity for ^{137}Cs measurements may became too low to allow accurate measurements by gamma spectrometry (Walling & Quine, 1992; Zhang et al., 2019). Another potential limitation, in some parts of the world, is that activity of ^{137}Cs in soils can be significantly influenced by Cs fallout from nuclear power plant accidents; which resulted in highly heterogeneous fallout (Parsons & Foster, 2011). In many European countries, this can lead to difficulties in calculating erosion accurately as ^{137}Cs was deposited in considerable amounts by the Chernobyl fallout in 1986 (Schimmack et al., 2001; Zollinger et al., 2015). However, the effects of nuclear power plant accidents are localised and so do not affect tropical soils significantly (Gudiksen et al., 1989; Korsakissok et al., 2013).

The determination of ^{137}Cs is typically measured via radiometric techniques; namely gamma spectroscopy due to its energy of emission being within the gamma range of the electromagnetic spectrum (662.66 KeV). The advantage of using gamma spectroscopy analysis is that the sample preparation for analysis is simple and non-destructive (Chappell et al., 1998; Poreba, 2006; Zhidkin et al., 2020).

$^{239+240}$Plutonium

An alternative to using Cs is using Plutonium (Pu) isotopes. Similarly to ^{137}Cs, $^{239+240}Pu$ isotopes aren't found in the environment naturally and were deposited globally during the 1950s and 60s as a result of nuclear weapons testing. Although this was the dominant global contributor of environmental Pu, other Pu sources exist such as nuclear power plant accidents and marine discharges of reprocessing wastes. These releases had more localised effects in the environment compared to ^{137}Cs (Kersting, 2013; Thakur et al., 2017). This is as a result of $^{239+240}Pu$ being contained within the non-volatile fraction of nuclear fuel debris, resulting in no significant long-range transport in the environment (Alewell et al., 2017; Ketterer & Szechenyi, 2008; Lal et al., 2013). The $^{239+240}Pu$ method has been used infrequently in the past (Hakonson et al., 1981; Joshi & Shukla, 1991; Muller et al., 1978). However, in 2001 the use of $^{239+240}Pu$ as an alternative to ^{137}Cs was investigated at a study site in southern Germany (Schimmack et al., 2001). Subsequently, there has been a number of studies utilising $^{239+240}Pu$ as a tracer for soil erosion (Alewell et al., 2014; Hoo et al., 2011; Lal et al., 2013; Meusburger et al., 2018; Portes et al., 2018; Raab et al., 2018; Schimmack et al., 2004; Xu et al., 2013, 2015; Zhang et al., 2019; Zollinger et al., 2015).

The element Pu belongs to the actinide series with the atomic number 94. In soil erosion studies the isotopes 239 and 240 are utilised with both being alpha emitters with the energies 5.16 MeV and 5.17 MeV respectively. Traditionally alpha spectrometry has been used to analyse Pu isotopes for use in soil erosion studies (Alewell et al., 2017). The chemistry of Pu in the environment is complicated as a result of its oxidation state being influenced by many geochemical factors (Geckeis et al., 2018; Kaplan et al., 2004).

The erosional behaviour of $^{239+240}$Pu is like that of ^{137}Cs, with the retention of Pu in sandy/clayey soils being of the same order of magnitude as Cs. In addition, Pu has been observed to have an even greater retention in some organic soils (Hakonson et al., 1981; Muller et al., 1978). It has been reported that Pu is preferentially adsorbed to organic matter and oxides within the soil supporting greater retention and the use of $^{239+240}$Pu as a soil erosion tracer, owing to the assumption that Pu isotopes are only redistributed within soil as a result of physical processes (Alewell et al., 2014). Lal et al., (2013) and Meusburger et al., (2016) have shown that the depth profile of $^{239+240}$Pu is similar to ^{137}Cs and follows an exponential depth function. However, it has also been suggested that it can follow a polynomial depth function, with the maximum peak lying between 3 and 6 cm below the soil surface (Alewell et al., 2014; Xu et al., 2013). The lower concentrations of Pu in the very top-soil may be due to plant uptake after fallout deposition, however, some studies have suggested that this is a consequence of higher downward migration of Pu compared to Cs, as a result of Pu being influenced by geochemical factors such as pH, content of organic matter, and ion salinity (Alewell et al., 2017; Chawla et al., 2010).

There has been very limited use of Pu in tropical sub-Saharan African soils with Wilken et al., (2020) successfully using $^{239+240}$Pu to estimate rates of soil erosion in DR Congo, Uganda, and Rwanda with rates between -51.4 and 20.2 Mg ha^{-1} yr^{-1} using the mass

balance model. This work highlights the potential for $^{239+240}$Pu to be used in the Southern Hemisphere as a replacement to ^{137}Cs due to the advantages the method offers over ^{137}Cs. Firstly, as a result of ^{239}Pu and ^{240}Pu's much longer half-lives (24110 and 6561 years respectively), about 99% of original activity still remains in soils which ensures much longer term availability in the future compared to ^{137}Cs which has a half-life of only 30 years (Lal et al., 2013; Xu et al., 2015). In addition to this, with recent advances of analytical measurements by isotope counting methods such as ICP-MS, sensitivity of detection is increased. More than six times as many atoms of Pu were originally dispersed in comparison to Cs although their environmental activity was significantly lower (Everett et al., 2008). Until recently the measurement of Pu at the environmental level was restricted to few facilities world-wide with the use of alpha-particle spectrometry and accelerator mass spectrometry (AMS) (Hrnecek et al., 2005). Recent advances in mass spectrometry techniques such as ICP-MS allow for a higher availability for analysis world-wide making the application of Pu isotopes for tracing soil erosion more attractive (Moldovan et al., 2004; Muramatsu et al., 2001; Xu et al., 2022).

The determination of Pu isotopes in samples can be achieved in two different ways either using decay counting (radiometric techniques) or atom counting methods (mass spectrometric techniques). For the determination of $^{239+240}$Pu isotopes the radiometric technique used is alpha spectrometry. When using alpha spectrometry to measure $^{239+240}$Pu isotopes a sum of activities is usually reported as the two isotopes cannot be resolved due to their similar alpha energy of emission (5.16 MeV for ^{239}Pu and 5.17 MeV for ^{240}Pu) (Boulyga et al., 2001; Seferinoğlu et al., 2014; Varga et al., 2007; Esaka et al., 2017; Hrnecek et al., 2005). For this reason, the sum of ^{239}Pu and ^{240}Pu has continued to be used in soil erosion studies. This method is attractive for the measurement of Pu isotopes in environmental samples as a result of low cost of instrumentation, high

selectivity for alpha particles and high sensitivity resulting from a low background signal (Mabit et al., 2008).

The mass spectrometric technique traditionally used for $^{239+240}$Pu measurements in environmental samples is AMS. This method has high sensitivity with limits of detection as low as 0.001 mBq for ^{239}Pu isotope due to the absence of interferences (Hrnecek et al., 2005). The main limitation faced when using the AMS method to analyse Pu isotopes is the availability of specialist facilities where beam time must be applied for to access the facilities (Xu et al., 2013). More recently work has been focused around the use of ICP-MS techniques which are more widely available in laboratories world-wide. Prior to analysis via ICP-MS samples require radiochemical separation which pre-concentrates the Pu isotopes as well as removes possible interferences such as $^{238}U^{1}H^{+}$ on the ^{239}Pu isotope (Cao et al., 2016; Hou et al., 2019; Muramatsu et al., 2001; Xu et al., 2022; Liu et al., 2016; Metzger et al., 2019). When analysing soil and sediment samples for Pu isotopes the sample preparation involves spiking the sample with a Pu isotope not found in the sample, most commonly ^{242}Pu (Alewell et al., 2014; Ketterer & Szechenyi, 2008). Following this the Pu is selectively separated from the matrix components using methods such as co-precipitation, ion extraction or through using chromatographic techniques (Ketterer et al., 2004).

Alongside the AMS and ICP-MS methods, there are also some alternative mass spectrometric techniques such as thermal ionization mass spectrometry (TIMS) and resonance ionization mass spectrometry (RIMS) which are highly sensitive for the detection of Pu isotopes (Grüning et al., 2004; Lee et al., 2015; Wallenius & Mayer, 2000). However, the use of these mass spectrometry techniques is limited by the low global availability and high cost of setting up an analytical facility (Alewell et al., 2017;

Ketterer & Szechenyi, 2008). The TIMS instrument has a higher sensitivity for ^{239}Pu and ^{240}Pu than ICP-MS and interferences due to U present in the sample are less significant. However, TIMS requires time-consuming sample preparation to produce a thin filament source (Lee et al., 2015; Wallenius & Mayer, 2000). On the other hand, RIMS is an analytical technique which uses laser beams which are tuned for the selective excitation of Pu atoms making it highly sensitive for the measurement of ^{239}Pu detecting ^{239}Pu activities as low as 107 atoms per sample, which is in the range of 0.01 mBq. The RIMS instrumentation is available at only a few laboratories worldwide (Grüning et al., 2004).

Unsupported ^{210}Lead

Another commonly used radionuclide technique is using Lead (Pb) which, in contrast to anthropogenic radionuclides such as ^{137}Cs and $^{239+240}$Pu, is a natural radioisotope. It is a heavy metal with the atomic number 82 and in soil erosion studies the isotope utilised is ^{210}Pb which is a gamma emitter (46.5 KeV) with a Half-life of 22.26 years (Al-Tuweity et al., 2021; Moustakim et al., 2022). Similarly to ^{137}Cs, ^{210}Pb has proven to be an effective tracer of soil erosion worldwide (Mabit et al., 2014; Walling et al., 2003). Unsupported ^{210}Pb has had applications in soil science for more than five decades, being widely used as a tool for dating sediments as well as to investigate sedimentation processes across the globe. However, it wasn't until the 1990s that studies started to use the fallout $^{210}Pb_{ex}$ as a tool for determining rates of soil redistribution processes within agricultural landscapes (Joint FAO/IAEA, 2014). It has a high affinity for soil particles and so is adsorbed onto soil both rapidly and irreversibly allowing for the assumption that any subsequent redistribution of ^{210}Pb in the soil will be as a result of transport processes (Walling et al., 2003). In addition, ^{210}Pb has been shown to behave in the environment in a similar way to ^{137}Cs (He & Walling, 1997; Zapata, 2003).

^{210}Pb exists in the environment because of the decay of ^{226}Ra. In theory ^{210}Pb in the soil should be in secular equilibrium with its parent isotope ^{226}Ra, however, due to the diffusional behaviour the gaseous short-lived daughter, ^{222}Rn, this is not the case (Joint FAO/IAEA, 2014; Meusburger et al., 2018). In natural materials, a small proportion of the ^{222}Rn daughter diffuses out of the soil and enters the atmosphere where it rapidly decays to ^{210}Pb and is deposited back into the soil through precipitation (Appleby & Oldfield, 1978). This ^{210}Pb is considered unsupported or excess ($^{210}Pb_{ex}$) as it is not in equilibrium with the parent ^{226}Ra. The remaining ^{222}Rn decays to form ^{210}Pb within the soil, and this is considered supported ^{210}Pb which exists in secular equilibrium with the parent ^{226}Ra (Walling et al., 2011, 2003). The determination of unsupported ^{210}Pb is possible by subtracting the supported ^{210}Pb from the total which is determined using the ratio of either the parent radionuclide ^{226}Ra or one of the daughters (^{214}Pb / ^{214}Bi) with ^{210}Pb. The daughters of ^{226}Ra are often used due to the difficulty in distinguishing the ^{226}Ra peak at 186.21KeV with the intense peak of ^{235}U at 185.72KeV (Appleby & Oldfield, 1978). As ^{226}Ra is found in most rocks and soils, ^{210}Pb as a tracer has global potential and fallout of $^{210}Pb_{ex}$ is essentially constant through time (Meusburger et al., 2018).

The soil radionuclide inventories for unsupported ^{210}Pb are typically greater than those found for other elements, due to its constant input into the environment (Walling et al., 2011; Moustakim et al., 2022). This annual fallout can vary as a result of seasonal variations in atmospheric fallout, and it is reported that between 23 and 367 Bq m^{-2} $year^{-1}$ is deposited globally (Sedighi et al., 2020; Turekian et al., 1977). The depth profile of ^{210}Pb is similar to that found for ^{137}Cs, however, the maximum activity peak is typically

found at the surface of soil rather than a small depth below, due to its continuous deposition onto the earth (Walling et al., 2003).

The main advantage of using ^{210}Pb as a tracer of soil erosion over ^{137}Cs is its global applicability, resulting from the continuous fallout of ^{210}Pb compared to the bomb derived fallout of ^{137}Cs, which decreases consistently (Hoo et al., 2011; Meusburger et al., 2018). The biggest impact of this is seen in the southern hemisphere where deposition was up to 3x lower than that in the northern hemisphere (Rabesiranana et al., 2016; Zhang et al., 2019). The similar behaviour of fallout ^{210}Pb to ^{137}Cs makes it a good alternative radionuclide to investigate soil erosion rates, especially in areas where ^{137}Cs measurements may be unsuitable. This includes areas where there has been significant ^{137}Cs input from nuclear power plant accidents or where the levels of bomb-derived ^{137}Cs fallout are below detection limits (Khodadadi et al., 2021; Schimmack et al., 2001). The input of bomb-derived ^{137}Cs fallout has ceased and ^{137}Cs inventories are decreasing due to radioactive decay meaning less than 30% of the originally deposited ^{137}Cs remains (Hoo et al., 2011). Soon, the use of ^{137}Cs will no longer be possible, especially in southern hemisphere where fallout was much lower than in the northern hemisphere. Since the fallout of $^{210}Pb_{ex}$ is effectively continuous, the use of this radionuclide does not face these problems (Joint FAO/IAEA, 2014). Within sub-Saharan Africa there has been previous studies employing the $^{210}Pb_{ex}$ method (*Table 4*).

Table 4 - Previous soil erosion studies utilising unsupported ^{210}Pb within sub-Saharan Africa.

Reference	Study location	^{210}Pb reference inventory (Bq m^{-2})	Average erosion rate (t ha^{-1} yr^{-1})
(Rabesiranana et al., 2016)	Madagascar	3078	-5.9
(Walling et al., 2003)	Zambia	2602	-4.5

The use of ^{210}Pb as a soil erosion tracer does however have some disadvantages compared to the use of ^{137}Cs. This includes challenges associated with the analysis of ^{210}Pb. Radiometric analysis is typically used for the detection of ^{210}Pb which has a gamma emission at 46.5 KeV (Appleby & Oldfield, 1978; Moustakim et al., 2022). Due to its low energy of emission, detection by gamma spectroscopy requires a N-type HPGe detector which has a low counting efficiency (Al-Tuweity et al., 2021). In addition, the gamma emission of ^{210}Pb has a low absolute intensity (approximately 4%), resulting in greater uncertainty in the determination of $^{210}Pb_{ex}$ (L'Annunziata, 2012). Although the sample preparation is non-destructive, it can be time consuming as samples are required to be sealed in airtight containers and stored for at least 20 days to ensure equilibrium between ^{226}Ra and its daughter ^{222}Rn ($t_{1/2}$ 3.8 days) allowing the determination of unsupported ^{210}Pb (Appleby & Oldfield, 1978). It is worth noting that additional adjustments are needed to the resulting value of unsupported ^{210}Pb if the analysed samples were collected many years previously to correct for radioactive decay of the ^{210}Pb (Mabit et al., 2008).

For the determination of unsupported ^{210}Pb, the approach uses results which are obtained indirectly, requiring assumptions of secular equilibrium between ^{226}Ra and supported ^{210}Pb which can compound potential errors associated with the measurement of $^{210}Pb_{ex}$ (Appleby & Oldfield, 1978). This results in a low precision on the final determined value for $^{210}Pb_{ex}$ and the uncertainty associated with estimates of $^{210}Pb_{ex}$ can be as high as 30-50%, particularly when concentrations of ^{210}Pb are low (Alewell et al., 2017). Other methods which can be used for the determination of ^{210}Pb in samples include alpha spectroscopy or beta/liquid scintillation counting and these methods, involve radiochemical separations. These alternative methods are more sensitive and can provide improved analytical precision, however the methods are not traditionally used for the

determination of ^{210}Pb as the analysis is both laborious and expensive (Sánchez-Cabezudo et al., 2021; Šešlak et al., 2017).

In conclusion, this chapter highlights the critical environmental problem of land degradation as a result of soil erosion, particularly in tropical areas such as the Winam Gulf watershed of Lake Victoria in Kenya. Agriculture, water quality, food security, and the sustainable management of land and water resources are all impacted by the effects of soil erosion. The chapter emphasises the requirement for accurate measurements of soil erosion rates for the development of efficient mitigation techniques. Traditional methodologies, although useful, have their limits, highlighting the need for reliable quantitative data to inform decision-making and support the use of predictive modelling. The use of FRN's provides a cost-effective tool for measuring soil erosion with $^{239+240}$Pu showing good potential to replace ^{137}Cs and ^{210}Pb in tropical soils. Determination of soil erosion rates according to land management, clearance scale and land use can benefit our understanding of the factors which influence soil erosion and is the first step towards supporting the implementation of future mitigation solutions into policy.

Aim and objectives

The aim of this research project is to determine small scale soil redistribution patterns under a range of land use histories and management practices to improve understanding of the driving factors for soil erosion across the rift valley region of the Winam Gulf catchment of Lake Victoria in western Kenya. To achieve this aim the following objectives need to be met:

1 accurately determine fallout Pu activity concentrations in tropical soils for the subsequent determination of soil erosion rates with an improved separation and analysis method for ultra-trace Pu determination by;

1 (a) adapting and optimising a separation method using TEVA cartridges for the removal of matrix interferences with pre-concentration of ultra-trace Pu isotopes to reduce waste and increase throughput;

1 (b) establishing a robust analytical method for the determination of ultra-trace level Pu isotopes with sufficient sensitivity for African soil samples using oxygen as a reaction gas for ICP-MS/MS;

2 demonstrate the utility of $^{239+240}$Pu as a soil erosion tracer for the retrospective evaluation of soil redistribution that overcomes regional challenges in existing tracer-based approach using ^{137}Cs by;

2 (a) identification of a suitable area within the Winam Gulf of Lake Victoria on which to estimate soil redistribution occurring over differing timescales within the lake catchment;

2 (b) collection of soil samples to test the applicability of fallout radionuclide tracers, ^{137}Cs, $^{210}Pb_{ex}$ and $^{239+240}$Pu for the estimation of soil loss in Western Kenya;

2 (c) identifying the robustness of each FRN and assessing the improved applicability of $^{239+240}$Pu compared to other FRNs;

3 evaluate erosion dynamins, according to different land uses and clearance scale within a typical small scale agricultural plot of the Winam Gulf catchment of Lake Victoria using $^{239+240}$Pu by;

3 (a) identifying the radionuclide inventory across plots with different land use and clearance scale;

3 (b) modelling experimental outputs to relate sample site inventory with reference sites to calculate rates of erosion and deposition using the MODERN model;

3 (c) comparison scale of erosion according to different land use and management practices.

Thesis structure

During the study, a portion of the conducted research was submitted for publication after being subjected to peer-review. Therefore, chapters 2, 3 and 4 have been published and chapter 5 is undergoing peer review. All chapters are provided in "paper format," with author contributions explicitly specified at the beginning of each chapter. These constitute the thesis' core chapters.

The first chapter gave a general introduction to the thesis, including background information on the research question and an outline of the aim objectives of the research.

The second chapter is a literature review assessing methods of measurement for Pu isotopes. This paper reviewed the common methods reported in the literature for the separation and subsequent detection of Pu isotopes are compared to recent advances in analysis using ICP-MS/MS technology to improve understanding of Pu analysis to support the determination of soil erosion rates.

In chapter 3 the utilisation of TEVA resins and ICP-MS/MS analysis as a means of detecting ultra-trace Pu isotopes in African soils was evaluated. In addition, the development of analytical separation methods and analysis, previously outlined in Chapter 2, is completed to comment on the detection of ultra-trace Pu down a tropical African soil profile.

Chapter 4 evaluated the usefulness of Pu as a soil erosion tracer in comparison to the more regularly employed isotopes Cs and Pb, using the methods introduced in Chapter 3. An investigation into the variability of reference sites across the study area was conducted, to assess the improved applicability of $^{239+240}$Pu compared to other FRNs.

Chapter 5 assessed soil erosion patterns within a representative study site within Western Kenya using Pu isotopes and the MODERN model. The understanding of these erosion processes presented within the literature is currently incomplete and in order to determine best practices for mitigation strategies, a much better understanding of soil erosion patterns and ultimate land degradation is essential. In addition, an evaluation of the modelled soil erosion patterns according to varying land use, clearance, and management approaches was conducted in consideration of future mitigation strategies.

Chapter 6 concluded with a comprehensive discussion and evaluation of the use of Pu isotopes to investigate soil erosion trends in tropical Africa as well as considerations for future research.

References

Abdulkareem, J. H., Pradhan, B., Sulaiman, W. N. A., & Jamil, N. R. (2019). Prediction of spatial soil loss impacted by long-term land-use/land-cover change in a tropical watershed. Geoscience Frontiers, 10(2), 389–403. https://doi.org/10.1016/j.gsf.2017.10.010

Alewell, C., Egli, M., & Meusburger, K. (2015). An attempt to estimate tolerable soil erosion rates by matching soil formation with denudation in Alpine grasslands. Journal of Soils and Sediments, 15(6), 1383–1399. https://doi.org/10.1007/s11368-014-0920-6

Alewell, C., Meusburger, K., Juretzko, G., Mabit, L., & Ketterer, M. E. (2014). Suitability of 239+240Pu and 137Cs as tracers for soil erosion assessment in mountain grasslands. Chemosphere, 103, 274–280 https://doi.org/10.1016/J.CHEMOSPHERE.2013.12.016

Alewell, C., Pitois, A., Meusburger, K., Ketterer, M., & Mabit, L. (2017). 239 + 240Pu from "contaminant" to soil erosion tracer: Where do we stand? Earth-Science Reviews, 172, 107–123. https://doi.org/10.1016/J.EARSCIREV.2017.07.009

Al-Tuweity, J., Kamleh, H., Al-Masri, M. S., Doubal, A. W., & Chakir, E. M. (2021). Self-absorption Correction Factors: Applying A Simplified Method to Analysis of Lead-210 in Different Environment Samples by Direct Counting of Low-energy Using HPGe Detector. E3S Web Conf, 240, https://doi.org/10.1051/e3sconf/202124003002

Appleby, P. G., & Oldfield, F. (1978). The calculation of lead-210 dates assuming a constant rate of supply of unsupported 210Pb to the sediment. CATENA, 5(1), 1–8. https://doi.org/10.1016/S0341-8162(78)80002-2

Arata, L., Alewell, C., Frenkel, E., A'Campo-Neuen, A., Iurian, A.-R., Ketterer, M. E., Mabit, L., & Meusburger, K. (2016a). Modelling Deposition and Erosion rates with RadioNuclides (MODERN) – Part 2: A comparison of different models to convert 239+240 Pu inventories into soil redistribution rates at unploughed sites. Journal of Environmental Radioactivity, 162–163, 97–106. https://doi.org/10.1016/j.jenvrad.2016.05.009

Arata, L., Meusburger, K., Frenkel, E., A'Campo-Neuen, A., Iurian, A.-R., Ketterer, M. E., Mabit, L., & Alewell, C. (2016b). Modelling Deposition and Erosion rates with RadioNuclides (MODERN) – Part 1: A new conversion model to derive soil redistribution rates from inventories of fallout radionuclides. Journal of Environmental Radioactivity, 162–163, 45–55. https://doi.org/10.1016/j.jenvrad.2016.05.008

Ashraf, M. A., Akib, S., Maah, Mohd. J., Yusoff, I., & Balkhair, K. S. (2014). Cesium-137: Radio-Chemistry, Fate, and Transport, Remediation, and Future Concerns. Critical Reviews in Environmental Science and Technology, 44(15), 1740–1793. https://doi.org/10.1080/10643389.2013.790753

Batista, P. V. G., Davies, J., Silva, M. L. N., & Quinton, J. N. (2019). On the evaluation of soil erosion models: Are we doing enough? Earth-Science Reviews, 197, 102898. https://doi.org/10.1016/j.earscirev.2019.102898

Boardman, J. (2006). Soil erosion science: Reflections on the limitations of current approaches. CATENA, 68(2–3), 73–86. https://doi.org/10.1016/j.catena.2006.03.007

Borrelli, P., Robinson, D. A., Fleischer, L. R., Lugato, E., Ballabio, C., Alewell, C., Meusburger, K., Modugno, S., Schütt, B., Ferro, V., Bagarello, V., Oost, K. Van, Montanarella, L., & Panagos, P. (2017). An assessment of the global impact of 21st century land use change on soil erosion. Nature Communications, 8(1), 2013. https://doi.org/10.1038/s41467-017-02142-7

Borrelli, P., Robinson, D. A., Panagos, P., Lugato, E., Yang, J. E., Alewell, C., Wuepper, D., Montanarella, L., & Ballabio, C. (2020). Land use and climate change impacts on global soil erosion by water (2015-2070). Proceedings of the National Academy of Sciences, 117(36), 21994–22001. https://doi.org/10.1073/pnas.2001403117

Boulyga, S. F., Testa, C., Desideri, D., & Becker, J. S. (2001). Optimisation and application of ICP-MS and alpha-spectrometry for determination of isotopic ratios of depleted uranium and plutonium in samples collected in Kosovo. Journal of Analytical Atomic Spectrometry, 16(11), 1283–1289. https://doi.org/10.1039/b103178n

Cao, L., Zheng, J., Tsukada, H., Pan, S., Wang, Z., Tagami, K., & Uchida, S. (2016). Simultaneous determination of radiocesium (135Cs, 137Cs) and plutonium (239Pu, 240Pu) isotopes in river suspended particles by ICP-MS/MS and SF-ICP-MS. Talanta, 159, 55–63. https://doi.org/10.1016/j.talanta.2016.06.008

Chappell, A., Warren, A., Taylor, N., & Charlton, M. (1998). Soil flux (loss and gain) in southwestern Niger and its agricultural impact. Land Degradation & Development, 9(4), 295–310. https://doi.org/10.1002/(SICI)1099-145X(199807/08)9:4<295::AID-LDR293>3.0.CO;2-J

Chawla, F., Steinmann, P., Pfeifer, H.-R., & Froidevaux, P. (2010). Atmospheric deposition and migration of artificial radionuclides in Alpine soils (Val Piora, Switzerland) compared to the distribution of selected major and trace elements. Science of The Total Environment, 408(16), 3292–3302. https://doi.org/10.1016/j.scitotenv.2010.03.012

Chibowski, S., Zygmunt, J., & Klimowicz, Z. (1999). Investigation of adsorption and vertical migration of 137Cs in three kinds of soil at Lublin vicinity. Journal of Radioanalytical and Nuclear Chemistry, 242(2), 287–295. https://doi.org/10.1007/BF02345555

Collier, P., & Dercon, S. (2014). African Agriculture in 50Years: Smallholders in a Rapidly Changing World? World Development, 63, 92–101 https://doi.org/10.1016/j.worlddev.2013.10.001

Collins, A. L., Walling, D. E., Sichingabula, H. M., & Leeks, G. J. L. (2001). Using 137Cs measurements to quantify soil erosion and redistribution rates for areas under different land use in the Upper Kaleya River basin, southern Zambia. Geoderma, 104(3–4), 299–323. https://doi.org/10.1016/S0016-7061(01)00087-8

deGraffenried, J. B., & Shepherd, K. D. (2009). Rapid erosion modeling in a Western Kenya watershed using visible near infrared reflectance, classification tree analysis and 137Cesium. Geoderma, 154(1–2), 93–100. https://doi.org/10.1016/j.geoderma.2009.10.001

Elwell, H. A. (1978). Modelling soil losses in Southern Africa. Journal of Agricultural Engineering Research, 23(2), 117–127. https://doi.org/10.1016/0021-8634(78)90043-4

Esaka, F., Yasuda, K., Suzuki, D., Miyamoto, Y., & Magara, M. (2017). Analysis of plutonium isotope ratios including 238Pu/239Pu in individual U–Pu mixed oxide particles by means of a combination of alpha spectrometry and ICP-MS. Talanta, 165, 122–127. https://doi.org/10.1016/J.TALANTA.2016.12.041

Everett, S. E., Tims, S. G., Hancock, G. J., Bartley, R., & Fifield, L. K. (2008). Comparison of Pu and 137Cs as tracers of soil and sediment transport in a terrestrial environment. Journal of Environmental Radioactivity, 99(2), 383–393. https://doi.org/10.1016/j.jenvrad.2007.10.019

Evrard, O., Chaboche, P.-A., Ramon, R., Foucher, A., & Laceby, J. P. (2020). A global review of sediment source fingerprinting research incorporating fallout radiocesium (137Cs). Geomorphology, 362, 107103. https://doi.org/10.1016/j.geomorph.2020.107103

Farnsworth, A., White, E., Williams, C. J. R., Black, E., & Kniveton, D. R. (2011). Understanding the Large Scale Driving Mechanisms of Rainfall Variability over Central Africa, 101–122. https://doi.org/10.1007/978-90-481-3842-5_5

Fusilli, L., Marzialetti, P., Laneve, G., & Santilli, G. (2014). Urban growth assessment around Winam Gulf of Kenya based on satellite imagery. Acta Astronautica, 93, 279–290. https://doi.org/10.1016/j.actaastro.2013.07.008

Geckeis H, Salbu B, Zavarin M, Lind OC, Skipperud L (2018) Environmental chemistry of plutonium. In: Clark D, GeesonD, Hanrahan R (eds) Plutonium handbook, 2nd Edn. American Nuclear Society, Illinois

Gharbi, F., AlSheddi, T. H., Ben Ammar, R., & Ahmed El-Naggar, M. (2020). Combination of 137Cs and 210Pb Radioactive Atmospheric Fallouts to Estimate Soil Erosion for the Same Time Scale. International Journal of Environmental Research and Public Health, 17(22), 8292. https://doi.org/10.3390/ijerph17228292

Grüning, C., Huber, G., Klopp, P., Kratz, J. V., Kunz, P., Passler, G., Trautmann, N., Waldek, A., & Wendt, K. (2004). Resonance ionization mass spectrometry for ultratrace analysis of plutonium with a new solid state laser system. International Journal of Mass Spectrometry, 235(2), 171–178. https://doi.org/10.1016/j.ijms.2004.04.013

Gudiksen, P. H., Harvey, T. F., & Lange, R. (1989). Chernobyl Source Term, Atmospheric Dispersion, and Dose Estimation. Health Physics , 57(5), 697–706.

Hakonson, T. E., Watters, R. L., & Hanson, W. C. (1981). The Transport of Plutonium in Terrestrial Ecosystems. Health Physics, 40(1), 63–69.

He, Q., & Walling, D. E. (1997). The distribution of fallout 137Cs and 210Pb in undisturbed and cultivated soils. Applied Radiation and Isotopes, 48(5), 677–690. https://doi.org/10.1016/S0969-8043(96)00302-8

Hoo, W. T., Fifield, L. K., Tims, S. G., Fujioka, T., & Mueller, N. (2011). Using fallout plutonium as a probe for erosion assessment. Journal of Environmental Radioactivity, 102(10), 937–942. https://doi.org/10.1016/J.JENVRAD.2010.06.010

Hossain, A., Krupnik, T. J., Timsina, J., Mahboob, M. G., Chaki, A. K., Farooq, M., Bhatt, R., Fahad, S., & Hasanuzzaman, M. (2020). Agricultural Land Degradation: Processes and Problems Undermining Future Food Security. In Environment, Climate, Plant and Vegetation Growth, 17–61. Springer International Publishing. https://doi.org/10.1007/978-3-030-49732-3_2

Hou, X., Zhang, W., & Wang, Y. (2019). Determination of Femtogram-Level Plutonium Isotopes in Environmental and Forensic Samples with High-Level Uranium Using Chemical Separation and ICP-MS/MS Measurement. Anal. Chem, 91 (18), 11553-11561. https://doi.org/10.1021/acs.analchem.9b01347

Hrnecek, E., Steier, P., & Wallner, A. (2005). Determination of plutonium in environmental samples by AMS and alpha spectrometry. Applied Radiation and Isotopes, 63(5-6), 633–638. https://doi.org/10.1016/J.APRADISO.2005.05.012

Joint FAO/IAEA Division of Nuclear Techniques in Food and Agriculture, Soil and Water Management and Crop Nutrition Section, Vienna (Austria) 2014. Guidelines for Using Fallout Radionuclides to Assess Erosion and Effectiveness of Soil Conservation Strategies (IAEA-TECDOC--1741). International Atomic Energy Agency (IAEA)

Joshi, S. R., & Shukla, B. S. (1991). AB initio derivation of formulations for 210Pb dating of sediments. Journal of Radioanalytical and Nuclear Chemistry 148(1), 73–79. https://doi.org/10.1007/BF02060548

Junge, B., Mabit, L., Dercon, G., Walling, D. E., Abaidoo, R., Chikoye, D., & Stahr, K. (2010). First use of the 137Cs technique in Nigeria for estimating medium-term soil redistribution rates on cultivated farmland. Soil and Tillage Research, 110(2), 211–220. https://doi.org/10.1016/j.still.2010.07.012

Kaplan, D. I., Powell, B. A., Demirkanli, D. I., Fjeld, R. A., Molz, F. J., Serkiz, S. M., & Coates, J. T. (2004). Influence of Oxidation States on Plutonium Mobility during Long-Term Transport through an Unsaturated Subsurface Environment. Environmental Science & Technology, 38(19), 5053–5058. https://doi.org/10.1021/es049406s

Kassab, M., Hegazi, A., Salem, M., & Benmansour, M. (2021). Using Beryllium-7 as a natural radionuclide for assessing short term soil erosion in arid agricultural land, Egypt. Arab Journal of Nuclear Sciences and Applications, 1–10. https://doi.org/10.21608/ajnsa.2021.91984.1505

Kelley, J. M., Bond, L. A., & Beasley, T. M. (1999). Global distribution of Pu isotopes and 237Np. Science of The Total Environment, 237–238, 483–500. https://doi.org/10.1016/S0048-9697(99)00160-6

Kelly, C., Wynants, M., Munishi, L. K., Nasseri, M., Patrick, A., Mtei, K. M., Mkilema, F., Rabinovich, A., Gilvear, D., Wilson, G., Blake, W., & Ndakidemi, P. A. (2020). 'Mind the Gap': Reconnecting Local Actions and Multi-Level Policies to Bridge the Governance Gap. An Example of Soil Erosion Action from East Africa. Land, 9(10), 352. https://doi.org/10.3390/land9100352

Kersting, A. B. (2013). Plutonium Transport in the Environment. Inorganic Chemistry, 52(7), 3533–3546. https://doi.org/10.1021/ic3018908

Ketterer, M. E., Hafer, K. M., Jones, V. J., & Appleby, P. G. (2004). Rapid dating of recent sediments in Loch Ness: inductively coupled plasma mass spectrometric measurements of global fallout plutonium. Science of The Total Environment, 322(1–3), 221–229. https://doi.org/10.1016/J.SCITOTENV.2003.09.016

Ketterer, M. E., & Szechenyi, S. C. (2008). Determination of plutonium and other transuranic elements by inductively coupled plasma mass spectrometry: A historical perspective and new frontiers in the environmental sciences. In Spectrochimica Acta - Part B Atomic Spectroscopy, 63 (7), 719–737). https://doi.org/10.1016/j.sab.2008.04.018

Khodadadi, M., Alewell, C., Mirzaei, M., Ehssan-Malahat, E., Asadzadeh, F., Strauss, P., & Meusburger, K. (2021). Deforestation effects on soil erosion rates and soil physicochemical properties in Iran: a case study of using fallout radionuclides in a Chernobyl contaminated area. https://doi.org/10.5194/soil-2021-2

Korsakissok, I., Mathieu, A., & Didier, D. (2013). Atmospheric dispersion and ground deposition induced by the Fukushima Nuclear Power Plant accident: A local-scale simulation and sensitivity study. Atmospheric Environment, 70, 267–279. https://doi.org/10.1016/j.atmosenv.2013.01.002

Labrière, N., Locatelli, B., Laumonier, Y., Freycon, V., & Bernoux, M. (2015). Soil erosion in the humid tropics: A systematic quantitative review. Agriculture, Ecosystems & Environment, 203, 127–139. https://doi.org/10.1016/j.agee.2015.01.027

Lal, D. (1983). Poverty of Development Economics. Cambridge, MA: MIT Press.

Lal, R. (2001). Soil degradation by erosion. Land Degradation & Development, 12(6), 519–539. https://doi.org/10.1002/ldr.472

Lal, R., Tims, S. G., Fifield, L. K., Wasson, R. J., & Howe, D. (2013). Applicability of 239Pu as a tracer for soil erosion in the wet-dry tropics of northern Australia. Nuclear Instruments and Methods in Physics Research, Section B: Beam Interactions with Materials and Atoms, 294, 577–583. https://doi.org/10.1016/j.nimb.2012.07.041

L'Annunziata, M. F. (2012). Handbook of Radioactivity Analysis (L'Annunziata M. F, Ed.; 3rd ed., Vol. 1). Academic Press. https://doi.org/10.1016/C2009-0-64509-8

Laurance, W. F., Sayer, J., & Cassman, K. G. (2014). Agricultural expansion and its impacts on tropical nature. Trends in Ecology & Evolution, 29(2), 107–116. https://doi.org/10.1016/j.tree.2013.12.001

Lee, C.-G., Suzuki, D., Esaka, F., Magara, M., & Song, K. (2015). Ultra-trace analysis of plutonium by thermal ionization mass spectrometry with a continuous heating technique without chemical separation. Talanta, 141, 92–96. https://doi.org/10.1016/j.talanta.2015.03.060

Liu, B., Shi, K., Ye, G., Guo, Z., & Wu, W. (2016). Method development for plutonium analysis in environmental water samples using TEVA microextraction chromatography separation and low background liquid scintillation counter measurement. Microchemical Journal, 124, 824–830. https://doi.org/10.1016/J.MICROC.2015.10.007

Loba, A., Waroszewski, J., Sykuła, M., Kabala, C., & Egli, M. (2022). Meteoric 10Be, 137Cs and 239+240Pu as Tracers of Long- and Medium-Term Soil Erosion; A Review. Minerals, 12(3), 359. https://doi.org/10.3390/MIN12030359

Lokuruka, M. N. I. (2021). Food and nutrition security in east Africa (Kenya, Uganda and Tanzania): Status, challenges, and prospects. In Mahoud Baraat (Ed.), Food Security in Africa 1, 93–96. IntechOpen. https://doi.org/10.5772/intechopen.77894

Lorenz, K., Lal, R., & Ehlers, K. (2019). Soil organic carbon stock as an indicator for monitoring land and soil degradation in relation to United Nations' Sustainable Development Goals. Land Degradation & Development, 30(7), 824–838. https://doi.org/10.1002/ldr.3270

Mabit, L., Benmansour, M., Abril, J. M., Walling, D. E., Meusburger, K., Iurian, A. R., Bernard, C., Tarján, S., Owens, P. N., Blake, W. H., & Alewell, C. (2014). Fallout 210Pb as a soil and sediment tracer in catchment sediment budget investigations: A review. Earth-Science Reviews, 138, 335–351. https://doi.org/10.1016/j.earscirev.2014.06.007

Mabit, L., Benmansour, M., & Walling, D. E. (2008). Comparative advantages and limitations of the fallout radionuclides 137Cs, 210Pbex and 7Be for assessing soil erosion and sedimentation. Journal of Environmental Radioactivity, 99(12), 1799–1807. https://doi.org/10.1016/j.jenvrad.2008.08.009

Mabit, L., & Blake, W. (2019). Assessing Recent Soil Erosion Rates through the Use of Beryllium-7 (Be-7). Springer International Publishing. https://doi.org/10.1007/978-3-030-10982-0

Mabit, L., Chhem-Kieth, S., Toloza, A., Vanwalleghem, T., Bernard, C., Amate, J. I., González de Molina, M., & Gómez, J. A. (2012). Radioisotopic and physicochemical background indicators to assess soil degradation affecting olive orchards in southern Spain. Agriculture, Ecosystems & Environment, 159, 70–80. https://doi.org/10.1016/j.agee.2012.06.014

Mabit, L., Chhem-Kieth, S., Dornhofer, P., Toloza, A., Benmansour, M., Bernard, C., Fulajtar, E., Walling, D.E. (2014) 137Cs: A Widely Usedand Validated Medium-Term Soil Tracer; IAEA publication: Vienna, Austria, 27–77.

Marriott, A. L., Osano, O. F., Coffey, T. J., Humphrey, O. S., Ongore, C. O., Watts, M. J., & Aura, C. M. (2023). Considerations for environmental biogeochemistry and food security for aquaculture around Lake Victoria, Kenya. Environmental Geochemistry and Health, 45(8), 6137–6162. https://doi.org/10.1007/s10653-023-01585-w

Metzger, S. C., Rogers, K. T., Bostick, D. A., McBay, E. H., Ticknor, B. W., Manard, B. T., & Hexel, C. R. (2019). Optimization of uranium and plutonium separations using TEVA and UTEVA cartridges for MC-ICP-MS analysis of environmental swipe samples. Talanta, 198, 257–262. https://doi.org/10.1016/J.TALANTA.2019.02.034

Meusburger, K., Mabit, L., Ketterer, M., Park, J.-H., Sandor, T., Porto, P., & Alewell, C. (2016). A multi-radionuclide approach to evaluate the suitability of 239+240Pu as soil erosion tracer. Science of The Total Environment, 566–567, 1489–1499. https://doi.org/10.1016/j.scitotenv.2016.06.035

Meusburger, K., Porto, P., Mabit, L., La Spada, C., Arata, L., & Alewell, C. (2018). Excess Lead-210 and Plutonium-239+240: Two suitable radiogenic soil erosion tracers for mountain grassland sites. Environmental Research, 160, 195–202. https://doi.org/10.1016/J.ENVRES.2017.09.020

Missana, T., García-Gutiérrez, M., & Alonso, Ú. (2004). Kinetics and irreversibility of cesium and uranium sorption onto bentonite colloids in a deep granitic environment. Applied Clay Science, 26(1–4), 137–150. https://doi.org/10.1016/j.clay.2003.09.008

Moldovan, M., Krupp, E. M., Holliday, A. E., & Donard, O. F. X. (2004). High resolution sector field ICP-MS and multicollector ICP-MS as tools for trace metal speciation in environmental studies: a review. Journal of Analytical Atomic Spectrometry, 19(7), 815–822. https://doi.org/10.1039/B403128H

Montgomery, D. R. (2007). Soil erosion and agricultural sustainability. Proceedings of the National Academy of Sciences, 104(33), 13268–13272. https://doi.org/10.1073/pnas.0611508104

Moustakim, M., Benmansour, M., Nouira, A., Benkdad, A., & Damnati, B. (2022). Caesium-137 re-sampling approach and excess Lead-210 sediment dating to assess the impacts of climate change and agricultural practices on soil erosion and sedimentation in Northwest Morocco. Environmental Earth Sciences, 81(10), 278. https://doi.org/10.1007/s12665-022-10409-6

Muller, R. N., Sprugel, D. G., & Kohn, B. (1978). Erosional Transport and Deposition of Plutonium and Cesium in Two Small Midwestern Watersheds. Journal of Environmental Quality, 7(2), 171–174. https://doi.org/10.2134/JEQ1978.00472425000700020003X

Muramatsu, Y., Hamilton, T., Uchida, S., Tagami, K., Yoshida, S., & Robison, W. (2001). Measurement of 240Pu/239Pu isotopic ratios in soils from the Marshall Islands using ICP-MS. The Science of the Total Environment, 278(1–3), 151–159. https://doi.org/10.1016/S0048-9697(01)00644-1

Mutie, F. M., Rono, P. C., Kathambi, V., Hu, G. W., & Wang, Q. F. (2020). Conservation of Wild Food Plants and Their Potential for Combatting Food Insecurity in Kenya as Exemplified by the Drylands of Kitui County. Plants, 9(8), 1017. https://doi.org/10.3390/plants9081017

Nassali, J., Yongji, Z., & Fangninou, F. F. (2020). A Systematic Review of Threats to the Sustainable Utilization of Transboundary Fresh Water Lakes: A Case Study of Lake Victoria. International Journal of Scientific and Research Publications (IJSRP), 10(2), p9890. https://doi.org/10.29322/IJSRP.10.02.2020.p9890

Njagi, D. M., Routh, J., Odhiambo, M., Luo, C., Basapuram, L. G., Olago, D., Klump, V., & Stager, C. (2022). A century of human-induced environmental changes and the combined roles of nutrients and land use in Lake Victoria catchment on eutrophication. Science of The Total Environment, 835, 155425. https://doi.org/10.1016/j.scitotenv.2022.155425

Odada, E. O., Olago, D. O., Bugenyi, F., Kulindwa, K., Karimumuryango, J., West, K., Ntiba, M., Wandiga, S., Aloo-Obudho, P., & Achola, P. (2003). Environmental assessment of the East African Rift Valley lakes. Aquatic Sciences - Research Across Boundaries, 65(3), 254–271. https://doi.org/10.1007/s00027-003-0638-9

Pálsson, S. E., Howard, B. J., & Wright, S. M. (2006). Prediction of spatial variation in global fallout of 137Cs using precipitation. Science of The Total Environment, 367(2–3), 745–756. https://doi.org/10.1016/j.scitotenv.2006.01.011

Parsons, A. J., & Foster, I. D. L. (2011). What can we learn about soil erosion from the use of 137Cs? Earth-Science Reviews, 108(1–2), 101–113. https://doi.org/10.1016/j.earscirev.2011.06.004

Parwada, C., Chipomho, J., & Tibugari, H. (2023). Comparison of conventional and artificial fallout radionuclide (FRNs) methods in assessing soil erosion. Sustainable Environment, 9(1). https://doi.org/10.1080/27658511.2023.2236406

Pennock, D. J. (2000) Suitability of 137 Cs Redistribution as an Indicator of Soil Quality. Acta geológica hispánica, 35 (3), 213-217, https://raco.cat/index.php/ActaGeologica/article/view/75614

Pimentel, D. (2006). Soil Erosion: A Food and Environmental Threat. Environment, Development and Sustainability, 8(1), 119–137. https://doi.org/10.1007/s10668-005-1262-8

Pimentel, D., & Burgess, M. (2013). Soil Erosion Threatens Food Production. Agriculture, 3(3), 443–463. https://doi.org/10.3390/agriculture3030443

Poreba, G. J. (2006). Caesium-137 as a soil erosion tracer: a review. Geochronometria, 25(37–46).

Portes, R., Dahms, D., Brandová, D., Raab, G., Christl, M., Kühn, P., Ketterer, M., & Egli, M. (2018). Evolution of soil erosion rates in alpine soils of the Central Rocky Mountains using fallout Pu and δ13C. Earth and Planetary Science Letters, 496, 257–269. https://doi.org/10.1016/J.EPSL.2018.06.002

Prăvălie, R. (2014). Nuclear Weapons Tests and Environmental Consequences: A Global Perspective. AMBIO 2014 43:6, 43(6), 729–744. https://doi.org/10.1007/S13280-014-0491-1

Quine, T. A., Walling, D. E., and Mandiringana, O.T. (1993). An investigation of the influence of edaphic, topographic and land- use controls on soil erosion on agricultural land in the Borrowdale and Chinamora areas, Zimbabwe, based on caesium-137 measurements. Sediment Problems. Proc. International Symposium, Yokohama, 217, 185–196

Raab, G., Scarciglia, F., Norton, K., Dahms, D., Brandová, D., de Castro Portes, R., Christl, M., Ketterer, M. E., Ruppli, A., & Egli, M. (2018). Denudation variability of the Sila Massif upland (Italy) from decades to millennia using 10Be and 239+240Pu. Land Degradation & Development, 29(10), 3736–3752. https://doi.org/10.1002/LDR.3120

Rabesiranana, N., Rasolonirina, M., Solonjara, A. F., Ravoson, H. N., Raoelina Andriambololona, & Mabit, L. (2016). Assessment of soil redistribution rates by 137Cs and 210Pbex in a typical Malagasy agricultural field. Journal of Environmental Radioactivity, 152, 112–118. https://doi.org/10.1016/j.jenvrad.2015.11.007

Ritchie JC, Ritchie CA (2005) Bibliography of publications of 137cesium studies related to erosion and sediment deposition. USDA-Agricultural Research Service, Beltsville.

Ritchie, J. C., Spraberry, J. A., & McHenry, J. R. (1974). Estimating Soil Erosion from the Redistribution of Fallout 137Cs. Soil Science Society of America Journal, 38(1), 137–139. https://doi.org/10.2136/sssaj1974.03615995003800010042x

Ruecker, G. R., Park, S. J., Brunner, A. C., & Vlek, P. L. G. (2008). Assessment of Soil Redistribution on Two Contrasting Hillslopes in Uganda Using Caesium-137 Modelling. *Erdkunde*, *62*(3), 259–272. http://www.jstor.org/stable/25648129

Ruecker, G. R., Park, S. J., Brunner, A. C., & Vlek, P. L. G. (2008). Assessment of Soil Redistribution on Two Contrasting Hillslopes in Uganda Using Caesium-137 Modelling. *Erdkunde*, *62*(3), 259–272. http://www.jstor.org/stable/25648129

Russell, B. C., Croudace, I. W., & Warwick, P. E. (2015). Determination of 135Cs and 137Cs in environmental samples: A review. Analytica Chimica Acta, 890, 7–20. https://doi.org/10.1016/j.aca.2015.06.037

Sánchez-Cabezudo, A. I., Crespo, M. T., Roteta, M., & Navarro, N. (2021). Standardization of non-equilibrium 210Pb solutions by LSC and 2πα counting. Applied Radiation and Isotopes, 170, 109587. https://doi.org/10.1016/j.apradiso.2021.109587

Schimmack, W., Auerswald, K., & Bunzl, K. (2001). Can 239+240Pu replace 137Cs as an erosion tracer in agricultural landscapes contaminated with Chernobyl fallout? Journal of Environmental Radioactivity, 53(1), 41–57. https://doi.org/10.1016/S0265-931X(00)00117-X

Schimmack, W., Auerswald, K., & Bunzl, K. (2004). Estimation of soil erosion and deposition rates at an agricultural site in Bavaria, Germany, as derived from fallout radiocesium and plutonium as tracers. Naturwissenschaften 2001 89:1, 89(1), 43–46. https://doi.org/10.1007/S00114-001-0281-Z

Sedighi, F., Darvishan, A. K., Golosov, V., & Zare, M. R. (2020). Relationship between Mean Annual Precipitation and Inventories of Fallout Radionuclides (137Cs and 210Pbexcess) in Undisturbed Soils around the World: A Review. Eurasian Soil Science, 53(9), 1332–1341. https://doi.org/10.1134/S1064229320090148

Seferinoğlu, M., Aslan, N., Kurt, A., Erden, P. E., & Mert, H. (2014). Determination of plutonium isotopes in bilberry using liquid scintillation spectrometry and alpha-particle spectrometry. Applied Radiation and Isotopes, 87, 81–86. https://doi.org/10.1016/J.APRADISO.2013.11.097

Šešlak, B., Vukanac, I., Kandić, A., Đurašević, M., Erić, M., Jevremović, A., & Benedik, L. (2017). Determination of 210Pb by direct gamma-ray spectrometry, beta counting via 210Bi and alpha-particle spectrometry via 210Po in coal, slag, and ash samples from thermal power plant. Journal of Radioanalytical and Nuclear Chemistry, 311(1), 719–726. https://doi.org/10.1007/s10967-016-5028-6

Seutloali, K. E., Dube, T., & Sibanda, M. (2018). Developments in the remote sensing of soil erosion in the perspective of sub-Saharan Africa. Implications on future food security and biodiversity. Remote Sensing Applications: Society and Environment, 9, 100–106. https://doi.org/10.1016/j.rsase.2017.12.002

Smith, H. G., & Blake, W. H. (2014). Sediment fingerprinting in agricultural catchments: A critical re-examination of source discrimination and data corrections. Geomorphology, 204, 177–191. https://doi.org/10.1016/j.geomorph.2013.08.003

Soto, J., & Navas, A. (2008). A simple model of Cs-137 profile to estimate soil redistribution in cultivated stony soils. Radiation Measurements, 43(7), 1285–1293. https://doi.org/10.1016/j.radmeas.2008.02.024

Suchara, I., Sucharová, J., Holá, M., Pilátová, H., & Rulík, P. (2016). Long-term retention of 137Cs in three forest soil types with different soil properties. Journal of Environmental Radioactivity, 158–159, 102–113. https://doi.org/10.1016/j.jenvrad.2016.04.010

Sultan, B., & Gaetani, M. (2016). Agriculture in West Africa in the Twenty-First Century: Climate Change and Impacts Scenarios, and Potential for Adaptation. Frontiers in Plant Science, 7. https://doi.org/10.3389/fpls.2016.01262

Sutherland, R. A. (1996). Caesium-137 soil sampling and inventory variability in reference locations: A literature survey. Hydrological Processes, 10(1), 43–53. https://doi.org/10.1002/(SICI)1099-1085(199601)10:1<43::AID-HYP298>3.0.CO;2-X

Thakur, P., Khaing, H., & Salminen-Paatero, S. (2017). Plutonium in the atmosphere: A global perspective. Journal of Environmental Radioactivity 175–176, 39–51. https://doi.org/10.1016/j.jenvrad.2017.04.008

Thiessen, K. M., Thorne, M. C., Maul, P. R., Pröhl, G., & Wheater, H. S. (1999). Modelling radionuclide distribution and transport in the environment. Environmental Pollution, 100(1–3), 151–177. https://doi.org/10.1016/S0269-7491(99)00090-1

Turekian, K. K., Nozaki, Y., & Benninger, L. K. (1977). Geochemistry of Atmospheric Radon and Radon Products. Annual Review of Earth and Planetary Sciences, 5(1), 227–255. https://doi.org/10.1146/annurev.ea.05.050177.001303

Varga, Z., Surányi, G., Vajda, N., & Stefánka, Z. (2007). Determination of plutonium and americium in environmental samples by inductively coupled plasma sector field mass spectrometry and alpha spectrometry. Microchemical Journal, 85(1), 39–45. https://doi.org/10.1016/J.MICROC.2006.02.006

Wallenius, M., & Mayer, K. (2000). Age determination of plutonium material in nuclear forensics by thermal ionisation mass spectrometry. Fresenius' Journal of Analytical Chemistry, 366(3), 234–238. https://doi.org/10.1007/s002160050046

Walling, D. E., Collins, A. L., & Sichingabula, H. M. (2003). Using unsupported lead-210 measurements to investigate soil erosion and sediment delivery in a small Zambian catchment. Geomorphology, 52(3–4), 193–213. https://doi.org/10.1016/S0169-555X(02)00244-1

Walling, D.E., Zhang, Y., & He, Q. (2011). Models for Deriving Estimates of Erosion and Deposition Rates from Fallout Radionuclide (Caesium-137, Excess Lead-210, and Beryllium-7) Measurements and the Development of User-Friendly Software for Model Implementation (IAEA-TECDOC--1665). International Atomic Energy Agency (IAEA)

Walling, D.E., Quine, T.A., (1992). The use of caesium-137 measurements in soil erosion surveys. Eros. sediment Monit. Program. river basins. Proc. Int. Symp. Oslo, 1992 143-152.

Whitlow, R. (1988a). Potential versus actual erosion in Zimbabwe. Applied Geography, 8(2), 87–100. https://doi.org/10.1016/0143-6228(88)90026-4

Whitlow, R. (1988b). Land degradation in Zimbabwe: a geographical study. Harare: UZ/ Department of Natural Resources.

Wilken, F., Fiener, P., Ketterer, M., Meusburger, K., Muhindo, D. I., Van Oost, K., & Doetterl, S. (2020). Assessing soil erosion of forest and cropland sites in wet tropical Africa using 239+240 Pu fallout radionuclides. https://doi.org/10.5194/soil-2020-95

Wynants, M., Kelly, C., Mtei, K., Munishi, L., Patrick, A., Rabinovich, A., Nasseri, M., Gilvear, D., Roberts, N., Boeckx, P., Wilson, G., Blake, W. H., & Ndakidemi, P. (2019). Drivers of increased soil erosion in East Africa's agro-pastoral systems: changing interactions between the social, economic, and natural domains. Regional Environmental Change, 19(7), 1909–1921. https://doi.org/10.1007/s10113-019-01520-9

Xu, Y., Li, C., Yu, H., Fang, F., Hou, X., Zhang, C., Li, X., & Xing, S. (2022). Rapid determination of plutonium isotopes in small samples using single anion exchange separation and ICP-MS/MS measurement in NH3–He mode for sediment dating. Talanta, 240, 123152. https://doi.org/10.1016/J.TALANTA.2021.123152

Xu, Y., Qiao, J., Hou, X., & Pan, S. (2013). Plutonium in Soils from Northeast China and Its Potential Application for Evaluation of Soil Erosion. Scientific Reports, 3(1), 1–8. https://doi.org/10.1038/srep03506

Xu, Y., Qiao, J., Pan, S., Hou, X., Roos, P., & Cao, L. (2015). Plutonium as a tracer for soil erosion assessment in northeast China. Science of the Total Environment, 511, 176–185. https://doi.org/10.1016/J.SCITOTENV.2014.12.006

Zapata, F. (2003). The use of environmental radionuclides as tracers in soil erosion and sedimentation investigations: recent advances and future developments. Soil and Tillage Research, 69(1–2), 3–13. https://doi.org/10.1016/S0167-1987(02)00124-1

Zhang, W., Xing, S., & Hou, X. (2019). Evaluation of soil erosion and ecological rehabilitation in Loess Plateau region in Northwest China using plutonium isotopes. Soil and Tillage Research, 191, 162–170. https://doi.org/10.1016/J.STILL.2019.04.004

Zhidkin, A. P., Shamshurina, E. N., Golosov, V. N., Komissarov, M. A., Ivanova, N. N., & Ivanov, M. M. (2020). Detailed study of post-Chernobyl Cs-137 redistribution in the soils of a small agricultural catchment (Tula region, Russia). Journal of Environmental Radioactivity, 223–224, 106386. https://doi.org/10.1016/j.jenvrad.2020.106386

Zollinger, B., Alewell, C., Kneisel, C., Meusburger, K., Brandová, D., Kubik, P., Schaller, M., Ketterer, M., & Egli, M. (2015). The effect of permafrost on time-split soil erosion using radionuclides (137Cs, 239 + 240Pu, meteoric 10Be) and stable isotopes (δ 13C) in the eastern Swiss Alps. Journal of Soils and Sediments, 15(6), 1400–1419. https://doi.org/10.1007/s11368-014-0881-9

Chapter 2 - Ultra-Trace Analysis of Fallout Plutonium Isotopes in Soil: Emerging Trends and Future Perspectives

This chapter has been published in *Chemistry Africa*

https://doi.org/10.1007/s42250-023-00659-7

Author contributions:

Review conceived by SD, OSH and MJW

All tables and figures produced by SD

Construction of the paper by SD

All authors were involved during manuscript development

Dowell, S.M., Humphrey, O.S., Blake, W.H., Osano, O., Chenery, S., Watts, MJ. 2023. Ultra-Trace Analysis of Fallout Plutonium Isotopes in Soil: Emerging Trends and Future Perspectives. Chemistry Africa. https://doi.org/10.1007/s42250-023-00659-7

Ultra-trace analysis of fallout plutonium isotopes in soil: emerging trends and future perspectives

Sophia M. Dowell [a,b], Olivier S. Humphrey [a], William H. Blake [b], Odipo Osano [c], Simon Chenery [a] Michael J. Watts [a]

[a] Inorganic Geochemistry, Centre for Environmental Geochemistry, British Geological Survey, Nottingham, NG12 5GG, UK

[b] School of Geography, Earth and Environmental Sciences, University of Plymouth, Plymouth, Devon, PL4 8AA, UK

[c] School of Environmental Sciences, University of Eldoret, Eldoret, Kenya

Highlights

- This review assesses the current trends employed for the detection of Pu isotopes
- Challenges associated with the determination of soil redistribution rates
- Traditional analysis of plutonium isotopes is expensive
- Mass spectrometry techniques are reliant on extensive separation prior to analysis
- ICP-MS/MS boasts advantages for the analysis of plutonium for quantification of soil erosion

Keywords

Plutonium, soil erosion, mass spectrometry, radiometric, ICP-MS/MS

Graphical abstract

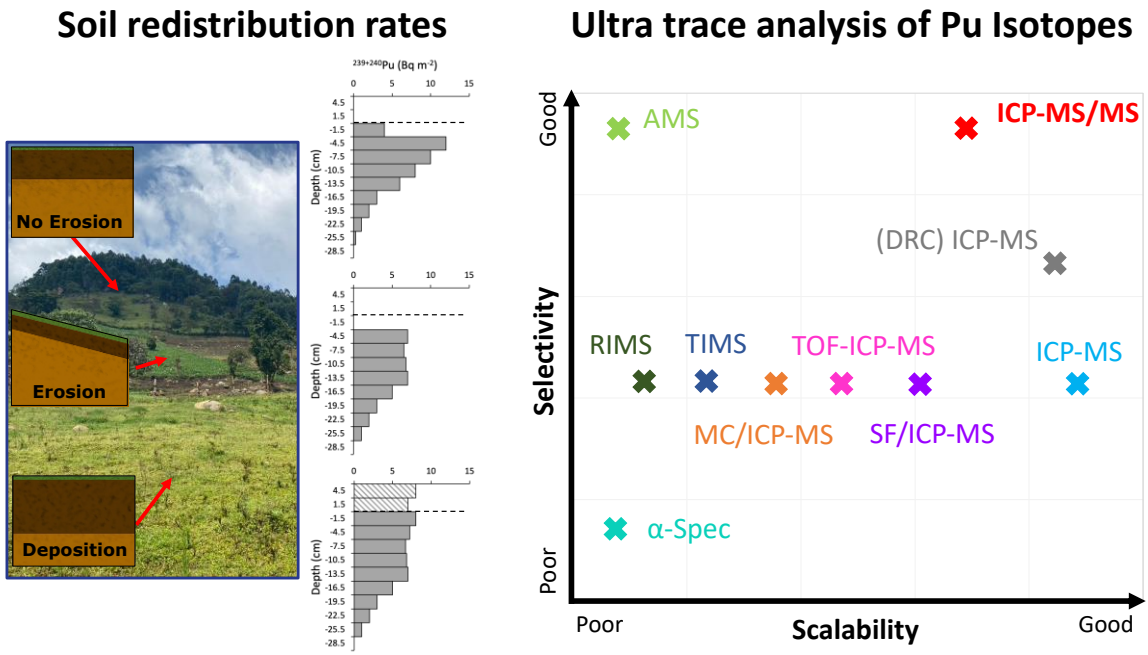

Abstract

The measurement of isotopic abundances and ratio variations of plutonium (Pu) can provide important information about the sources and behaviours of radiogenic isotopes in the environment. The detection of ultra-trace isotopes of Pu is increasing interest in the scientific literature for the determination of soil erosion rates due to their long retention times in the environment. The characteristics of Pu within the environment make it an ideal tracer for the determination of soil redistribution rates and its robustness presents the opportunity to replace more commonly used radioisotopes such as ^{137}Cesium and ^{210}Lead. However, ultra-trace analysis of Pu (fg g^{-1}) presents analytical challenges which must be overcome in a variety of soil types. Inductively Coupled Plasma Mass Spectrometry has proven valuable for detection of Pu in a range of environmental samples. However, severe polyatomic interferences from uranium isotopes significantly limits its application. Due to the improvements in detection sensitivity and reaction cell technology, inductively coupled plasma tandem mass spectrometry, which is also commonly referred to as triple quadrupole inductively coupled plasma tandem mass spectrometry (ICP-MS/MS), has emerged as an exceptional tool for ultra-trace elemental analysis of Pu isotopes in environmental samples overcoming the limitations of standard quadrupole ICP-MS such as limited sensitivity and cost of analysis. In this review, common methods reported in the literature for the separation and subsequent detection of Pu isotopes are compared to recent advances in analysis using ICP-MS/MS technology.

1. Introduction

Plutonium (Pu) is an anthropogenic element, ubiquitous in the environment as a result of fallout from nuclear weapons testing in the 1950s and 60s, nuclear power plant accidents and marine discharges of reprocessing waste [1], [2]. However, distribution of Pu from the latter is more localised, owing to $^{239+240}$Pu being contained within the non-volatile fraction of nuclear fuel debris [3], [4]. A total of 520 atmospheric nuclear weapons tests were conducted worldwide between 1945–1980 [5]. Due to their high radiotoxicity and long retention times, ^{239}Pu and ^{240}Pu isotopes are considered important transuranic nuclides in the environment with half-lives of 24,110 years and 6,561 years, respectively [6], [7]. The geographical distribution of Pu in the environment largely varies due to the spatial distribution of weapons testing as well as post-test global weather patterns. The highest deposition is in the northern hemisphere temperate latitudes [8], as only 10% of the overall tests were conducted in the southern hemisphere [9]. This presents a challenge for the analysis of environmental samples in the tropics due to a much lower fallout compared to the mid-latitudes of the northern hemisphere. This can be seen when comparing Europe with Africa, with Europe's minimum activity per unit area being two times larger than Africa's maximum caused by the high volume of tests in the northern hemisphere in comparison to a much smaller number in the southern hemisphere (*Table 1*). For the African continent, 14 nuclear weapons tests were conducted within the Tanezrouft region of Algeria, of which only four tests were atmospheric [10], [11].

Table 1: Geographical distribution of $^{239+240}$Pu inventories [8]

Continent	**$^{239+240}$Pu range (MBq km^{-2})**
Africa	3.33 – 19.2
South America	4.44 – 22.6
Australia	6.66 – 24.8
Asia	55.5 – 70.3
Europe	40.7 – 115
North America	12.2 – 148

The analysis of long-lived Pu isotopes are applied as tracers in geochemistry, geochronology, nuclear forensics and as part of environmental monitoring to inform decontamination and remediation strategies [2]. The accurate determination of Pu isotopes could be useful for the identification of contamination sources. For example, global atmospheric fallout has a $^{240}Pu/^{239}Pu$ ratio of 0.18 while much lower ratios (0.02 - 0.07) are observed via fallout from historical nuclear weapon testing and much higher ratios (0.30 - 0.41) are observed from releases originating from nuclear power plant accidents and incidents [12]–[15]. Commonly a sum of both the ^{239}Pu and ^{240}Pu isotopes is reported due to the historic use of alpha spectroscopy for their detection. Due to the isotopes similar energies of emission, alpha spectrometry cannot distinguish between the two isotopes [16].

1.1. Environmental analysis

Isotopes of Pu are considered hazardous pollutants in the environment due to their radiological toxicities and long radioactive half-lives, leading to millennial persistence in the environment [4], [5]. Attention has focused on the impact of these radionuclides on the environment and interest in the biogeochemical behaviour of Pu has been increasing, in particular as an environmental tracer to investigate the origin and delivery pathways [17]–[19]. The concentrations of Pu isotopes ($^{239+240}Pu$) in environmental samples are normally very low, $(0.04–400) \times 10^{-16}$ g m^{-3} in the atmosphere, $(10–9000) \times 10^{-16}$ g g^{-1} in soil and sediment, and $(0.5–22) \times 10^{-16}$ g L^{-1} in seawater samples [7]. Since the development of atomic energy from 1940's, nuclear facilities have been established all over the world. With the lifetime of a typical nuclear power plant being between 40 and 60 years, a major concern is the decommissioning of facilities to ensure environmental protection and safety [5]. In order to effectively decommission an area, baseline levels of radionuclides from atmospheric fallout must first be determined within the area close to

the site. The analysis of isotopes ^{238}Pu, ^{239}Pu and ^{240}Pu in a variety of samples matrices is essential to plan decommissioning processes for matrices including concrete, graphite, metals, resin, and filters [19], [20]. Appropriate information for radiological and chemical characterisation is an important factor for legacy waste decommissioning [5].

1.2 Soil redistribution tracer

Fallout radionuclides (FRN) provide an alternative approach to quantify soil erosion, compared to relatively expensive long-term monitoring techniques such as run-off plot testing. Methods using FRN, in contrast to traditional methods, can be performed within a single sampling campaign and can be applied to the calculation of both erosion and deposition rates. Previously FRN tracing has utilised ^{137}Cs and ^{210}Pb, however, Pu isotopes offers a new alternative method which can overcome some of the challenges faced when using both ^{137}Cs and ^{210}Pb [4], [21]. Recent advancements, in the quantification of soil redistribution rates, have employed Pu isotopes to determine rates of soil erosion using $^{239+240}$Pu inventory as a measure of soil redistribution [17], [22]. Due to ^{239}Pu and ^{240}Pu's much longer half-lives, about 99% of original activity still remains in soils, providing stable and long term use for application compared to ^{137}Cs which has a half-life of only 30 years [23], [24]. Approximately 75% of ^{137}Cs has already decayed away since the peak of bomb testing and in the northern hemisphere the high spatial variability of fallout from nuclear power plant accidents, such as Chernobyl, make use of ^{137}Cs as redistribution tracer challenging. More than six times as many atoms of $^{239+240}$Pu were originally dispersed in comparison to ^{137}Cs, but the specific activity of ^{137}Cs exceeds that of the Pu isotopes; this makes the Pu isotope more amenable to detection by atom counting methods such as ICP-MS whereas for ^{137}Cs decay counting by radiometric (gamma) spectrometry is more appropriate [3], [18], [25]–[28].

The use of $^{239+240}$Pu to determine soil erosion has been reported infrequently in the past [29], [30]. However, in 2001 the use of $^{239+240}$Pu as an alternative to ^{137}Cs was investigated at a study site in Scheyern farm, southern Germany [22]. Subsequently, there has been an increasing interest in utilising $^{239+240}$Pu as a tracer for soil erosion shown by the increasing number of publications using Pu isotopes for determining rates of soil erosion [24], [31], [32] (*Table 2*). Due to the increased environmental lifetime and low spatial variability of Pu isotopes compared to ^{137}Cs, there is an increasing potential for Pu isotopes to replace ^{137}Cs in the tropics as a soil erosion tracer [4]. Therefore, this review aims to critically assess the current trends in analytical methodologies employed for the detection of Pu isotopes with the following objectives, (i) identification of common methods reported for the determination of Pu isotopes in environmental samples, and (ii) comparison of these methods to identify the usefulness in terms of the determination of soil redistribution rates.

Table 2: Application of Pu analysis for the determination of soil redistribution rates

Analysis method	Reference	Location	Country
Alpha spectrometry	Schimmack et al., [22]	Scheyern farm	Germany
	Schimmack et al., [33]	Scheyern farm	Germany
AMS	Hoo *et al.*, [31]	Camberra	Australia
	Lal *et al.*, [24]	Northern territory	Australia
	Lal *et al.*, [32]	Daly River	Australia
ICP-MS with a high efficiency ultrasonic nebuliser	Xu *et al.*, [34]	Liaodong Bay	China
	Alewell *et al.*, [17]	The Urseren Valley	Switzerland
	Xu *et al.*, [23]	Liaodong Bay	China
	Zhang *et al.*, [35]	Liaodong Bay	China
	Zollinger et al., [36]	Upper Engadine	Switzerland
	Meusburger *et al.*, [37]	Haean catchment	South Korea
	Meusburger *et al.*, [18]	The Urseren Valley	Switzerland
	Raab et al., [26]	Sila Massif upland	Italy
	Calitri et al., [27]	Uckermark region	Germany
	Musso et al., [38]	Klausenpass	Switzerland
	Wilken et al., [39]	Various	Uganda, Rwanda, DR Congo
	Wilken et al., [40]	Weichselian glacial belt	Germany
	Khodadadi et al., [3]	Zarivar Lake	Iran
ICP-MS/MS	Zhang *et al.*, [28]	Loess Plateau, Qingyang	China
ICP-MS/MS with a high efficiency ultrasonic nebuliser	Portes et al., [25]	Wyoming	America
	Calitri *et al.*, [41]	Uckermark region	Germany

2. Methods for plutonium determination

2.1. Radiochemical separation of plutonium

The accurate determination of trace Pu isotopes requires a high level of enrichment prior to analysis due to their low abundance in environmental samples, which is reliant on atmospheric fallout. Using specialised separation techniques, the Pu isotopes can be both removed from the matrix and interfering substances, and pre-concentrated to ensure maximum sensitivity is achieved [42]. For analysis by α-spectrometry the samples require complete separation of Pu from the matrix to both avoid spectroscopic interferences (^{241}Am on ^{238}Pu) and obtain a thin alpha source for measurement which must not exceed a few micrometres. This is due to the short range of alpha radiation particles resulting in a degradation of the resolution of Pu peaks in the spectrum as distance increases. This review focuses on the separation techniques employed for mass spectrometry techniques and a more detailed explanation of separation for radiometric techniques can be found in Qiao *et al.* [16].

The matrix elements (salt), peak tailing, and hydrides of ^{238}U and other polyatomic ions are the major interferences in the measurement of Pu isotopes using ICP-MS [7]. The mass concentrations of Pu are normally very low in environmental samples, and so to maximise the number of atoms counted, large starting masses/volumes of sample are used to pre-concentrate the Pu in the final measured sample aliquot sample. When analysing solid samples, Pu first needs to be released from the solid sample matrix into solution prior to chemical separation. The first preparation step for Pu separation is to remove the organic matter in the sample as otherwise the Pu may bind to these and disrupt the chromatography. Organic matter in the solid samples is commonly decomposed by dry ashing in muffle furnaces at 400–700 °C for 2–24 h [43], although it should be noted that many published studies do not give details of the ashing temperature.

Prior to extraction, samples are spiked with a low abundance isotope such as ^{242}Pu which can be used as a tracer to calculate recovery following chemical separation and to validate the success of the separation by correction for Pu loss during the analytical process [19], [44], [35]. Concentrated nitric acid is often employed for the extraction of Pu from soil but methods using 8M nitric acid and aqua regia have also been used [23], [42], [46], [47]. An alternative commonly used, is a lithium metaborate fusion for samples containing refractory species of Pu, such as samples which have been collected from highly contaminated sites of nuclear weapons tests and nuclear accidents. These refractory species are not fully dissolved by acid leaching which could lead to underestimation of analytical results [48], [50]. However, despite fusion methods being most effective for the digestion of soil samples containing Pu, drawbacks of the method include that additional interfering elements and matrices can also be decomposed leading to unreliable recovery and practicality of fusing large volumes of sample [6].

Co-precipitation, solvent extraction, ion exchange chromatography, and extraction chromatography are often applied for separation and purification of Pu in environmental samples, especially for removal of U [7]. Among the methods in recent years, ion exchange and extraction chromatography are becoming the most popular technique. These methods are based on anionic complexes of Pu with NO_3^- and Cl^- bonding with the organic functional group within the chromatographic resin [7]. These methods are reliant on Pu existing in the correct oxidation state prior to separation. Since both ion exchange chromatography and extraction chromatography rely on Pu to be in the oxidation state Pu(IV), $NaNO_2$ is frequently employed as a valence adjuster to convert Pu to the tetravalent state with the nitrite ion playing an important role in Pu aqueous processing. It is capable of oxidising Pu(III) to Pu(IV) and of reducing Pu(VI) to Pu(IV).

Often another reducing agent, such as ferrous ion is also added to increase the rate of the reaction because the Pu(VI) to Pu(IV) reduction by nitrite is slow [16]. An additional step widely reported to increase the rate of reaction, was the conversion of Pu species to Pu(III) using a reducing agent such as $K_2S_2O_5$ prior to the addition of $NaNO_2$ [51], [52]. Co-precipitation with reagents such as Ca, Bi or Fe can be used to reduce the effects of matrix elements on Pu in the sample prior to chromatographic separation [48]. This is often useful for analysis of low mass samples (~1g) to preconcentrate Pu, but is not practical for larger mass soils (e.g., > 50g) owing to the use of additional chemicals and time-consuming steps.

Nygren *et al*. [49] investigated the separation of Pu from soil and sediment using different chromatographic methods and found that the TEVA resin (Eichrom Technologies) showed the highest yield of Pu. The potential of this method was further realised when incorporated into a full analytical protocol using ICP-MS by Ketterer *et al.* [53], [54]. With > 80 citations in google scholar, this paper has become pivotal in the literature, with TEVA resins widely adopted as the standard separation method for Pu isotope measurements for the majority of analytical techniques. This can be attributed to relatively low uranium content within the TEVA resin and relatively large differences in the nitric acid dependency factors of k' (k' = distribution coefficient between resin and solution) [55]. The TEVA-resin is based on an aliphatic (R = C8 and C10) quaternary ammonium salt as extractant [49]. To maximise decontamination factors of U isotopes multi-step separations can be used with a combination of resins. Examples of this include Varga *et al.* [56] where a UTEVA column was used in tandem with a TRU resin, Metzger *et al.* [57] used a TEVA column in tandem with UTEVA and Puzas *et al.* [58] using an AG1-x8 followed by a UTEVA column in tandem with TRU. Through the use of these

separation techniques, decontamination factors of U isotopes with respect to Pu of up to 10^7 have been achieved [7].

2.2. Radiometric method for measurement of plutonium

The determination of Pu isotopes in samples can be achieved in two fundamentally different ways either using: (i) decay counting (radiometric techniques) or (ii) atom counting methods (mass spectroscopy techniques). Alpha spectrometry is the most used radiometric technique for the determination of isotopes ^{238}Pu, $^{239+240}$Pu, ^{242}Pu and ^{244}Pu. However, α-spectrometry is unable to distinguish between isotopes with similar energy of emission due to the limited energy resolution of alpha detectors (*Table 3*) [16]. As a result $^{239+240}$Pu isotopes are reported as a sum of activities and the method is also unable to distinguish between ^{238}Pu and interfering isotope ^{241}Am [59]. In addition, α-spectroscopy detection of long-lived ^{242}Pu and ^{244}Pu isotopes in environmental samples is challenging due to their ultra-trace level concentrations in the environment and their low specific activity [60].

A typical detection limit of α-spectrometry is in the order 10^{-4} Bq (0.05pg) ^{239}Pu [16], [48], [59], [61]. The low cost of instrumentation, high selectivity for alpha particles and high sensitivity resulting from a low background signal make this method attractive for the measurement of Pu isotopes in environmental samples [60]. Although α-spectrometry has these advantages it is a detection technique which requires very long counting times (1-30 days) and due to the short range of alpha radiation particles and increased thickness may result in a degradation of the resolution of Pu peaks in the spectrum [61]. This means that α-spectrometry detection is not a suitable method for emergency situations where results are required within a short timeframe or large-scale environmental surveys.

The ^{241}Pu isotope has a principal decay mode via a beta emission meaning that traditionally it has been determined directly by liquid scintillation counting (LSC). It can also be measured indirectly by α-spectrometry to determine the in-grown daughter ^{241}Am activity [20]. Both methods require a pre-concentration and separation step to allow for analysis and long counting times are required to achieve sufficient counts for an acceptable precision. One of the main challenges of the LSC method is the accurate determination of the counting efficiency which can vary between 30 - 43%, depending on the spectral quench parameter of the external standard and accounting for these low efficiencies is a challenge [62]. Although initial fallout of ^{241}Pu was high, this isotope is not applicable for use as a soil erosion tracer due to its short half-life and limited environmental lifetime [20].

Table 3: Nuclear properties of Pu isotopes [16], [63]. *Note all decays also produce gamma emission but their intensities are too low to be used analytically for environmental samples.*

Nuclide	Half-life (yr)	Decay mode	Specific activity (Bq g^{-1})	Energy of emission (MeV)
^{238}Pu	87.7	α	6.34 x 10^{11}	5.59
^{239}Pu	24100	α	2.30 x 10^{9}	5.16
^{240}Pu	6561	α	8.40 x 10^{9}	5.17
^{241}Pu	14.3	β	3.82 x 10^{12}	20.8* (KeV)
^{242}Pu	3.73 x 10^{5}	α	1.46 x 10^{8}	4.85
^{244}Pu	8.08 x 10^{7}	α	6.71 x 10^{5}	4.59

2.3. Mass spectrometry techniques

2.3.1. Accelerator mass spectrometry

The mass spectrometry technique traditionally used for $^{239+240}$Pu measurements in environmental samples is Accelerator Mass Spectrometry (AMS). The instrumental effort is much higher for AMS than for α-spectrometry, but the much increased sensitivity and ability to distinguish between the isotopes ^{239}Pu and ^{240}Pu has in the past made AMS an attractive option for Pu analysis and may be viewed as the "gold standard" technique [59]. The main limitation when using the AMS method to analyse Pu isotopes is the poor

availability of specialist facilities where beam time must be applied for to access the facilities and the relatively high cost of using these facilities [34]. However, despite these limitations AMS can achieve very high levels of sensitivity and the method stands out with setting detection limits as low as 0.001mBq for ^{239}Pu regardless of the matrix components of the sample, which is between 10-100 times better than detection limits achieved using alpha spectrometry [4], [59], [64]–[67]. This is possible due to the elimination of molecular isobars in the stripping process, which occurs in the terminal of an electrostatic tandem accelerator [66]. Another benefit of this stripping process is that the levels of U purification prior to analysis are lower than other MS techniques, allowing for the simplification of the radiochemical procedures prior to analysis [67].

2.3.2. Thermal Ionisation Mass Spectrometry and Resonance Ionisation Mass Spectrometry

In addition to AMS there are also some alternative mass spectroscopy techniques that are highly sensitive for the detection of Pu isotopes including Thermal Ionisation Mass Spectrometry (TIMS) and Resonance Ionisation Mass Spectrometry (RIMS). The TIMS method has a higher sensitivity for ^{239}Pu and ^{240}Pu than ICP-MS and interferences due to UH and UH_2 are less significant. This means that TIMS has become the method of choice for measuring isotope ratios with precision as low as 0.002% [68]. However, TIMS is limited by the relatively high cost of analytical facilities and the extensive sample preparation prior to analysis to produce a thin filament source, taking days to weeks of dissolution and separation steps [54]. The method used in RIMS, employs tuned laser beams for the selective excitation of the Pu atoms. It is both highly sensitive and selective for the measurement of ^{239}Pu with detection of ^{239}Pu activities as low as 100 atoms per

sample, equivalent to of 0.1 nBq. This method however, is only available at specialist laboratories worldwide [4].

2.3.3. Inductively Coupled Plasma Mass Spectrometry

An alternative to mass spectrometry methods described above is Inductively Coupled Plasma Mass Spectrometry (ICP-MS). This method has grown in popularity over the past 10 years which is shown by the increasing number of publications using the method and it has become a widely used technique for the detection of Pu isotopes due to its high sensitivity, short analytical times, and relatively simple operation. However, the method can be hindered by the formation of interferences due to polyatomic species, formed from matrix elements and plasma gases. These polyatomic interferences require removal as they have the same integer mass-to-charge ratios as the analyte of interest, leading to false detection or overestimation of results [14], [69]. For Pu isotopes, the major interfering ions are a consequence of the presence of ^{238}U which is ubiquitous in the environment. Uranium hydrides $^{238}UH^+$ and $^{238}UH_2^+$ cannot be resolved from $^{239}Pu^+$ and $^{240}Pu^+$ making analysis of these isotopes a challenge [66]. With the concentration of ^{238}U in environmental samples being up to 6-9 orders of magnitude higher than that of Pu, another issue for the analysis of ^{239}Pu as a result, in quadrupole ICP-MS is the peak tailing from ^{238}U [70]. Therefore, low-resolution ICP-MS cannot always reliably determine ^{239}Pu, relying heavily on the chemical purification steps prior to analysis, which are used to remove U isotopes from the matrix [71]. However, these procedures also bring additional U into the final sample solutions through atmospheric contamination of the glassware, and reagents [72]. There are also other minor polyatomic interferences which need to be taken into consideration such as plasma gas induced Hg and Pb interferences (*Table 4*).

Table 4: Polyatomic interferences for Pu isotopes using ICP-MS [6], [46], [73]

Isotope	Polyatomic interference
^{238}Pu	$^{198}Pt^{40}Ar^{+}$, $^{201}Hg^{37}Cl^{+}$, $^{198}Hg^{40}Ar^{+}$, $^{202}Hg^{36}Ar^{+}$, $^{205}Tl^{16}O_2{}^{1}H^{+}$, $^{203}Tl^{35}Cl^{+}$, $^{208}Pb^{14}N^{16}O^{+}$, $^{207}Pb^{14}N^{16}O^{1}H^{+}$, $^{206}Pb^{16}O_2{}^{+}$
^{239}Pu	$^{206}Pb^{33}S^{+}$, $^{207}Pb^{16}O_2{}^{+}$, $^{208}Pb^{31}P^{+}$, $^{205}Tl^{34}S^{+}$, $^{203}Tl^{36}Ar^{+}$, $^{202}Hg^{37}Cl^{+}$, $^{199}Hg^{40}Ar^{+}$, $^{203}Tl^{36}Ar^{+}$,$^{204}Pb^{35}Cl^{+}$,$^{177}Hf^{14}N^{16}O_3{}^{+}$, $^{176}Hf^{14}N^{16}O_3{}^{1}H^{+}$,$^{191}Ir^{16}O_3{}^{+}$, $^{193}Ir^{14}N^{16}O_2{}^{+}$, $^{198}Pt^{40}Ar^{1}H^{+}$, $^{208}Pb^{14}N^{16}O^{1}H^{+}$, $^{209}Bi^{14}N^{16}O^{+}$
^{240}Pu	$^{204}Pb^{36}Ar^{+}$, $^{206}Pb^{34}S^{+}$, $^{207}Pb^{33}S^{+}$, $^{208}Pb^{32}S^{+}$, $^{205}Tl^{35}Cl^{+}$, $^{203}Tl^{37}Cl^{+}$, $^{205}Hg^{35}Cl^{+}$ $^{200}Hg^{40}Ar^{+}$,$^{208}Pb^{16}O_2{}^{+}$,$^{178}Hf^{14}N^{16}O_3{}^{+}$, $^{177}Hf^{14}N^{16}O_3{}^{1}H^{+}$, $^{191}Ir^{16}O_3{}^{1}H^{+}$, $^{193}Ir^{14}N^{16}O_2{}^{1}H^{+}$, $^{194}Pt^{14}N^{16}O_2{}^{+}$, $^{207}Pb^{16}O_2{}^{1}H^{+}$, $^{209}Bi^{14}N^{16}O^{1}H^{+}$

2.3.4. Dynamic Reaction Cell / Collision Reaction Cell - Inductively Coupled Plasma Mass Spectrometry

Some studies have focused on the use of dynamic reaction cell (DRC) or collision reaction cell (CRC) ICP-MS to eliminate the UH^{+} interference. The different reactivities of Pu and U with specific gases provide a promising way for the spectro-chemical resolution of $^{238}Pu^{+}$ from isobaric $^{238}U^{+}$ and polyatomic interference i.e. UH^{+} in ICP-MS [70]. Through the introduction of He gas it was reported that the sensitivity of Pu isotopes could be enhanced by about three times, however, the signal of UH species is also enhanced, making it an unsuitable gas to use within the reaction cell [7]. Vais et al. [74] found that the $^{238}UH^{+}$ signal interfering with ^{239}Pu could be reduced by 10 orders of magnitude by using NH_3 gas while the Pu signal was only reduced slightly [74]. Tanner et al. [75] and Gourgiotis et al. [76] investigated the use of CO_2 gas for the reduction of interference, finding that the reaction efficiency of UH^{+} was significantly higher than that of Pu^{+}; ultimately reducing the interference. The different reactivity observed for U and Pu towards CO_2 gas is linked to the need to promote the ground-state ions to a reactive configuration with the Pu^{+} ion requiring a greater energy to promote the electron during reaction (1.08eV) compared to U^{+} (0.04eV) [75], [76].

2.3.5. Inductively Coupled Plasma Tandem Mass Spectrometry

An emerging technique for the analysis of Pu isotopes is ICP-MS/MS which is also commonly referred to as triple quadrupole ICP-MS (ICP-QQQ-MS). The method has gained popularity over recent years due to the method's achievable low detection limits and ability to remove interferences using collision cell technology (*Table 5*). This advancement in interference removal efficiency has led to more applications in nuclear materials analysis and other complementary radiometric techniques [70]. The additional quadrupole mass filter located in the front of the collision-reaction cell allows the pre-selection of species, which prevents the formation of secondary polyatomic interference and improves the efficiency of the cell chemistry in the collision cell (*Figure 1*) [73], [77]. Using a second quadrupole peak tailing will be reduced which in turn has the advantage of improving the mass resolution reducing effects of peak tailing. Ammonia (NH_3), carbon dioxide (CO_2) and oxygen gas (O_2) are among the different reaction gases proposed for the removal of UH^+ and UH_2^+ interferences by ICP-MS/MS [6], [7], [78], [79].

The reaction of U^+ and UH^+ interferences within the reaction cell of the ICP-MS/MS with NH_3, work effectively to mass shift interferences away from the Pu isotopes. This is possible as a result of Pu isotopes not reacting with the gas and therefore remaining at the original m/z ratio while U^+ and UH^+ are shifted to a higher ratio [7].

$$U^+ + NH_3 \rightarrow U(NH_m)_n{}^+$$

$$UH^+ + NH_3 \rightarrow UH(NH_m)_n{}^+$$

(m/n = 1-2)

Xu *et al*. [79] reported that both the U^+ and UH^+ interferences were effectively eliminated using 0.4 ml min^{-1} NH_3 as a reaction gas and 6.4 ml min^{-1} He, reducing the overall interference to $<2.4 \times 10^{-7}$. In addition, Pu sensitivity was increased by the collisional

focusing effect of He gas to a sensitivity of 13,900 Mcps (mg L^{-1})$^{-1}$. Despite the ability of NH_3 to react with the U interference, the use of NH_3 gas poses several safety concerns, including its potential corrosive nature, requiring mitigation for its use in a laboratory that could be prohibitively costly [80]. In addition, the ratio of UH^+/U^+, although significantly reduced, is not sufficient to meet the needs of measurement of ultra-low-level Pu in samples containing comparatively higher U concentrations [77].

Another commonly used gas is CO_2 which has been successfully used to eliminate UH^+ interference by converting hydrides within the sample to oxides, while keeping the intensity of the Pu signal. Both the tailing effect of ^{238}U on abundance sensitivity and the polyatomic interference UH^+ are eliminated, reducing the overall interference of uranium to three orders of magnitude better than conventional ICP-MS [7].

$$U^+ + CO_2 \rightarrow UO_n{}^+$$

$$UH^+ + CO_2 \rightarrow UO_n{}^+$$

(n = 1-2)

Hou *et al*. [7] reported that the optimal conditions to eliminate U interferences was 1.2 ml min^{-1} CO_2 and 8 ml min^{-1} He, which reduced overall interference on ^{239}Pu to <1 x10^{-8}. However, it was reported that although this high flow rate is optimal for the removal of interfering ions, increasing flow rates above 1.2ml min^{-1} of CO_2 results in declining intensity of PuO^+ signal. This was attributed to the increased production of $PuO_2{}^+$ within the collision cell [7]. Similar results were reported by Childs *et al*. [77] where significant U interferences were observed when comparing a U spiked Pu standard with an un-spiked standard; therefore it was deemed that Pu quantification was not possible using high flow rates of CO_2 [77]. As the m/z ratio for $PuO_2{}^+$ >271 is beyond the mass range for older ICP-MS/MS instruments, the loss of Pu signal measured at the Pu^+ mass rather than shifted to an oxide form can have a negative impact on the measurement sensitivity. User

requirements, particularly the nuclear industry, for analysing heavy elements in mass shift modes has meant that new instruments such as the Agilent 8900 have an extended m/z detection range up to 275, allowing for the detection of the mass shifted Pu isotope [73]. This highlights a need for manufacturers to extend the m/z range in future instruments to improve reaction cell chemistry and therefore allow for greater research into elements with complex interferences, further reducing detection limits and increasing sensitivity.

In addition to NH_3 and CO_2, O_2 has also been used as a reaction gas with the Pu^+ ion readily converted to both PuO^+ and PuO_2^+ [73]. Of these two ions the favoured one for analysis is PuO_2^+ as it is subject to lesser interference than PuO^+ which experiences dominant interference from uranium oxides, $^{238}U^{16}O^+$, $^{238}U^{16}O^1H^+$ and $^{238}U^{16}O^1H_2^+$ for the measurement of $^{239}Pu^{16}O^+$ and $^{240}Pu^{16}O^+$ ions, causing a less efficient elimination of the uranium interference [7].

$$U^+ + O_2 \rightarrow UO_n^+$$

$$UH^+ + O_2 \rightarrow UO_n^+$$

(n = 1-2)

Zhang *et al*. [28] found that both $^{238}U^+$ and $^{238}U^1H^+$ preferably reacted with O_2 to form $^{238}U^{16}O_2^+$ and therefore the interference was significantly reduced. The optimal conditions in order to observe maximal sensitivity of $^{242}Pu^+$ (880 Mcps (mg L^{-1})$^{-1}$) at m/z 274 (PuO_2^+) was obtained using 0.09 ml min^{-1} O_2 as a reaction gas and 12 ml min^{-1} He [73]. The Pu^+ signal decreases exponentially by more than 600 times when using O_2/He gas mode as opposed to He only mode and this can be attributed to the formation of PuO_2^+ when subjected to relatively high O_2 levels in the reaction cell. The use of this reaction gas is however limited to detectors with m/z reaching > 271. The reaction mechanism for

the removal of uranium interferences can be seen in *Figure 1*. It should be noted that there may still be some tailing of the $^{238}U^{16}O_2^+$ on to $^{239}Pu^{16}O_2^+$.

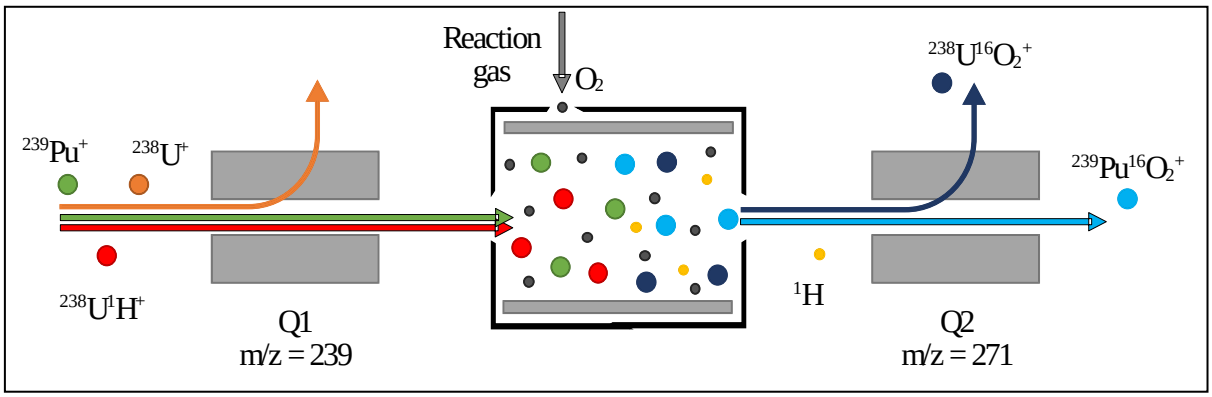

Figure 1: Reaction mechanism of O_2 gas using ICP-MS/MS and m/z of 239 and 271

Table 5 summarises the detection limits achieved for ICP-MS/MS analysis using reaction gasses. With older ICP-MS/MS instruments being limited to detect m/z ratios no greater than >271 one of the most commonly used reaction gases reported in ICP-MS/MS has been NH_3. However, with the need for safe gas handling due to the corrosive nature of NH3 and the availability of quadrupole systems capable of >271 amu, alternative methods are beginning to be favoured. With recent advancements in ICP-MS/MS technology allowing for m/z ratios >271 to be detected, oxygen gas presents an exciting development in the detection of Pu isotopes in the presence of U in samples with detection limits exceeding that of NH_3 and CO_2.

Table 5: Method Detection limits of ^{239}Pu and ^{240}Pu reported in the literature using different gas modes with ICP-MS/MS.

Reference	Sample introduction system	Instrument	Gas mode	Detection limit (fg g^{-1})	
				^{239}Pu	^{240}Pu
Xing *et al*. [42]	None	Agilent 8800	NH_3	0.55	0.09
Xing *et al*. [6]	None	Agilent 8800	NH_3	0.55	0.09
Bu *et al*. [47]	APEX-Ω	Agilent 8900	NH_3	0.30	0.20
Xu *et al*. [79]	APEX-Ω	Agilent 8900	NH_3	0.16	0.05
Hou *et al*. [7]	None	Agilent 8800	CO_2	0.11	0.07
Zhang *et al*. [73]	None	Agilent 8900	O_2	0.06	0.06

2.3.6. Sector field Inductively Coupled Plasma Mass Spectrometry

Limitations in the mass resolution of quadrupole ICP-MS has led to the development of high-resolution mass spectrometers. Sector field ICP-MS (SF-ICP-MS) which is based on the magnetic field approach and uses double focusing, to improve the mass resolution of ion peaks [81], [82]. This is achieved using an electrostatic analyser (ESA) before or after the magnetic field before passing the sample through an exit slit to filter the isotopes. Consequently, compared to a quadrupole system either an improvement in selectivity in high resolution mode or an improvement in the sensitivity as well as a reduction of the noise level can be achieved in low resolution mode (similar to quadrupole); this results in low achievable detection limits in the pg kg^{-1} range [83]–[85]. Another advantage of SF-ICP-MS over traditional ICP-MS is the ability to measure the signals on flat-topped peaks at lower resolutions. This offers an improvement in the measurement of isotope ratio precision over quadrupole based ICP-MS; however, it is important to note that precision is reduced with increasing resolution due to the deterioration of peak shape and is still poorer than that of MC-ICP-MS, where true simultaneous ratio measurements are made. Similarly to traditional quadrupole ICP-MS, SF-ICP-MS requires a high level of decontamination prior to analysis to remove interferences from UH^+ as even high

resolution mode is insufficient to fully remove this interference [86], [87]. This alongside the relatively higher cost of instrumentation and subsequently less common availability, make SF-ICP-MS a less attractive method for the determination of Pu in soil erosion studies. However, SF-ICP-MS is an more appropriate option in cases where a higher degree of specificity is required (e.g. forensic identification of Pu source using isotope ratios) compared to the requirement for soil erosion studies [83], [88].

2.3.7. Multi collector Inductively Coupled Plasma Mass Spectrometry

Multi-collector ICP-MS (MC-ICP-MS) is based on the simultaneous detection of isotopes, eliminating classical sources of uncertainty from the sequential scanning used in ICP-MS [89]. Typically, MC-ICP-MS instruments will have up to nine faraday cages making up the detection assembly and newer instruments make use of ion counting systems to improve the abundance selectivity. Therefore, MC-ICP-MS can be used for measuring isotope compositions with both high precision and accuracy, and has the advantage of a high ionisation efficiency in comparison to the TIMS, allowing for a larger theoretical mass range of isotopes to be measured [81]. Similarly, to SF-ICP-MS, this analysis method has a requirement for the removal of UH^+ via extensive separation prior to analysis and one of the challenges which must be overcome using MC-ICP-MS is the limited 'practical' mass range – needing repeat analyses to cover broad mass range, hence longer analysis time compared to ICP-MS/MS, limiting sample throughput. A consequence of this is the need to select an internal standard which falls into the mass range which is usually limited between 10 and 30% [90], [91]. Similarly to the SF-ICP-MS instrumentation, MC-ICP-MS is relatively more expensive than ICP-MS/MS, therefore with less availability and slower sample throughput is not suitable to soil erosion studies which need quick analysis of large quantity of samples.

2.3.8. Time of flight Inductively Coupled Plasma Mass Spectrometry

An alternative analysis method is time of flight ICP-MS (ICP-TOF-MS). This technique pushes a packet of sample ions from the ICP into a ion flight tube, accelerates them and then separates the ions of different mass to charge ratio by their drift time [92]. Counting of the ions proceeds in a temporal succession on a microsecond time scale and because the packet of ions was sampled at the same time from the ICP this method of detection is essentially simultaneous [93]. This gives it an advantage of requiring a low sample volume and quick analysis time. However, prior to analysis a high degree of separation is required, and selectivity is similar to that of traditional quadrupole ICP-MS. Although this method does not offer advantages over ICP-MS/MS in terms of analysis for the purpose of soil erosion measurement, it does have a high potential to be used alongside laser ablation for high resolution analysis of impurities in nuclear fuels, nanomaterials and biological matrices [94]–[97].

3. Discussion

This review summarised the advancements of Pu isotope analysis over the past 20 years, by identifying common methods reported for the determination of Pu isotopes in environmental samples and comparing these methods for their respective advantages for the measurement of soil redistribution rates. A future challenge which must be addressed is the need for ultra-trace analysis of Pu isotopes in soils, so that Pu can be used as an effective tool for the quantification of soil erosion in areas where global fallout is minimal (tropics). Wilken *et al*. [39] demonstrated the applicability of using $^{239+240}$Pu in tropical Africa for the determination of soil erosion for study sites along the East African Rift Valley system. Despite lower global fallout in the tropics, a relatively high $^{239+240}$Pu baseline inventory was found at the reference sites. Cultivated sites showed signs of substantial soil erosion and sedimentation that exceeded 40 cm over 55 years. However, half of the slope sites at the cropland site in DR Congo fell below the detection limit of

ICP-MS analysis, which makes the drawing of conclusions from data generated by traditional techniques very difficult if not impossible. This challenge could be addressed using ICP-MS/MS, through which the removal of UH^+ interferences greater selectivity can be achieved (*Table 4*). The observation of extensive soil erosion, yet inability to determine measurable quantities of Pu emphasised the value of Pu isotopes measured by ICP-MS/MS to study the impact of erosion in tropical Africa where the baseline Pu signal is likely to relatively much lower than in other global regions. With the advancements of Pu analysis using reaction cell technology, analysis challenges such as limited sensitivity and cost of analysis associated with traditional methods of analysis can be overcome. The improved detection limits using ICP-MS/MS can be seen in *Table 6* and the use of Pu isotopes to determine soil redistribution rates in challenging environments (low signal), increasing its viability for use in geochemical surveys associated with soil erosion studies.

Both radiometric and mass spectrometry techniques require extensive and time-consuming sample preparation steps prior to analysis which consist of the digestion of soil samples and radiochemical separation from the matrix elements. Radiometric measurements using both alpha-particle spectrometry and LSC are simple and cost-effective techniques for the determination of ^{238}Pu, $^{239+240}Pu$ and ^{241}Pu. However, these methods do not have the ability to detect isotopes ^{239}Pu and ^{240}Pu individually. In addition, they require relatively long counting times compared to mass spectrometry methods for accurate quantification of Pu at environmental levels summarised in *Table 6*. Not all of the papers in Table 6 provided sufficient details to provide an in-depth comparison between methods, with many papers missing crucial details about operating conditions. An ideal format for the comparison of methods and to guide future studies would follow the presentation of experimental details by Kazi *et al.* [98] and Wang *et al.* [99]. In contrast, mass spectroscopy techniques can provide shorter analysis times and are highly

sensitive with detection limits as low as 10^{-3} mBq g^{-1}. Furthermore, these methods have the capability to provide individual isotopic concentrations of ^{239}Pu and ^{240}Pu. However, the availability and cost of some mass spectroscopy techniques is a limiting factor. In some cases depending on the intended purpose of the analysis a combination of both radiometric and mass spectroscopy techniques may be used [16]. Although AMS can be considered the gold standard for ICP-MS analysis, the cost of instrumentation set up (approximately $4 million for the set-up of each facility) and therefore availability of analytical facilities is a major limiting factor, making this method for the determination of Pu in environmental samples unattractive. Alternative mass spectrometric techniques such as SF-ICP-MS and MC-ICP-MS, have the advantage of increased resolution for the determination of isotopic ratios compared to traditional quadrupole ICP-MS, however, they require a comparable level of decontamination prior to analysis to remove interferences from UH^+. This challenge can be overcome using reaction cell technology via developments in recent years of ICP-MS/MS to selectively mass shift interferences during analysis, taking advantage of the high throughput capabilities of this instrumentation over other instruments, enabling its broader application to survey scale studies on soil

Table 6: Comparison of analytical techniques for the determination of Pu activity concentrations

Detection method	Reference	Sample introduction technique	Instrument	Detection limit (mBq)	Detection limit (Bq kg^{-1})	Mass of sample (g)	Pu recovery (%)	Analysis time (s)
α-spectrometry	[59]		Ortec	0.40		2.5 - 6		4.0×10^4
	[98]		Ortec Spectrum Master 920-8	0.20		1 – 10	95.5 ± 4.6	7.2×10^3 – 3.6×10^5
	[100]		Alpha Analyst		0.01	50	87.6	
	[101]		Canberra	2.95×10^3				3.65×10^3
	[48]		Ortec	0.31		20	84	1.73×10^5
LSC	[102]		Wallac 1220 Quantulus		0.73	20	75 – 80	1.44×10^4
	[103]		Tri-Carb 3180TR/SL		6×10^{-3}	5×10^3	80 - 95	3600
	[104]		PERALS Model 8100AB		6.5×10^3	2	84 ± 7.2	250
AMS	[65]		Australian National University	4.5×10^{-7}				
	[105]		Compact AMS system TANDY at ETH Zurich	8.74×10^{-7}				3600
	[106]		Centro Nacional de Aceleradores	0.05			60 - 90	30

Detection method	Reference	Sample introduction technique	Instrument	Detection limit (mBq)	Detection limit (Bq kg^{-1})	Mass of sample (g)	Pu recovery (%)	Analysis time (s)
AMS	[98]		Isotrace Laboratory	0.11		1 – 10	95.5 ± 4.6	
	[66]		CNA		0.013		70 – 88	
TIMS	[107]				5×10^{-4}	1–20	75 - 90	
	[108]		Triton, Thermo Fisher Scientific	1.38×10^{-8}		1×10^{-12}		
ICP-MS	[74]		ELAN DRC II Perkin-Elmer		0.16			
	[75]		ELAN DRC II Perkin-Elmer		1.38			
	[109]	APEX-Ω	ELAN5000		9.2		70 – 100	660
	[110]	APEX-Ω	ELAN-DRCII, PerkinElmer		6.67	10	87–102	
	[52]		X SeriesII Ther mo Fisher Scientific		2.76	1–20	90	
ICP-MS/MS	[48]		Agilent 8800	0.08		5		
	[42]		Agilent 8800		1.3	1 - 20	80 – 90	
	[5]		Agilent 8800		0.25		70 – 85	300
	[6]		Agilent 8800		1.3	10		

Detection method	Reference	Sample introduction technique	Instrument	Detection limit (mBq)	Detection limit (Bq kg^{-1})	Mass of sample (g)	Pu recovery (%)	Analysis time (s)
ICP-MS/MS	[70]	APEX-Ω	Agilent 8900		0.69		80	120
	[73]		Agilent 8900		0.14			
	[79]	APEX-Ω	Agilent 8900		0.37	1 - 2		
SF-ICP-MS	[61]	Aridus	ELEMENT		0.30			
	[111]		Element 1 Finnigan-MAT		3.91			
	[84]	APEX-Ω	Finnigan Element 2 Bremen		0.32	0.03 – 0.5		150
	[83]		PlasmaTrace 2 Micromass		0.018			
	[85]	APEX-Ω	Axiom SC VG Elemental		0.23			
	[99]	APEX-Ω	Element XR, Thermo Scientific		0.015	1	80	130
MC-ICP-MS	[91]	MCN 6000 CETAC	IsoProbe Micromass		9.2			
	[90]	APEX-Ω	NEPTUNE Thermo Fisher		0.046	2		
	[112]	Aridus II	NU Instruments		0.023			

2

redistribution rates. Although not reported in the literature at this point in time, exciting developments in the field of analytical chemistry using reaction cell technology paired with high resolution SF-ICP-MS and MC-ICP-MS show promise for the future detection of isotopic ratios. However, for the purpose of soil erosion studies the additional costs associated with the setup of these analysis methods and the surplus ability to determine accurate ratios to the requirement of soil erosion measurement, makes it unlikely these methods will be used for this purpose in the future.

4. Conclusion

The development of ICP-MS/MS has opened many novel fields of research involving the analysis of Pu isotopes in soils where ultra-trace detection is required, including as a soil erosion tracer. The developments of reaction cell technology clearly demonstrates that ICP-MS/MS can be a routine tool to support Pu analysis in areas of research such as nuclear decommissioning and soil erosion tracing. The advantages that ICP-MS/MS analysis can offer relative to other instrumentation is the increased rate of analysis and subsequent lower costs per sample, meaning that the method has better availability and can be deployed for survey scale research. However, to improve the detection limits of Pu isotopes, developments in mass spectroscopy measurements using oxygen as the reaction gas are necessary in order to detect high end m/z ratios (>271) to further enhance the selectivity for Pu through removal of polyatomic interferences. Additionally, there is a need to refine the separation process prior to analysis to allow for the effective pre-concentration of ultra-trace Pu. This has the potential to increase Pu's applicability to be used as a soil redistribution tracer in challenging environments, such as tropical Africa, where Pu concentrations will be present in soils at ultra-trace levels. This data has the potential to inform land management practices via the better understanding of the rate of soil losses in the tropics.

Declarations

The authors declare that there is no financial/personal interest or belief that could affect their objectivity.

Acknowledgements

This work is published with the permission of the Executive Director, British Geological Survey. This work has originated from research conducted with the financial support of the following funders: BGS-NERC grant NE/R000069/1 entitled 'Geoscience for Sustainable Futures' and BGS Centre for Environmental Geochemistry programmes for financial support, the NERC National Capability International Geoscience programme entitled 'Geoscience to tackle global environmental challenges' (NE/X006255/1). In addition, The Royal Society international collaboration awards 2019 grant ICA/R1/191077 entitled 'Dynamics of environmental geochemistry and health in a lake wide basin', Natural Environment Research Councils ARIES Doctoral Training Partnership (grant number NE/S007334/1) and the British Geological Survey University Funding Initiative (GA/19S/017). Additional support provided from the British Academy Early Career Researchers Writing Skills Workshop (WW21100104). The authors would like to thank Drs' Andrew Marriott for checking of the manuscript.

References

[1] Hu QH, Weng JQ, Wang JS (2010) Sources of anthropogenic radionuclides in the environment: a review. J. Environ. Radioact 101:426–437 DOI: 10.1016/j.jenvrad.2008.08.004

[2] Goldstein SJ, Price AA, Hinrichs KA, Lamont SP, Nunn AJ, Amato RS, Cardon AM, Gurganus DW (2021) High-precision measurement of U-Pu-Np-Am concentrations and isotope ratios in environmental reference materials by mass spectrometry. J. Environ. Radioact 237:106689 DOI: 10.1016/j.jenvrad.2021.106689

[3] Khodadadi M, Alewell C, Mirzaei M, Ehssan-Malahat EE, Asadzadeh F, Strauss P, Meusburger K (2021) Deforestation effects on soil erosion rates and soil physicochemical properties in Iran: a case study of using fallout radionuclides in a Chernobyl contaminated area. SoilD (Preprint) DOI:10.5194/soil-2021-2

[4] Alewell C, Pitois A, Meusburger K, Ketterer M, Mabit L (2017) 239 + 240Pu from 'contaminant' to soil erosion tracer: Where do we stand?. Earth-Science Rev 172:107–123 DOI:10.1016/j.earscirev.2017.07.009

[5] Hou X (2019) Radioanalysis of ultra-low level radionuclides for environmental tracer studies and decommissioning of nuclear facilities. J. Radioanal. Nucl. Chem 322:1217–1245 DOI:10.1007/s10967-019-06908-9

[6] Xing S, Luo M, Yuan N, Liu D, Yang Y, Dai X, Zhang W, Chen N (2021) Accurate determination of plutonium in soil by tandem quadrupole icp-ms with different sample preparation methods. At. Spectrosc., 42:62–70 DOI:10.46770/AS.2021.011

[7] Hou X, Zhang W, Wang Y (2019) Determination of Femtogram-Level Plutonium Isotopes in Environmental and Forensic Samples with High-Level Uranium Using Chemical Separation and ICP-MS/MS Measurement. Anal. Chem 91:11553–11561 DOI:10.1021/acs.analchem.9b01347

[8] Hardy EP, Krey PW, Volchok HL (1973) Global inventory and distribution of fallout plutonium. Nature 241:444–445 DOI:10.1038/241444a0

[9] Thakur P, Khaing H, Salminen-Paatero S (2017) Plutonium in the atmosphere: A global perspective. . J. Environ. Radioact, 175–176:39–51 DOI:10.1016/j.jenvrad.2017.04.008

[10] Danesi PR, Moreno J, Makarewicz M, Louvat D (2008) Residual radionuclide concentrations and estimated radiation doses at the former French nuclear weapons test sites in Algeria. Appl. Radiat. Isot 66:1671–1674 DOI:10.1016/j.apradiso.2007.08.022

[11] Prăvălie R (2014) Nuclear Weapons Tests and Environmental Consequences: A Global Perspective. AMBIO 43:729–744 DOI:10.1007/s13280-014-0491-1

[12] Kelley JM, Bond LA, Beasley TM (1999) Global distribution of Pu isotopes and 237Np. Sci. Total Environ 237–238:483–500 DOI:10.1016/s0048-9697(99)00160-6

[13] Eriksson M, Lindahl P, Roos P, Dahlgaard H, Holm E (2008) U, Pu, and Am nuclear signatures of the thule hydrogen bomb debris. Environ. Sci. Technol 42:4717–4722 DOI:10.1021/es800203f

[14] Muramatsu Y, Rühm W, Yoshida S, Tagami K, Uchida S, Wirth E (2000) Concentrations of 239Pu and 240Pu and Their Isotopic Ratios Determined by ICP-MS in Soils Collected from the Chernobyl 30-km Zone. Environ. Sci. Technol 34:2913–2917 DOI:10.1021/es0008968

[15] Zheng J, Tagami K, Uchida S (2013) Release of Plutonium Isotopes into the Environment from the Fukushima Daiichi Nuclear Power Plant Accident: What Is Known and What Needs to Be Known. Environ. Sci. Technol 47:9584–9595 DOI:10.1021/es402212v

[16] Qiao J, Hou X, Miró M, Roos P (2009) Determination of plutonium isotopes in waters and environmental solids: A review. Anal. Chim. Acta 652:66–84 DOI:10.1016/j.aca.2009.03.010

[17] Alewell C, Meusburger K, Juretzko G, Mabit L, Ketterer ME (2014) Suitability of 239+240Pu and 137Cs as tracers for soil erosion assessment in mountain grasslands. Chemosphere 103:274–280 DOI:10.1016/j.chemosphere.2013.12.016

[18] Meusburger K, Porto P, Mabit L, La Spada C, Arata L, Alewell C (2018) Excess Lead-210 and Plutonium-239+240: Two suitable radiogenic soil erosion tracers for mountain grassland sites. Environ. Res 160:195–202 DOI:10.1016/j.envres.2017.09.020

[19] Yang G, Zheng J, Kim E, Zhang S, Seno H, Kowatri M, Aono T, Kurihara O (2021) Rapid analysis of 237Np and Pu isotopes in small volume urine by SF-ICP-MS and ICP-MS/MS. Anal. Chim. Acta 1158:338431 DOI:10.1016/j.aca.2021.338431

[20] Thakur P, Ward AL (2018) 241Pu in the environment: insight into the understudied isotope of plutonium. J. Radioanal. Nucl. Chem 317:757–778 DOI:10.1007/s10967-018-5946-6

[21] Loba A, Waroszewski J, Sykuła K, Kabala C, Egli M (2022) Meteoric 10Be, 137Cs and 239+240Pu as Tracers of Long- and Medium-Term Soil Erosion- A Review. Miner 12: 359 DOI:10.3390/min12030359

[22] Schimmack W, Auerswald K, Bunzl K (2001) Can 239+240Pu replace 137Cs as an erosion tracer in agricultural landscapes contaminated with Chernobyl fallout?. J. Environ. Radioact 53:41–57 DOI: 10.1016/s0265-931x(00)00117-x

[23] Xu Y, Qiao J, Pan S, Hou X, Roos P, Cao L (2015) Plutonium as a tracer for soil erosion assessment in northeast China. Sci. Total Environ 511:176–185 DOI: 10.1016/j.scitotenv.2014.12.006

[24] Lal R, Tims SG, Fifield LK, Wasson RJ, Howe D (2013) Applicability of 239Pu as a tracer for soil erosion in the wet-dry tropics of northern Australia. Nucl. Instruments Methods Phys. Res. Sect. B Beam Interact. with Mater. Atoms 294:577–583 DOI: 10.1016/j.nimb.2012.07.041

[25] Portes R, Dahms D, Brandova D, Raab G, Christl M, Kuhn P, Ketterer M, Egli M (2018) Evolution of soil erosion rates in alpine soils of the Central Rocky Mountains using fallout Pu and δ13C. Earth Planet. Sci. Lett 496:257–269 DOI: 10.1016/j.epsl.2018.06.002

[26] Raab G, Scarciglia F, Norton K, Dahms D, Brandova D, Portes R, Christl M, Ketterer M, Ruppli A, Egli M (2018) Denudation variability of the Sila Massif upland (Italy) from decades to millennia using 10Be and 239+240Pu. L. Degrad. Dev 29:3736–3752 DOI: 10.1002/ldr.3120

[27] Calitri F, Sommer M, Norton K, Temme A, Brandova D, Portes R, Christl M, Ketterer M, Egli M (2019) Tracing the temporal evolution of soil redistribution rates in an agricultural landscape using 239+240Pu and 10Be. Earth Surf. Process. Landforms 44:1783–1798 DOI: 10.1002/esp.4612

[28] Zhang W, Xing S, Hou X (2019) Evaluation of soil erosion and ecological rehabilitation in Loess Plateau region in Northwest China using plutonium isotopes. Soil Tillage Res 191:162–170 DOI: 10.1016/j.still.2019.04.004

[29] Muller RN, Sprugel DG, Kohn B (1978) Erosional Transport and Deposition of Plutonium and Cesium in Two Small Midwestern Watersheds. J. Environ. Qual 7:171–174 DOI: 10.2134/jeq1978.00472425000700020003x

[30] Joshi SR, Shukla BS (1991) AB initio derivation of formulations for 210Pb dating of sediments. J. Radioanal. Nucl. Chem 148:73–79 DOI: 10.1007/BF02060548

[31] Hoo WT, Fifield LK, Tims SG, Fujioka T, Mueller N (2011) Using fallout plutonium as a probe for erosion assessment. J. Environ. Radioact 102:937–942 DOI: 10.1016/j.jenvrad.2010.06.010

[32] Lal R, Fifield LK, Tims SG, Wasson RJ, Howe D (2020) A study of soil erosion rates using 239Pu, in the wet-dry tropics of northern Australia. J. Environ. Radioact 211:106085 DOI: 10.1016/j.jenvrad.2019.106085

[33] Schimmack W, Auerswald K, Bunzl K (2002) Estimation of soil erosion and deposition rates at an agricultural site in Bavaria, Germany, as derived from fallout radiocesium and plutonium as tracers. Naturwissenschaften 89:43–46 DOI: 10.1007/s00114-001-0281-z

[34] Xu Y, Qiao J, Hou X, Pan S (2013) Plutonium in Soils from Northeast China and Its Potential Application for Evaluation of Soil Erosion. Sci. Reports 3:1–8 DOI: 10.1038/srep03506

[35] Zhang K, Pan S, Xu Y, Cao L, Hao Y, Wu M, Xu W, Ren S (2016) Using 239+240Pu atmospheric deposition and a simplified mass balance model to re-estimate the soil erosion rate: a case study of Liaodong Bay in China. J Radioanal Nucl Chem 307:599–604 DOI: 10.1007/s10967-015-4208-0

[36] Zollinger B, Alewell C, Kneisel C, Meusburger K, Brandová D, Kubik P, Schaller M, Ketterer M, Egli M (2015) The effect of permafrost on time-split soil erosion using radionuclides (137Cs, 239 + 240Pu, meteoric 10Be) and stable isotopes (δ 13C) in the eastern Swiss Alps. . J Soils Sediments 15:1400–1419 DOI: 10.1007/s11368-014-0881-9

[37] Meusburger K, Mabit L, Ketterer M, Park J, Sandor T, Porto P, Alewell C (2016) A multi-radionuclide approach to evaluate the suitability of 239 + 240Pu as soil erosion tracer. Science of The Total Environment 566:1489-1499 DOI: 10.1016/j.scitotenv.2016.06.035

[38] Musso A, Ketterer M, Greinwald K, Geitner C, Egli M (2020) Rapid decrease of soil erosion rates with soil formation and vegetation development in periglacial areas. Earth Surf. Process. Landforms 45:2824–2839 DOI: 10.1002/esp.4932

[39] Wilken F, Fiener P, Ketterer M, Meusburger K, Muhindo DI, van Oost K, Doetterl S (2021) Assessing soil erosion of forest and cropland sites in wet tropical Africa using 239+240 Pu fallout radionuclides 7:399-414 DOI: 10.5194/soil-7-399-2021

[40] Wilken F, Ketterer M, Koszinski S, Sommer M, Fiener P (2020) Understanding the role of water and tillage erosion from 239+240Pu tracer measurements using inverse modelling. SOIL 6:549-564 DOI: 10.5194/soil-6-549-2020

[41] Calitri F, Sommer M, van der Meij MW, Egli M (2020) Soil erosion along a transect in a forested catchment: Recent or ancient processes?. CATENA 194:104683 DOI: 10.1016/j.catena.2020.104683

[42] Xing S, Zhang W, Qiao J, Hou X (2018) Determination of ultra-low level plutonium isotopes (239Pu, 240Pu) in environmental samples with high uranium. Talanta 187:357–364 DOI: 10.1016/j.talanta.2018.05.051

[43] Wang Z, Yang G, Zheng J, Cao L, Yu H, Zhu Z, Tagami K, Uchida S (2015) Effect of ashing temperature on accurate determination of plutonium in soil samples. Anal. Chem 87:5511–5515 DOI: 10.1021/acs.analchem.5b01472

[44] Jerome SM, Smith D, Woods MJ, Woods SA (1995) Metrology of plutonium for environmental measurements. Appl. Radiat. Isot 46:1145–1150 DOI: 10.1016/0969-8043(95)00157-9

[45] Gao RQ, Hou XL, Zhang LY, Zhang WC, Zhang MT (2020) Determination of Ultra-Low Level Plutonium Isotopes in Large Volume Environmental Water Samples. Chinese J. Anal. Chem 48:765–773 DOI: 10.1016/S1872-2040(20)60027-5

[46] Wang Z, Zheng J, Ni Y, Men W, Tagami K, Uchida S (2017) High-Performance Method for Determination of Pu Isotopes in Soil and Sediment Samples by Sector Field-Inductively Coupled Plasma Mass Spectrometry. Anal. Chem 89: 2221–2226 DOI: 10.1021/acs.analchem.6b04975

[47] Bu W, Zheng J, Guo Q, Aono T, Otosaka S, Tagami K, Uchida S (2015) Temporal distribution of plutonium isotopes in marine sediments off Fukushima after the Fukushima Dai-ichi Nuclear Power Plant accident. J. Radioanal. Nucl. Chem 303:1151–1154 DOI: 10.1007/s10967-014-3437-y

[48] Luo M, Xing S, Yang Y, Song L, Ma Y, Wang Y, Dai X, Happel S (2018) Sequential analyses of actinides in large-size soil and sediment samples with total sample dissolution. J. Environ. Radioact 187:73–80 DOI: 10.1016/j.jenvrad.2018.01.028

[49] Nygren U, Rodushkin I, Nilsson C, Baxter DC (2003) Separation of plutonium from soil and sediment prior to determination by inductively coupled plasma mass spectrometry. J. Anal. At. Spectrom 18:1426–1434 DOI: 10.1039/B306357G

[50] Maxwell SL, Culligan B, Hutchison JB, McAlister DR (2015) Rapid fusion method for the determination of Pu, Np, and Am in large soil samples. J. Radioanal. Nucl. Chem 305:599–608 DOI: 10.1007/s10967-015-3992-x

[51] Cao L, Bu W, Zheng J, Pan S, Wang Z, Uchida S (2016) Plutonium determination in seawater by inductively coupled plasma mass spectrometry: A review. Talanta 151:30–41 DOI: 10.1016/j.talanta.2016.01.010

[52] Qiao J, Hou X, Roos P, Miró M (2010) Rapid and simultaneous determination of neptunium and plutonium isotopes in environmental samples by extraction chromatography using sequential injection analysis and ICP-MS. J. Anal. At. Spectrom 25:1769–1779 DOI: 10.1039/C003222K

[53] Ketterer ME, Hafer KM, Jones VJ, Appleby PG (2004) Rapid dating of recent sediments in Loch Ness: inductively coupled plasma mass spectrometric measurements of global fallout plutonium. Sci. Total Environ 322:221–229 DOI: 10.1016/j.scitotenv.2003.09.016

[54] Ketterer ME, Szechenyi SC (2008) Determination of plutonium and other transuranic elements by inductively coupled plasma mass spectrometry: A historical perspective and new frontiers in the environmental sciences. Spectrochimica Acta - Part B Atomic Spectroscopy 63:719–737 DOI:10.1016/j.sab.2008.04.018

[55] Horwitz EP, Dietz ML, Chiarizia R, Diamond H, Maxwell SL, Nelson MR (1995) Separation and preconcentration of actinides by extraction chromatography using a supported liquid anion exchanger: application to the characterization of high-level nuclear waste solutions. Anal. Chim. Acta 310:63–78 DOI: 10.1016/0003-2670(95)00144-O

[56] Varga Z, Surányi G, Vajda N, Stefánka Z (2007) Determination of plutonium and americium in environmental samples by inductively coupled plasma sector field mass spectrometry and alpha spectrometry. Microchem. J 85:39–45 DOI: 10.1016/j.microc.2006.02.006

[57] Metzger SC, Rogers KT, Bostock DA, McBay EH, Ticknor BW, Manard BT, Hexel CR (2019) Optimization of uranium and plutonium separations using TEVA and UTEVA cartridges for MC-ICP-MS analysis of environmental swipe samples. Talanta 198:257–262 DOI: 10.1016/j.talanta.2019.02.034

[58] Puzas A, Genys P, Remeikis V, Druteikienė R (2014) Challenges in preparing soil samples and performing a reliable plutonium isotopic analysis by ICP-MS. J. Radioanal. Nucl. Chem 303:751–759 DOI: 10.1007/s10967-014-3411-8

[59] Hrnecek E, Steier P, Wallner A (2005) Determination of plutonium in environmental samples by AMS and alpha spectrometry. Appl. Radiat. Isot 63:633–638 DOI: 10.1016/j.apradiso.2005.05.012

[60] Hou X, Roos P (2008) Critical comparison of radiometric and mass spectrometric methods for the determination of radionuclides in environmental, biological, and nuclear waste samples. Anal. Chim. Acta 608:105–139 DOI: 10.1016/j.aca.2007.12.012

[61] Boulyga SF, Testa C, Desideri D, Becker JS (2001) Optimisation and application of ICP-MS and alpha-spectrometry for determination of isotopic ratios of depleted uranium and plutonium in samples collected in Kosovo. J. Anal. At. Spectrom 16:1283–1289 DOI: 10.1039/B103178N

[62] Corcho Alvarado JA, Nedjadi Y, Bochud F (2011) Determining the activity of 241Pu by liquid scintillation counting. J. Radioanal. Nucl. Chem 289:375–379 DOI: 10.1007/s10967-011-1105-z

[63] Morss LR, Edelstein NM, Fuger J (2006) The Chemistry of the Actinide and Transactinide Elements. Chem. Actin. Trans. Elem 3rd ed 1-5 DOI: 10.1007/1-4020-3598-5

[64] McAninch JE, Hamilton TF, Brown TA, Jokela TA, Knezovich JP, Ognibene TJ, Proctor ID, Roberts ML, Sideras-Haddad E, Southon JR, Vogel JS (2000) Plutonium measurements by accelerator mass spectrometry at LLNL. Nucl. Instruments Methods Phys. Res. Sect. B Beam Interact. with Mater. Atoms 172:711–716 DOI: 10.1016/S0168-583X(00)00091-4

[65] Fifield LK, Cresswell RG, Tada ML, Ophel TR, Day JP, Clacher AP, King SJ, Priest ND (1996) Accelerator mass spectrometry of plutonium isotopes. Nucl. Instruments Methods Phys. Res. Sect. B Beam Interact. with Mater. Atoms 117:295–303 DOI: 10.1016/0168-583X(96)00287-X

[66] López-Lora M, Chamizo E, Villa-Alfageme M, Hurtado-Bermúdez S, Casacuberta N, García-León M (2018) Isolation of 236U and 239,240Pu from seawater samples and its determination by Accelerator Mass Spectrometry. Talanta 178:202–210 DOI: 10.1016/j.talanta.2017.09.026

[67] López-Lora M, Levy I, Chamizo E (2019) Simple and fast method for the analysis of 236U, 237Np, 239Pu and 240Pu from seawater samples by Accelerator Mass Spectrometry. Talanta 200:22–30 DOI: 10.1016/j.talanta.2019.03.036

[68] Thakur P (2019) Radiochemical methods | food and environmental applications. Encyclopedia of Analytical Science, Academic Press 1–14 DOI: 10.1016/B978-0-12-409547-2.14223-4

[69] Muramatsu Y, Hamilton T, Uchida S, Tagami K, Yoshida S, Robison W (2001) Measurement of 240Pu/239Pu isotopic ratios in soils from the Marshall Islands using ICP-MS. Sci. Total Environ 278:151–159 DOI: 10.1016/s0048-9697(01)00644-1

[70] Bu W, Gu M, Ding X, Ni Y, Shao X, Liu X, Yang C, Hu S (2021) Exploring the ability of triple quadrupole inductively coupled plasma mass spectrometry for the determination of Pu isotopes in environmental samples. J. Anal. At. Spectrom 36:2330–2337 DOI: 10.1039/D1JA00288K

[71] Zheng J, Yamada M (2005) Vertical distributions of 239+240Pu activities and 240Pu/239Pu atom ratios in sediment cores: implications for the sources of Pu in the Japan Sea. J. Radioanal. Nucl. Chem 340:199–211 DOI: 10.1007/s10967-006-7001-2

[72] Olufson KP, Moran G (2016) Polyatomic interference removal using a collision reaction interface for plutonium determination in the femtogram range by quadrupole ICP-MS. J. Radioanal. Nucl. Chem 308:639–647 DOI: 10.1007/s10967-015-4483-9

[73] Zhang W, Lin J, Fang S, Li C, Yi X, Hou X, Chen N, Zhang H, Xu Y, Dang H, Wang W, Xu J (2021) Determination of ultra-trace level plutonium isotopes in soil samples by triple-quadrupole inductively coupled plasma-mass spectrometry

with mass-shift mode combined with UTEVA chromatographic separation. Talanta 234:122652 DOI: 10.1016/j.talanta.2021.122652

[74] Vais V, Li C, Cornett J (2004) Separation of plutonium from uranium using reactive chemistry in a bandpass reaction cell of an inductively coupled plasma mass spectrometer. Anal. Bioanal. Chem 380:235–239 DOI: 10.1007/s00216-004-2673-3

[75] Tanner SD, Li C, Vais V, Baranov VI, Bandura DR (2004) Chemical Resolution of Pu+ from U+ and Am+ Using a Band-Pass Reaction Cell Inductively Coupled Plasma Mass Spectrometer. Anal. Chem 76:3042–3048 DOI: 10.1021/ac049899j

[76] Gourgiotis A, Granet M, Isnard H, Nonell A, Gautier C, Stadelmann G, Aubert M, Durand D, Legand S, Chartier F (2010) Simultaneous uranium/plutonium separation and direct isotope ratio measurements by using CO2 as the gas in a collision/reaction cell based MC-ICPMS. J. Anal. At. Spectrom 25:1939–1945 DOI: 10.1039/C0JA00092B

[77] Childs DA, Hill JG (2018) The use of carbon dioxide as the reaction cell gas for the separation of uranium and plutonium in quadrupole inductively coupled plasma mass spectrometry (ICP-MS) for nuclear forensic samples. J. Radioanal. Nucl. Chem 318:139–148 DOI: 10.1007/s10967-018-5973-3

[78] Amr MA, Helal AFI, Al-Kinani AT, Balakrishnan P (2016) Ultra-trace determination of 90Sr, 137Cs, 238Pu, 239Pu, and 240Pu by triple quadruple collision/reaction cell-ICP-MS/MS: Establishing a baseline for global fallout in Qatar soil and sediments. J. Environ. Radioact 153:73–87 DOI: 10.1016/j.jenvrad.2015.12.008

[79] Xu Y, Li C, Yu H, Fang F, Hou X, Zhang C, Li Xiaofei, Xing S (2022) Rapid determination of plutonium isotopes in small samples using single anion exchange separation and ICP-MS/MS measurement in NH3–He mode for sediment dating. Talanta 240:123152 DOI: 10.1016/j.talanta.2021.123152

[80] Tiong LYD, Tan S (2019) In situ determination of 238Pu in the presence of uranium by triple quadrupole ICP-MS (ICP-QQQ-MS). J. Radioanal. Nucl. Chem 322:399–406 DOI: 10.1007/s10967-019-06695-3

[81] Moldovan M, Krupp EM, Holliday AE, Donard OFX (2004) High resolution sector field ICP-MS and multicollector ICP-MS as tools for trace metal speciation in environmental studies: a review. J. Anal. At. Spectrom 19:815–822 DOI: 10.1039/B403128H

[82] Jakubowski N, Moens L, Vanhaecke F (1998) Sector field mass spectrometers in ICP-MS. Spectrochim. Acta Part B At. Spectrosc 53:1739–1763 DOI: 10.1016/S0584-8547(98)00222-5

[83] Donard OFX, Bruneau F, Moldovan M, Garraud H, Epov VN, Boust D (2007) Multi-isotopic determination of plutonium (239Pu, 240Pu, 241Pu and 242Pu) in marine sediments using sector-field inductively coupled plasma mass spectrometry. Anal. Chim. Acta 587:170–179 DOI: 10.1016/j.aca.2007.01.047

[84] Zheng J, Yamada M (2006) Inductively coupled plasma-sector field mass spectrometry with a high-efficiency sample introduction system for the determination of Pu isotopes in settling particles at femtogram levels. Talanta 69:1246–1253 DOI: 10.1016/j.talanta.2005.12.047

[85] Pointurier F, Pottin AC, Hémet P, Hubert A (2011) Combined use of medium mass resolution and desolvation introduction system for accurate plutonium determination in the femtogram range by inductively coupled plasma-sector-field mass spectrometry. Spectrochim. Acta - Part B At. Spectrosc 66:261–267 DOI: 10.1016/j.sab.2011.03.003

[86] Liao H, Zheng J, Wu F, Yamada M, Tan M, Chen J (2008) Determination of plutonium isotopes in freshwater lake sediments by sector-field ICP-MS after separation using ion-exchange chromatography. Appl. Radiat. Isot 66:1138–1145 DOI: 10.1016/j.apradiso.2008.01.001

[87] Guan Y, Sun S, Sun S, Wang H, Ruan X, Liu Z, Terrasi F, Gialanella L, Shen H (2018) Distribution and sources of plutonium along the coast of Guangxi, China. Nucl. Instruments Methods Phys. Res. Sect. B Beam Interact. with Mater. Atoms 437:61–65 DOI: 10.1016/j.nimb.2018.09.047

[88] Huang Z, Ni Y, Wang H, Zheng J, Yamazaki S, Sakaguchi A, Long X, Uchida S (2019) Simultaneous determination of ultra-trace level 237Np and Pu isotopes in soil and sediment samples by SF-ICP-MS with a single column chromatographic separation. Microchem. J 148:597–604 DOI: 10.1016/j.microc.2019.05.044

[89] Taylor RN, Warneke T, Milton JA, Croudace IW, Warwick PE, Nesbitt RW (2003) Multiple ion counting determination of plutonium isotope ratios using multi-collector ICP-MS. J. Anal. At. Spectrom 18:480-484 DOI: 10.1039/B300432E

[90] Lindahl P, Keith-Roach M, Worsfold P, Choi MS, Shin HS, Lee SH (2010) Ultra-trace determination of plutonium in marine samples using multi-collector inductively coupled plasma mass spectrometry. Anal. Chim. Acta 671:61–69 DOI: 10.1016/j.aca.2010.05.012

[91] Taylor RN, Warneke T, Milton JA, Croudace IW, Warwick PE, Nesbitt RW (2001) Plutonium isotope ratio analysis at femtogram to nanogram levels by multicollector ICP-MS. J. Anal. At. Spectrom 16:279-284 DOI: 10.1039/B009078F

[92] Ronzani AL, Pointurier F, Rittner M, Borovinskaya, Tanner M, Hubert A, Humbert AC, Aupiais J, Dacheux N (2018) Capabilities of laser ablation – ICP-TOF-MS coupling for isotopic analysis of individual uranium micrometric particles. J. Anal. At. Spectrom 33:1892–1902 DOI: 10.1039/C8JA00241J

[93] Cizdziel JV (2007) Determination of lead in blood by laser ablation ICP-TOF-MS analysis of blood spotted and dried on filter paper: a feasibility study. Anal. Bioanal. Chem 388:603–611 DOI: 10.1007/s00216-007-1242-y

[94] Baalousha M, Wang J, Erfani M, Goharian E (2021) Elemental fingerprints in natural nanomaterials determined using SP-ICP-TOF-MS and clustering analysis. Sci. Total Environ 792:148426 DOI: 10.1016/j.scitotenv.2021.148426

[95] Greenhalgh CJ, Voloaca OM, Shaw P, Donard A, Cole LM, Clench MR, Managh AJ, Haywood-small SL (2020) Needles in haystacks: using fast-response LA chambers and ICP-TOF-MS to identify asbestos fibres in malignant mesothelioma models. J. Anal. At. Spectrom 35:2231–2238 DOI: 10.1039/D0JA00268B

[96] Bauer OB, Hachmoller O, Borovinskaya O, Sperling M, Schurek HJ, Ciarimboli G, Karst U (2019) LA-ICP-TOF-MS for rapid, all-elemental, and quantitative bioimaging, isotopic analysis and the investigation of plasma processes J. Anal. At. Spectrom 34:694–701 DOI: 10.1039/C8JA00288F

[97] Saha A, Deb SB, Saxena MK (2016) Determination of trace impurities in advanced metallic nuclear fuels by inductively coupled plasma time-of-flight mass spectrometry (ICP-TOF-MS). J. Anal. At. Spectrom 31:1480–1489 DOI: 10.1039/C6JA00138F

[98] Kazi ZH, Cornett JR, Zhao X, Kieser L (2014) Americium and plutonium separation by extraction chromatography for determination by accelerator mass spectrometry. Anal. Chim. Acta 829:75–80 DOI: 10.1016/j.aca.2014.04.044

[99] Wang ZT, Zheng J, Imanaka T, Uchida S (2017) A rapid method for accurate determination of 241 Am by sector field inductively coupled plasma mass spectrometry and its application to Sellafield site soil samples. J. Anal. At. Spectrom 32:2034–2040 DOI: 10.1039/C7JA00201G

[100] Shin C, Choi H, Kwon H, Jo H, Kim H, Yoon H, Kim D, Kang G (2017) Determination of plutonium isotopes (238,239,240Pu) and strontium (90Sr) in seafood using alpha spectrometry and liquid scintillation spectrometry. J. Environ. Radioact 177:151–157 DOI:10.1016/j.jenvrad.2017.06.025

[101] Mhatre AM, Chappa S, Paul S, Pandey AK (2017) Phosphate-bearing polymer grafted glass for plutonium(IV) ion-selective alpha spectrometry. J. Anal. At. Spectrom 32:1566–1570 DOI: 10.1039/C7JA00156H

[102] Seferinoğlu M, Aslan N, Kurt A, Erden PE, Mert H (2014) Determination of plutonium isotopes in bilberry using liquid scintillation spectrometry and alpha-

particle spectrometry. Appl. Radiat. Isot 87:81–86 DOI: 10.1016/j.apradiso.2013.11.097

[103] Liu B, Shi K, Ye G, Guo Z, Wu W (2016) Method development for plutonium analysis in environmental water samples using TEVA microextraction chromatography separation and low background liquid scintillation counter measurement. Microchem. J 124:824–830 DOI: 10.1016/j.microc.2015.10.007

[104] Yamamoto M, Taguchi S, Do VK, Kuno T, Surugaya N (2019) Development of an online measurement system using an alpha liquid scintillation counter and a glass-based microfluidic solvent extraction device for plutonium analysis. Appl. Radiat. Isot 152:37–44 DOI: 10.1016/j.apradiso.2019.06.027

[105] Dai X, Christl M, Kramer-Tremblay S, Synal HA (2012) Ultra-trace determination of plutonium in urine samples using a compact accelerator mass spectrometry system operating at 300 kV. J. Anal. At. Spectrom 27:126–130 DOI: 10.1039/C1JA10264H

[106] Strumińska-Parulska DI (2013) Accelerator mass spectrometry (AMS) in plutonium analysis J. Radioanal. Nucl. Chem 298:593–598 DOI: 10.1007/s10967-013-2448-4

[107] Kaplan DI, Demirkanli DI, Molz FJ, Beals DM, Cadieux JR, Halverson JE (2010) Upward movement of plutonium to surface sediments during an 11-year field study. J. Environ. Radioact 101:338–344 DOI: 10.1016/j.jenvrad.2010.01.007

[108] Lee CG, Suzuki D, Esaka F, Magara M, Song K (2015) Ultra-trace analysis of plutonium by thermal ionization mass spectrometry with a continuous heating technique without chemical separation. Talanta 141:92–96 DOI: 10.1016/j.talanta.2015.03.060

[109] Epov VN, Benkhedda K, Cornett RJ, Evans RD (2005) Rapid determination of plutonium in urine using flow injection on-line preconcentration and inductively coupled plasma mass spectrometry. J. Anal. At. Spectrom 20:424–430 DOI: 10.1039/B501218J

[110] Epov VN, Benkhedda K, Evans RD (2005) Determination of Pu isotopes in vegetation using a new on-line FI-ICP-DRC-MS protocol after microwave digestion. J. Anal. At. Spectrom 20:990–992 DOI: 10.1039/B504569J

[111] Truscott JB, Jones P, Fairman BE, Evans EH (2001) Determination of actinide elements at femtogram per gram levels in environmental samples by on-line solid phase extraction and sector-field-inductively coupled plasma-mass spectrometry. Anal. Chim. Acta 433:245–253 DOI: 10.1016/S0003-2670(01)00784-X

[112] Mitroshkov AV, Olsen KB, Thomas ML (2015) Estimation of the formation rates of polyatomic species of heavy metals in plutonium analyses using a

multicollector ICP-MS with a desolvating nebulizer. J. Anal. At. Spectrom 30:487–493 DOI: 10.1039/C4JA00282B

Chapter 3 – Optimisation of plutonium separations using TEVA cartridges and ICP-MS/MS analysis for applicability to large-scale studies in tropical soils

This chapter has been published in *Analytical Methods*

https://doi.org/10.1039/D3AY01030A

Author contributions:

Study conceived by SMD, OSH, WHB, OO, MJW

Experiments and analysis performed by SMD, TSB and SRC

All figures produced by SMD

Construction of the paper by SMD

All authors were involved in the study and manuscript development

Dowell, S.M., Barlow, T.S., Chenery, S.R., Humphrey, O.S., Isaboke, J., Blake, W.H., Osano, O., Watts, M.J. 2023. Optimisation of plutonium separations using TEVA cartridges and ICP-MS/MS analysis for applicability to large-scale studies in tropical soils. Anal. Methods. https://doi.org/10.1039/D3AY01030A

Supplementary data associated with this chapter can be found in appendices section A3.

Optimisation of plutonium separations using TEVA cartridges and ICP-MS/MS analysis for applicability to large-scale studies in tropical soils

Sophia M. Dowell [a,b], Thomas S. Barlow [a], Simon R. Chenery [a], Olivier S. Humphrey [a], Job Isaboke [c], William H. Blake [b], Odipo Osano [c], Michael J. Watts [a*]

[a] Inorganic Geochemistry, Centre for Environmental Geochemistry, British Geological Survey, Nottingham, NG12 5GG, UK
[b] School of Geography, Earth and Environmental Sciences, University of Plymouth, Plymouth, Devon, PL4 8AA, UK
[c] School of Environmental Sciences, University of Eldoret, Eldoret, Kenya

Graphical abstract

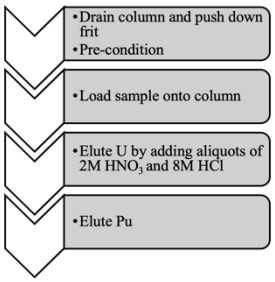

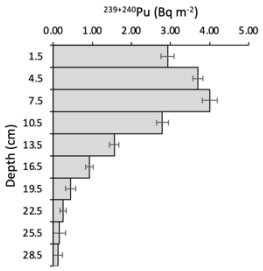

The optimisation of a TEVA column separation provides a simple, robust, and cost-effective method with low achievable detection limits, applicable to the detection of ultra-trace fallout Pu in African soils.

Abstract

The analysis of plutonium (Pu) in soil samples can inform the understanding of soil erosion processes globally. However, there are specific challenges associated for analysis in tropical soils and so an optimal analytical methodology ensuring best sensitivity is critical. This method aimed to demonstrate the feasibility of sample preparation and analysis of Pu isotopes in African soils, considering the environmental and cost implications applicable to low-resource laboratories. The separation procedure builds upon previous work using TEVA columns, further demonstrating their usefulness for the reduction of uranium (U) interference in ICP-MS analysis with enhanced selectivity for Pu. Here several steps were optimised to enhance Pu recovery, reducing method blank concentration, and improving the separation efficiency through the determination of the elution profiles of U and Pu. The elimination of the complexing agent in the eluent,

increased the spike recovery by improving matrix tolerance of the plasma, and simplified the separation procedure, improving throughput by 20%. The subsequent method was validated through the analysis of Certified Reference Material IAEA-384, where high accuracy and improved precision of measurement were demonstrated (measured value 114 ± 12 verses certified value 108 ± 13 Bq kg^{-1}). Optimisation of the column separation, along with the analysis of the samples using O_2 gas in ICP-MS/MS mode to mass shift Pu isotopes away from interfering molecular U ions provided a simple, robust, and cost-effective method with low achievable method detection limits of 0.18 pg kg^{-1} $^{239+240}$Pu, applicable to the detection of ultra-trace fallout Pu in African soils.

Keywords
Plutonium, mass spectrometry, ICP-MS/MS, Tropics, separation chemistry, soil erosion

1. Introduction

Plutonium (Pu) originates in the environment primarily as a consequence of nuclear weapons testing, 520 atmospheric tests were conducted worldwide between 1945 and 1980 [1,2]. However, only 10% of these experiments were conducted in the southern hemisphere, resulting in significantly less fallout in the tropics than in the mid-latitudes of the northern hemisphere. This makes the analysis of ultra-trace Pu isotopes in tropical soils challenging [3,4]. Due to their long retention time and minimal spatial variability, Pu isotopes have been recently utilised as an alternative fallout radionuclide tracer for determining soil erosion rates. Due to the much longer half-lives of ^{239}Pu and ^{240}Pu (24,110 and 6,561 years, respectively), approximately 99% of the original activity remains in soils, allowing for their stable and long-term use as a tracer compared to ^{137}Cs, which has a half-life of only 30 years [5,6]. In addition, more than six times as many atoms of $^{239+240}$Pu were initially dispersed compared to ^{137}Cs, despite the latter's significantly higher activity in the environment. This combination of long half-life and higher atom

content makes mass spectrometry techniques better suited to Pu isotopes, whereas radiometric decay counting techniques are more appropriate for the higher specific activity ^{137}Cs. Consequently, recent developments in mass spectrometry techniques have the potential to increase the sensitivity of quantification of Pu isotopes and subsequently the availability of analytical methods applicable to tropical soils [7,8]. This raises the potential of using Pu as a soil erosion tracer in the tropics, where the risk of soil degradation is increasing due to extreme weather patterns [3].

Radiometric and mass spectroscopy techniques, such as alpha spectrometry, accelerator mass spectrometry (AMS), and inductively coupled plasma mass spectrometry (ICP-MS), can be used to analyse Pu in a variety of samples [7-10]. In recent years, ICP-MS has gained popularity due to its low detection limits, short analytical time, high sample throughput, relatively simple operation, and lower instrument cost [5,11-14]. Despite the benefits of ICP-MS, the technique is severely constrained by polyatomic interferences, most notably uranium hydrides (UH^+). In addition, ^{238}U tailing interferes with the detection of mass-to-charge ratio (m/z) 239 due to its concentration being several orders of magnitude greater than that of ^{239}Pu in soils [15]. This has placed a requirement for a high level of enrichment and elemental separation prior to analysis for the accurate determination of trace Pu isotopes [7]. The Pu isotopes can be separated from the interfering isotopes in the matrix and pre-concentrated to assure maximum sensitivity, using techniques such as coprecipitation, ion exchange chromatography, and extraction chromatography [16-19]. Utilising the selective TEVA column resin (Eichrom Technologies) to effectively remove U and pre-concentrate Pu is common for determination by ICP-MS [16,20]. Nygren et al. (2003) [19] reported that TEVA resin exhibited the maximum separation yield of Pu from soils and sediments compared to other methods. This finding is corroborated by the scientific literature and can be attributed to both the relatively low U content of the resin

and the large variation in acid dependency of k' which is greater than 3 orders of magnitude between U and Pu with nitric acid concentration between 2 and 4 M [21]. Therefore, this paper concentrates on improving the analysis of ultra-trace Pu isotopes in east African soils by further optimising the chemistry of TEVA columns for the latest generations of mass spectrometric instrumentation, applicable to analysis of large-scale studies in tropical soils.

As a result of recent developments in reaction cell technology, tandem ICP-MS (ICP-MS/MS), also known as triple quadrupole ICP-MS (ICP-QQQ-MS), provides an alternative method of analysis to determine Pu. This method is increasingly utilised for the determination of Pu isotopes due to its enhanced abundance sensitivity, which effectively eliminates the interference of the ^{238}U peak tailing on the measurement of ^{239}Pu and ^{240}Pu [7,8,14,22]. In addition, the main interference of $^{238}UH^+$ on ^{239}Pu can be eliminated by utilising different reaction gases in the collision-reaction cell [4,7,8,10,15,23]. The quadrupole mass filter positioned in front of the collision-reaction cell permits the pre-selection of species, thereby enhancing the reaction efficiency of the collision cell and prohibiting the formation of secondary polyatomic interference. In addition, the use of a second quadrupole reduces peak tailing, resulting in enhanced mass resolution. Gases, including ammonia (NH_3), carbon dioxide (CO_2), and oxygen (O_2), have been proposed for the elimination of UH^+ interferences by ICP-MS/MS [4,7,15]. The most frequently employed of these gases is NH_3, which effectively mass shifts the $^{238}U^1H$ interference away from ^{239}Pu via the preferential reaction of U with the NH_3 gas. Using this method, detection limits of 0.16 fg g^{-1} for ^{239}Pu have been achieved; however, despite the ability of NH_3 to react with the U interference, the use of NH_3 gas poses several safety concerns, making its use undesirable [8,24]. Using O_2, the lowest detection limits of 0.06 fg g^{-1} for ^{239}Pu have been reported; this can be attributed to the formation of PuO_2^+, which

effectively mass shifts the Pu isotopes to m/z 271 to avoid interference from $^{238}UH^{+}$ at m/z 239 [4]. The m/z ratio of PuO_2^{+} exceeds the mass range of many early ICP-MS/MS instruments; however, user demands for analysing heavy elements in mass shift modes has led instrument manufacturers developing instruments with an extended m/z range up to 275.

The aim of this study was to accurately determine fallout Pu activity concentrations in tropical soils for the subsequent determination of soil erosion rates with an improved separation and analysis method for ultra-trace Pu determination. The two objectives to achieve this aim are: 1) adapting and optimising a separation method using TEVA cartridges for the removal of matrix interferences with pre-concentration of ultra-trace Pu isotopes to reduce waste and increase throughput; and 2) establishing a robust analytical method for the determination of ultra-trace level Pu isotopes with sufficient sensitivity for African soil samples using oxygen as a reaction gas for ICP-MS/MS.

2. Materials and methods

2.1. Reagents and materials

All reagents used were of analytical grade. Water used throughout had a resistivity of 18.2 MΩ at 25°C and was obtained from a Milli-Q gradient system (Millipore, MA, USA). Extra-pure nitric acid (70%) was obtained from Thermo Fisher Scientific. Ultra-pure HCl was obtained from ROMIL. A solution of ^{242}Pu (2.1×10^{-3} kBq / 14.2 ng) of unknown origin was created from a stock solution (0.21 kBq) using a 100-fold dilution with a solution of 5% HNO_3 and 2.5% HCl in water. This ^{242}Pu solution was then used to spike soil samples prior to digestion. Samples were filtered using 0.45 μm hydrophilic PTFE syringe filters (Thermo Fisher Scientific, UK). Oxidation of Pu species was achieved using ≥ 97% purity $NaNO_2$ (Sigma-Aldrich). The elution of Pu from the

columns used a solution of 0.05 M ammonium oxalate, which was created by dissolving di-ammonium oxalate monohydrate (Supelco, Sigma-Aldrich) in water. Quality control was achieved using certified reference material obtained from the International Atomic Energy Agency (IAEA). The certified reference material IAEA-384 (radionuclides in Fangataufa Lagoon sediment with a certified value of 108 ± 13 Bq kg^{-1} $^{239+240}Pu$) was selected, as this reference soil has been widely used within the literature for the determination of Pu isotopes and no suitable soil CRM was available. To account for differences in the sediment CRM and the analysed soils, an in-house reference material was created using soils collected in the UK. Column separations of Pu isotopes were performed using TEVA pre-packed columns (2ml, 100-150 μm) from Eichrom Technologies. Elemental standard Ir (Spex CertiPrep) was used as an internal standard. Calibration of Pu concentrations via ICP-MS used a U elemental standard solution (Fisher chemical). Silicate sand, which was subjected to the same dissolution procedure as the CRM and samples, was used as the method blank.

2.2 Sample collection

As part of this study, two bulk reference soils were collected from farmland within the UK and Zambia. The UK soil was collected from a cattle farm (Hoveringham, Nottinghamshire, England) during August 2020. Soil was collected from 3 locations across the farm, down to a depth of 15 cm. The soil was then dried in an oven overnight, disaggregated, sieved to <2 mm and finally milled ≤53 μm using a planetary ball mill (Retsch GmbH, Germany), ready for dissolution. This UK reference soil was then homogenised and used throughout the method development as both a quality control sample and to optimise the separation method. The Zambian soil was created from the combination of agricultural soils collected from Kitwe, Zambia, by Hamilton *et al. (2020)* [25]. The analysed soils were prepared in the same way as the UK reference soil and were

used to verify the usefulness of the final method for use on African soils, where Pu levels are much lower than in the Northern Hemisphere.

To validate the method for the determination of soil redistribution rates, a soil core was collected within the Oroba valley, Nandi County, Kenya (*Figure 1*). Within the valley, a site with no overall soil re-distribution, representative of a reference site, was collected. Here, a core was taken to a depth of 30 cm and broken down into 10 sections to determine the Pu inventory within the site. To collect the sample, a pit was dug, and a bulk density tin with a diameter of 5 cm and a height of 3 cm, was inserted into the pit wall. The sample was then taken from the tin and dried in an overnight oven, weighed, disaggregated, and then sieved to <2 mm. The resulting soil was then weighed again to determine the soil density, before finally being milled to ≤53 μm using a planetary ball mill before dissolution. This sample was then analysed to determine the Pu inventory at the site and to demonstrate the methods usability at depth where levels of Pu are significantly lower.

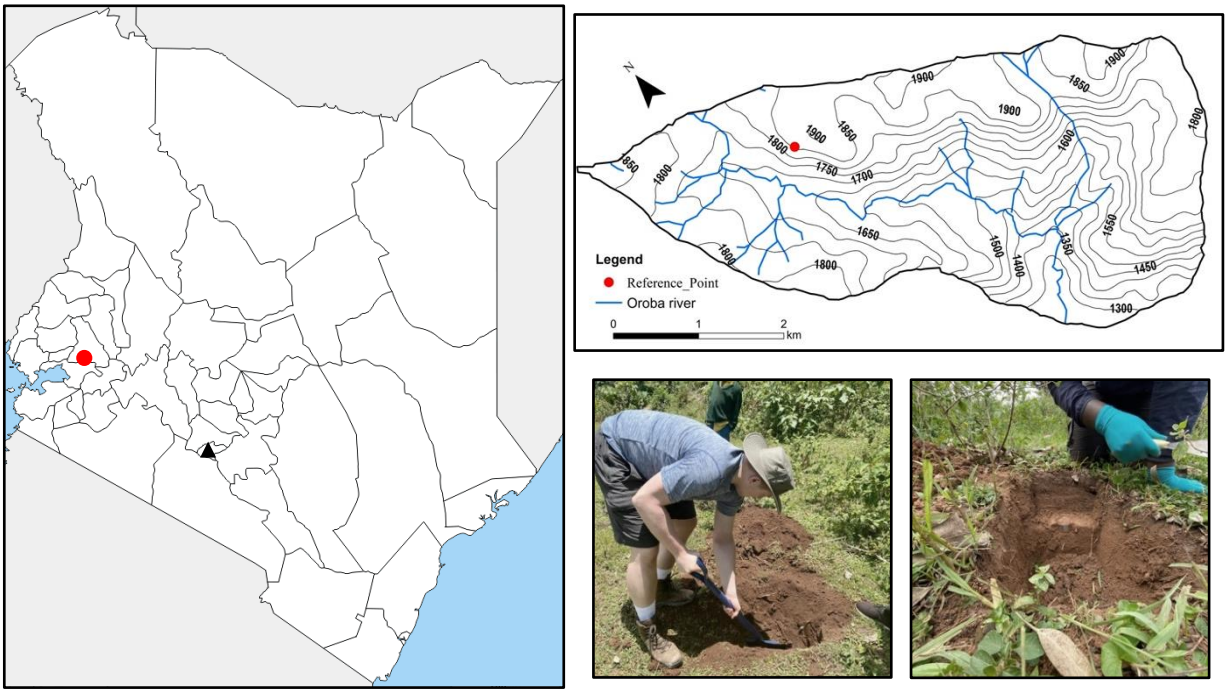

Figure 1 - Sample location of soil core within the Oroba valley, Nandi County, Kenya, and sampling technique

2.3. Sample preparation

2.3.1 Dissolution

Prior to analysis, all samples are weighed into glass beakers and then ignited (ashed) at 550°C for 12 hours to remove organic carbon. As Pu does not form volatile oxides it therefore would not be lost. The ashed sample was then weighed into a suitable PTFE beaker, and the volume of concentrated nitric acid required to leach Pu from soils was investigated, along with the optimum soil mass (soil/acid ratio) to ensure optimum sensitivity while limiting environmental impact by reducing waste. The first step of the optimisation was to determine the optimal mass of sample to use, determined using the UK reference soil (Newark, UK). Six masses ranging from 1 g to 50 g of soil were investigated (1, 5, 10, 20, 35, 50 g). To determine the optimal mass, the soils were digested in 2 ml HNO_3 per 1 g soil which is the minimum volume of HNO_3 suggested by Ketterer et al., (2004) [26]. The variability in measurement of $^{239+240}Pu$ by ICP-MS/MS was determined for three replicate samples at each mass over three separate analytical runs. Subsequently, the optimal volume of acid to digest the soil was investigated to ensure the minimum volume of acid was used to reduce waste and therefore the environmental impact, whilst ensuring the maximum extraction of $^{239+240}Pu$ from the soils. Volumes between 0.5 ml and 3 ml per gram of sample were investigated using the UK reference soil. To the leach mixture, 50 pg (70 µl of 0.2 Bq ml^{-1}) of the ^{242}Pu spike was added, and then the solution was covered by a watch glass. The soil solution was heated on a hotplate at 70°C for 24 hours, cooled to room temperature, and then centrifuged at 3000 rev min^{-1} for 15 minutes. The supernatant was then filtered through a 0.45 µm hydrophilic PTFE filter and collected in a PTFE beaker. A volume of water was added to the pellet in the centrifuge tube. The pellet was redistributed into the water through vigorous shaking and was subsequently centrifuged again. The supernatant was then filtered and added to the PTFE beaker, adjusting the concentration of HNO_3 to 8 M. For the Pu within the sample to be effectively separated using the TEVA column, it must first be in the IV oxidation

state. To do this, 0.02 g $NaNO_2$ per 1 ml of solution was added, and the sample was placed back on the hotplate at 40°C overnight due to the slow nature of the oxidation reaction. The Pu in the solution was then separated using a TEVA column separation.

2.3.2 Plutonium column separation

The separation used was modified using the method described in Ketterer et al., (2004) [26]. *Figure 2* shows the outline of steps within the column separation. The first step involved the pre-conditioning of the column with the first mobile phase to be used, and this ensured all air bubbles had been removed from the column bed and equilibrated the column chemistry for the sample solution matrix. Following this, the sample was loaded onto the column, and subsequently, the column was washed using 2 M HNO_3 and 8 M HCl. These two steps remove both major and trace elements from the TEVA resin, reducing the formation of molecular interferences within the plasma, primarily UH+ but also interferences originating from Hf, Ir, Pt, Hg, Tl, Pb, Bi, Th, and Pb. Due to the acid dependency (k') of tetravalent Pu on the TEVA resin being greatest in the region of 2 – 4 M HNO_3, it is well retained during the washing step with 2 M HNO_3 while hexavalent U is eluted. Following the washing steps, the Pu was eluted from the column by using an appropriate complexing agent or a dilute acid concentration [21]. The separation was optimised through a step-by-step process and is detailed in the results section. These steps include determining the volume of 2 M HNO_3 needed to ensure maximum elution of U isotopes to limit UH^+ interference on Pu measurements, the most suitable eluent for the elution of Pu isotopes (oxalate vs dilute HCl), and the volume of this eluent to ensure optimal elution of Pu isotopes. The steps were optimised to allow a cost-effective, robust method and to minimise laboratory waste disposal – applicable to laboratories with minimal resources for analysis and waste disposal. The column was then flushed and

stored with a 0.01 M HNO_3 matrix to be stored until the quantitative recovery was determined.

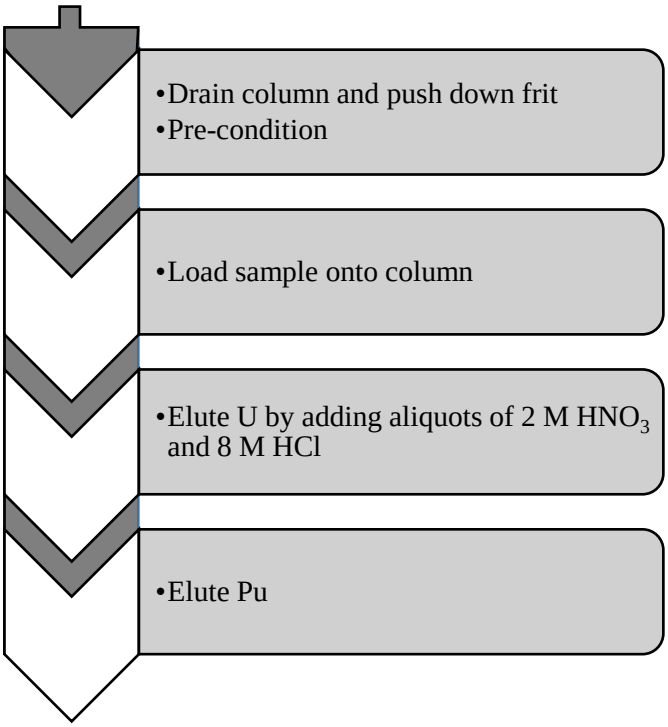

Figure 2 - Outline of column separation employed for the preparation of Pu isotopes in soil using a TEVA resin.

2.4 Instrumentation and setup

An ICP-MS/MS (Agilent 8900, Agilent Technologies, Japan) was used for the measurement of Pu isotopes in the soil samples. This instrument was equipped with a collision reaction cell (CRC) between two quadrupole mass filters. For the measurement of Pu isotopes, O_2 was used in the CRC to mass shift both Pu and U to PuO_2^+ and UO_2^+ ions for measurement, as demonstrated in Zhang *et al*. (2021) [4]. The operating gas modes and default internal standards for each isotope can be seen in *Table 1*. This mass shifting has the advantage of removing the major interference of UH^+ on Pu isotope measurements. The ICP-MS/MS was equipped with an Agilent IaS micro-autosampler and a Cetac Aridus 2 desolvating nebuliser (Teledyne CETAC Technologies, Omaha, USA). This combination required only 1 ml to be used for analysis, ensuring the maximum sensitivity of Pu in the sample through large pre-concentration factors for a

given sample size. The instrument was auto-tuned using the Agilent Masshunter software using a 1 μg kg^{-1} tune solution (SPEX CertiPrep #CL-TUNE-1) for general performance. Agilent typically enables autotuning up to mass 260, and therefore, autotuning on U^+ at mass 270 is not possible. The instrument was then manually tuned on $^{270}U^+$ specifically for Pu and U in oxygen mode. The key tuning parameters were O_2 flow rate, Q2 bias, energy discrimination, OctP bias, wait time offset, cell focus and axial acceleration. Optimised parameters used are shown in *Supplementary Table 1*. The instrument was calibrated for sensitivity using a ^{238}U standard as no certified Pu standard was available. It was assumed that the sensitivity of ^{238}U was the same as ^{239}Pu allowing for isotopic abundance (*Supplementary Table 2*).

Table 1 - Operating gas modes and default internal standards for each isotope.

Element	Isotope	Gas Mode	Reaction Product	Internal Standard
U	238 → 270	O_2	$^{238}UO_2^+$	^{193}Ir
Pu	239 → 271	O_2	$^{239}PuO_2^+$	^{193}Ir
Pu	240 → 272	O_2	$^{240}PuO_2^+$	^{193}Ir
Pu	242 → 274	O_2	$^{242}PuO_2^+$	^{193}Ir

2.5 Quality control

A variety of laboratory control samples were used to track instrumental performance within and between instrument analyses. These included a certified reference soil obtained from the IAEA, specifically IAEA-384 (Radionuclides in Fangataufa Lagoon sediment), with a certified value of 108 ± 13 Bq kg^{-1} $^{239+240}Pu$, which was digested in duplicate within each dissolution batch and then analysed. Background signals were identified by analysis of laboratory control samples (water with 5% HNO_3 and 2.5% HCl) and method blanks (20 g silicate sand, which was subjected to the same dissolution procedure as the CRM and samples). Detector performance was monitored using a 1 μg kg^{-1} tune solution (SPEX CertiPrep #CL-TUNE-1). Internal standard (^{193}Ir) was analysed to correct for instrumental drift and any matrix suppression effects. Soils were analysed

in triplicate within each dissolution batch to verify intra-batch analytical measurements for precision.

3. Results and discussion

3.1 Soil dissolution

Figure 3 shows the relative standard deviation (RSD) of $^{239+240}$Pu measurements according to different sample masses (g). To ensure the environmental impact (primarily the volume of acid required) of the method was accounted for, the minimum mass of sample with the lowest variability in measurement was selected, and the optimum mass for a UK sample was determined to be 20 g. The $^{239+240}$Pu concentration within the UK reference soil was found to be 38.86 ± 1.93 pg kg^{-1}. Due to the much lower fallout in the tropics compared to the mid-latitudes of the northern hemisphere, Pu activity in Europe is on average two-to-three times greater than that in Africa [2]. As a result, when working with African soils, it was decided that 50 g would be the preferred mass whilst retaining optimum sensitivity of Pu measurement. Previous studies utilising ICP-MS for the determination of Pu in soils in the northern hemisphere have used masses between 1 and 10 g [6,27-31], however, the results suggest that the error in measurements at these lower masses justifies the use of a greater mass for separation. The use of 50 g as the soil mass for dissolution is supported elsewhere in the literature, e.g. Wilken *et al. (2021)* [3] used 50 g of soil for the determination of Pu in African soils.

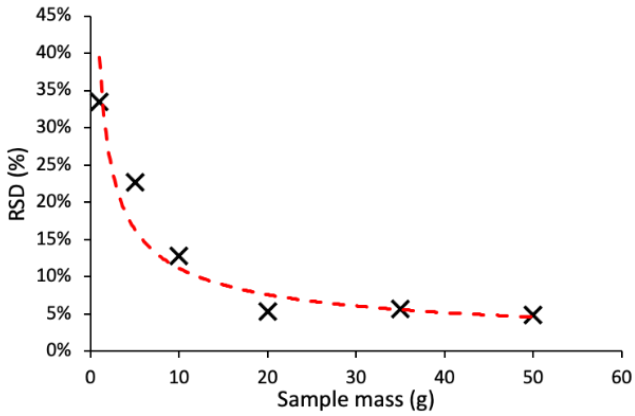

Figure 3 - Relative standard deviation (n = 3) in measurement of $^{239+240}$Pu isotope concentrations by ICP-MS/MS according to different sample mass of UK soil used for dissolution.

Figure 4 shows the recovery of the ^{242}Pu spike as a function of the volume of HNO_3 per gram of soil. Each sample was digested in triplicate, with the error bars representing two times the standard deviation of the measurements. The spike recovery of $^{239+240}$Pu, representative of the whole separation procedure, peaked at 2 ml with the addition of more digest acid, resulting in no significant increase in Pu extraction as the graph plateaus. This is likely as a result of both the decrease in viscosity of the digest solution passing through the column and the increased efficiency of dissolution. The maximum spike recoveries exceed 100% as a result of the overall uncertainty. This compliments with the method suggested by Ketterer et al. (2004) [26], which was widely reported in the literature. The benefits of the complete extraction of Pu isotopes from the soil using 2 ml of acid outweigh the environmental and cost implications of using a larger volume.

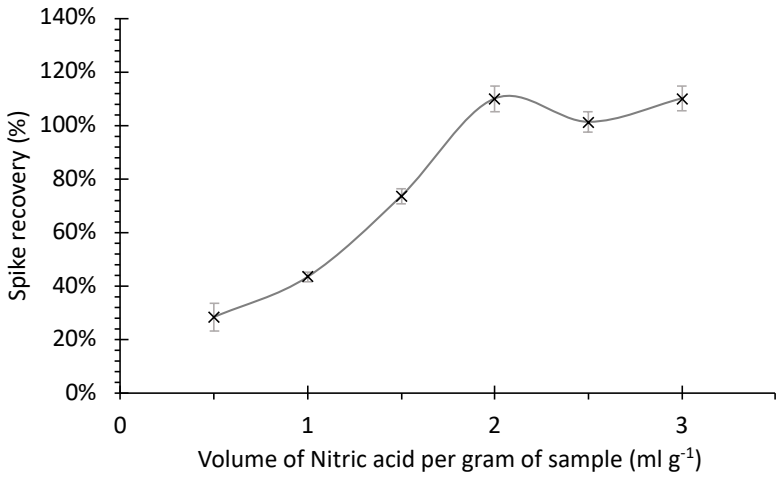

Figure 4 - ^{242}Pu spike recovery dependant on the volume of nitric acid used for the dissolution of soil samples.

The final step of the dissolution was to centrifuge the mixture to separate the digest from the residual solid. In the initial tests, it was found that spike recoveries were low (30 - 50%), and so the washing of the solid pellet after centrifugation was investigated. After the initial centrifugation step, the supernatant was transferred into a PTFE beaker, leaving behind a solid pellet. This was then re-distributed using an equivalent volume of DI water to the volume of acid used in the digestion. The centrifuge tube was then shaken vigorously until the solid pellet was fully redistributed into the water. The mixture was then centrifuged again at 3000 rpm min^{-1} for 15 minutes and the new supernatant was subsequently added to the PTFE beaker containing the digest to adjust the concentration of HNO_3 to 8 M. The results showed that the spike recovery was increased by 30% with the addition of a washing step, suggesting that some of the Pu remained within residual acid retained between pores of the centrifugated soil.

3.2 Optimisation of column separation

The Pu in the samples was separated from the sample matrix using a TEVA column. The separation involved preconditioning of the column, loading of the sample, elution of

matrix elements, including U isotopes, and finally the elution of Pu isotopes. As part of the method development, the elution of U isotopes and the elution of Pu isotopes were investigated. Due to the major interference caused by UH^+ on Pu isotopes during ICP-MS analysis, it was vital to elute and remove the greatest amount of the U isotopes present in the dissolution prior to analysis. The elution of U isotopes was achieved by loading the column with 2 M HNO_3 and discarding the eluent. The tetravalent Pu provided maximum uptake in the region of 2 – 4 M HNO_3, while the hexavalent U was eluted, Pu was retained on the resin during this step [32]. After loading the sample onto the column, 2 M HNO_3 was added to the column 5 ml at a time up to 80 ml. Each of the eluents for every addition of 5 ml was collected and subsequently analysed by ICP-MS/MS for ^{238}U to determine at what volume the maximum U had been eluted from the resin.

Figure 5 shows the percentage U eluted between 0 and 80 ml 2 M HNO_3. The greatest proportion of U was eluted within the first 10 ml of acid (98.5%); however, an additional 1.0% was removed up to 60 ml of acid, thereafter minimal U was eluted. For this reason, a volume of 60 ml acid was used to elute the U from the column to optimise the analysis due to the reduction in UH^+ formation in the plasma. Portes *et al. (2018)* [27] and Wilken *et al. (2021)* [3] used 5 ml per 30 mg of TEVA resin as the rinse volume of 2 M HNO_3 which would be equivalent to approximately 35 ml for the TEVA column used. Although 99% of the U had been eluted when using a volume of 30 ml, the benefit of adding an additional 30 ml of rinse acid had the benefit of reducing the overall U in the final sample for analysis, which is particularly important when working with ultra-trace Pu isotopes in African soils.

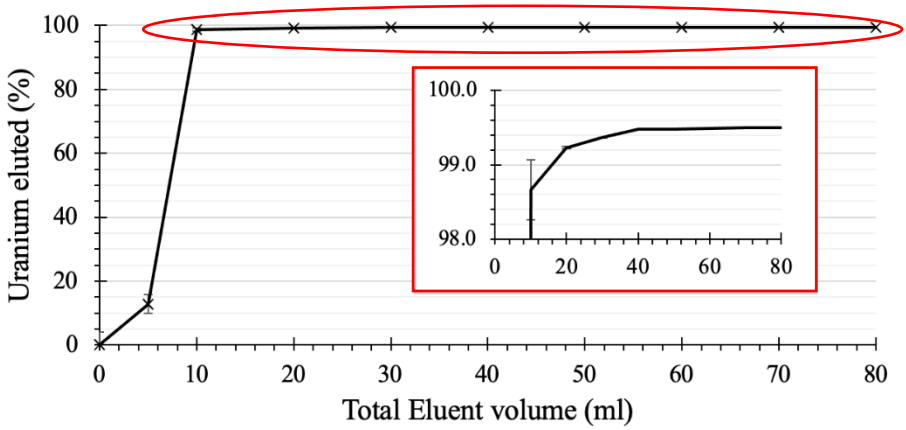

Figure 5 - Elution profile of ^{238}U isotope from TEVA resin using eluent 2 M nitric acid.

The elution of Pu isotopes from the TEVA resin has commonly used 0.05 M ammonium oxalate in the literature, as described in Ketterer *et al. (2004)* [26]. However, more recently, Metzger *et al. (2019)* [16] found that Pu can alternatively be removed from the TEVA resin using a low acid concentration. The Idaho National Engineering and Environmental Laboratory (INEEL) method uses 0.5 M HCl as the eluent of Pu, and so for this study, the use of both 0.05 M ammonium oxalate and 0.5 M HCl was investigated to optimise the elution of Pu from TEVA columns. The UK reference sample was prepared using the dissolution method detailed and loaded onto the column. After acid rinsing of the column, each sample was eluted using the different eluent matrices in triplicate. The oxalate samples were evaporated to dryness on a hot plate, followed by an addition of concentrated nitric acid and heating to decompose hydroxylamine in the samples, which would otherwise detriment the ICP-MS plasma efficiency. They were then reconstituted into 1 ml of the analysis matrix (5% HNO_3 and 2.5% HCl) and subsequently diluted to x5 with the addition of the internal standard for analysis. The HCl samples did not require removal of the matrix and were simply diluted using a solution of 5% HNO_3 and the internal standard. The samples were then analysed by ICP-MS/MS to determine the ^{242}Pu spike recovery. The spike recovery for the ammonium oxalate was 61 ± 11%, compared to the HCl spike recovery of 87 ± 17%. These findings agree with those of Metzger *et al.*

(2019) [16] and show that dilute HCl is a more suitable eluent for the determination of Pu than the commonly used ammonium oxalate. The presented method shows comparable spike recoveries with other methods utilising ICP-MS/MS analysis where reported values range between 70 – 90% [15,23,33]. Using HCl not only improved spike recovery, but it also eliminated the need for extra steps in the process of removing oxalate from the sample. This increased throughput by 20% and reduced the environment burden through the removal of the complexing agent.

The product sheet for TEVA resin indicated that the retention of U isotopes in dilute HCl is also very low and as a result any remaining U on the column after the rinsing steps is likely to elute alongside the Pu isotopes. In total 0.7 μg kg^{-1} ^{238}U was eluted in the collection step, contributing to 0.5% of the total ^{238}U in the sample. In comparison 0.2 μg kg^{-1} ^{238}U was eluted when using ammonium oxalate as the eluent. With the capabilities of ICP-MS/MS to remove the $^{238}UH^{+}$ interference through mass shifting of the Pu isotopes the increased throughput of the method when using dilute HCl outweighs the additional U isotopes being eluted into the sample.

To ensure that the maximum Pu was eluted from the column within the smallest volume to avoid dilution, the volume of eluent acid was investigated. The dilute HCl was added stepwise in 0.5 ml increments to the column and collected to determine the elution profile (*Figure 6*). To avoid dilution of the Pu isotopes prior to analysis, the eluent was collected between 1 ml and 4 ml where the maximum Pu was eluted (99%).

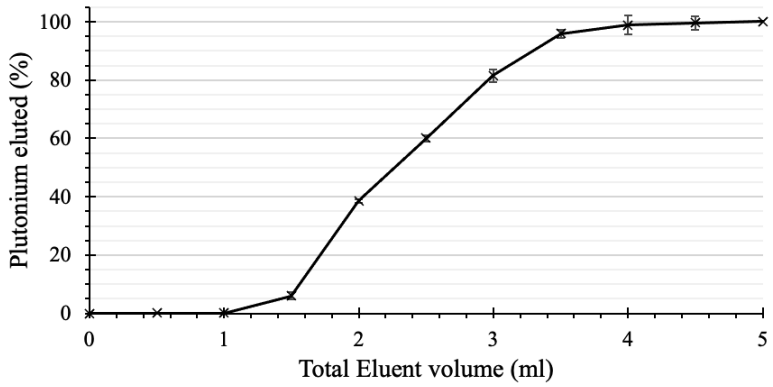

Figure 6 - Elution profile of $^{239+240}$Pu isotopes using eluent 0.5 M HCl.

3.3 Method performance

Blank samples were prepared in conjunction with the analysed soil samples, these consisted of finely milled silicate sand and enabled the determination of U and Pu originating from the whole dissolution and separation processes. While Pu does not occur naturally in the environment, naturally occurring U can be found throughout the environment, including in labware as well as within reagents. The use of clean acid-leached vials and ultra-pure reagents was employed to minimise the U background detected. In addition, analysis blanks containing the analysis matrix of 5% HNO_3 and 2.5% HCl were analysed as part of the analytical procedure. The amounts of U and Pu in the column blanks and ICP-MS measurement only blanks (analytical blanks) were estimated based on count rates and the sensitivity of the day. The analytical blanks yielded an average of 0.009 ± 0.014 μg kg^{-1} ^{238}U and 0.108 ± 0.105 pg kg^{-1} $^{239+240}$Pu (n = 32) with limits of detection of 0.021 μg kg^{-1} and 0.15 pg kg^{-1} respectively. The method blanks yielded an average (± 2σ) concentration of 0.012 ± 0.008 μg kg^{-1} ^{238}U and 0.066 ± 0.121 pg kg^{-1} $^{239+240}$Pu (n = 32) with limits of detection of 0.012 μg kg^{-1} and 0.18 pg kg^{-1} respectively. These detection limits were comparable with previous studies that used O_2 as the reaction gas, such as Zhang et al. (2021) [4] who reported detection limits of 0.06 pg kg^{-1}. The detection limits using this method are improved compared to methods using NH_3 as the reaction gas (0.16 – 0.55 pg kg^{-1}) owing to the formation of PuO_2^+ in the

reaction cell, effectively mass shifting the Pu isotopes to m/z 271 away from interfering $^{238}UH^{+}$ at m/z 239 [8,10,23].

Validation of the optimised separation method was conducted using the analysis of $^{239+240}Pu$ in CRM samples IAEA-384 over five separate analytical runs (n = 36). In addition, the UK reference soil was analysed as an indicator of precision within an analytical sequence as well as to monitor performance between different analytical batches. *Table 2* reports the measured values for both the CRM sample and the UK reference site (± 2σ). The measured value for IAEA-384 indicates both good accuracy and similar precision to the certified value, which was determined by a combination of radiometric (alpha and gamma spectroscopy) and mass spectroscopy techniques. Using a similar method with detection by Thermo X Series II quadrupole ICP-MS (Bremen, Germany), Wilken *et al. (2021)* [3] measured the IAEA-384 reference value to be 102 ± 20 Bq kg^{-1} over 11 measurements. The method presented shows improved precision through the optimisation of column separation and the use of O_2 in a collision cell ICP-MS/MS to reduce the error in measurements.

Table 2 - Analytical performance of measured values of CRM IAEA-384 (n = 36) and UK reference soil (n = 27).

	Certified Value (Bq kg^{-1})	Measured value (Bq kg^{-1})
IAEA 384 (Fangataufa Lagoon sediment) (n = 36)	108 ± 13	114 ± 12
UK reference sample (n = 27)	-	0.14 ± 0.02

Overall spike recoveries using the method in *Table 3* ranged between 67 – 100% with an average of 86% (n = 32). This is comparable with other reported results of spike recovery using ICP-MS/MS in the literature, which range from 70 – 90% [15,23,33]. This, along with the low detection limits, accuracy of measurement, and high precision supports the

application of this separation and analytical method for the detection of Pu isotopes in soils.

Table 3 - Separation scheme outline for the optimized method with volumes and reagents for Pu separation using 2ml volume TEVA resin.

Step	Description	Optimum volume (ml)	Column volumes	Reagent
1	Precondition	4	2	2 M HNO_3
2	Load sample	200	100	-
3	Wash TEVA	60	30	2 M HNO_3
4	Wash TEVA	20	10	8 M HCl
5	Load column with eluent	1	0.5	0.5 M HCl
6	Elute Pu isotopes	3	1.5	0.5 M HCl
7	Wash TEVA	2	1	0.5 M HCl
8	Wash TEVA	4	2	2 M HNO_3
9	Wash TEVA	4	2	0.01 M HNO_3
10	Store TEVA column	3	1.5	0.01 M HNO_3

3.4 Application for the determination of Pu isotopes in African soil samples

The method reported in *Table 3* was then tested on the African soil, which was collected in Zambia by Hamilton *et al. (2020)* [25]. The overall $^{239+240}$Pu in the topsoil samples was determined to be 29.59 ± 0.97 pg kg^{-1} (equivalent to 0.09 Bq kg^{-1}) with an average spike recovery of 81% (n = 3). This value is approximately 1.5 x smaller than the $^{239+240}$Pu concentration found within the UK reference soil and supports the use of 50 g as the sample mass for African soils to achieve maximum sensitivity down the soil profile. The measurement of soil erosion rates using Pu has increases significantly in the literature, and with improvements in the separation and measurement of Pu in soils, the method has the potential to improve understanding of processes influencing erosion and inform mitigation strategies globally [5,14]. Wilken *et al. (2021)* [3] demonstrated the usefulness of Pu as an alternative soil erosion tracer in East Africa, informing soil degradation patterns and highlighting the need for additional studies into erosion rates in tropical soils. This study reported measured mean values at sloped cropland sites in the DR Congo and Uganda of a similar magnitude, with reported values between 0.012 – 0.046 Bq kg^{-1}.

Through the detection of ultra-trace Pu in African soils as a tracer of soil erosion, the data collected can be used to reinforce sustainable soil conservation measures and aid in the validation of prediction models, allowing for a better understanding of the factors influencing accelerated erosion.

To validate the methods usability for studies into soil redistribution rates, Pu inventory was determined at a reference site in the Oroba valley, Nandi County, Kenya. The greatest concentration of $^{239+240}$Pu was found at the depth of 7.5 cm (32.30 pg kg^{-1} / 0.11 Bq kg^{-1}), whereafter concentrations exponentially decreased (*Figure 7*). The usability of the method for the detection of Pu isotopes in African soils is demonstrated by the ability to detect Pu at depths greater than 30 cm with concentrations being an order of magnitude greater than the methods detection limit. The total inventory for the reference site between 0 – 30 cm was determined as 16.86 Bq m^{-2} and the depth profile was consistent with examples in the literature globally [5,26,30,34,35]. The total inventory for the site is consistent with the estimated global fallout reported by Hardy *et al. (1973)* [2] and Kelley *et al. (1999)* [36] for Kenya of 19.2 Bq m^{-2} and the average latitudinal distribution (0 – 10° S) of 11.1 ± 7.4 Bq m^{-2}. In addition, the value is in line with the inventories reported by Wilken *et al. (2021)* [3], where although the inventories in this study were lower, they agree with the differences in annual precipitation (960 and 1400 mm yr^{-1} for Kenya and the White Nile-Congo rift respectively) [37].

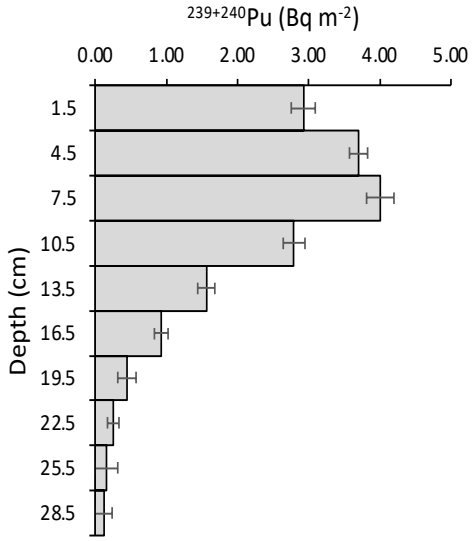

Figure 7 - Depth profile of $^{239+240}$Pu inventory at reference site.

4. Conclusion

A modified, robust analytical sequence for the pre-concentration and separation of ultra-trace Pu isotopes in African soils provided increased sensitivity using ICP-MS/MS with O_2 as a reaction gas to remove interferences. This improved the determination of fallout Pu activity concentrations in the southern hemisphere where Pu signals are relatively low compared to the northern hemisphere. Accuracy was improved through the elimination of the ammonium oxalate matrix in the eluent, with recoveries improved from 61-87%. Removal of the oxalate-sample matrix resulted in more stable plasma conditions, an increase in column separation throughput by 20%, and reduction in reagent consumption/disposal. This method reduced the acid requirement for separations by 80% compared to consensus literature reports, whilst maintaining maximum sensitivity and spike recovery. Additionally, O_2 use as a reaction gas provided low method blank measurements by ICP-MS/MS of 0.06 pg kg^{-1} $^{239+240}$Pu. The CRM sediment, IAEA-384, evidenced accuracy, with improved precision of measurement of: (± 2σ) of 114 ± 12 Bq kg^{-1} $^{239+240}$Pu. The total inventory (16.86 Bq m^{-2}) and depth profile at a reference site in

Kenya is in strong agreement with the literature which reinforces this methods usefulness in the determination of soil redistribution rates in tropical soils.

This method presents a simple, cost-effective, robust sequence with reduced laboratory waste disposal, which is vital to ensure the separation method is applicable to low-resource laboratories. Analysis via ICP-MS/MS with O_2 as a reaction gas offers a robust technique with high throughput compared to traditional techniques such as gamma spectroscopy, and therefore lends itself well to field and survey-scale soil erosion assessment. This outcome, along with the low detection limits that are comparable to alternative mass spectrometric methods, makes the method applicable to the detection of ultra-trace fallout Pu in African soils. Due to increasing concern regarding accelerated soil erosion and its impact on sustainable intensification of agriculture in developing countries, this work provides advancements in the detection of $^{239+240}$Pu which has proven to be a robust tracer for soil erosion. Furthermore, the optimised analytical method is a powerful tool to drive mitigation strategies through the analysis of ultra-trace Pu in African soils, ultimately improving the determination of soil erosion rates in tropical soils to better inform mitigation strategies.

Author contributions

SMD undertook fieldwork, method development, analyses and writing, TSB analyses, SRC analysis and validation, OSH fieldwork and conceptualisation, JI fieldwork and analyses, WHB conceptualisation and supervision, OO fieldwork, conceptualisation, validation, MJW conceptualisation, funding acquisition, administration, validation, writing and supervision. All authors contributed to the review and editing.

Conflicts of interest

There are no conflicts to declare.

Acknowledgements

This work is published with the permission of the Executive Director, British Geological Survey. This work has originated from research conducted with the financial support of the following funders: BGS-NERC grant NE/R000069/1 entitled ‘Geoscience for Sustainable Futures’ and BGS Centre for Environmental Geochemistry programmes for financial support, the NERC National Capability International Geoscience programme entitled ‘Geoscience to tackle global environmental challenges’ (NE/X006255/1). In addition, The Royal Society international collaboration awards 2019 grant ICA/R1/191077 entitled ‘Dynamics of environmental geochemistry and health in a lake wide basin’, Natural Environment Research Councils ARIES Doctoral Training Partnership (grant number NE/S007334/1) and the British Geological Survey University Funding Initiative (GA/19S/017). Additional support provided from the British Academy Early Career Researchers Writing Skills Workshop (WW21100104).

References

1 P. Thakur, H. Khaing, S. Salminen-Paatero, Plutonium in the atmosphere: A global perspective, J. Environ. Radioact, 2017, 175–176, 39–51 DOI:10.1016/j.jenvrad.2017.04.008

2 EP. Hardy, PW. Krey, HL. Volchok, Global inventory and distribution of fallout plutonium, Nature, 1973, 241, 444–445 DOI:10.1038/241444a0

3 F. Wilken, P. Fiener, M. Ketterer, K. Meusburger, DI. Muhindo, K. van Oost, S. Doetterl, Assessing soil erosion of forest and cropland sites in wet tropical Africa using 239+240 Pu fallout radionuclides, SOIL, 2021, 7, 399-414, DOI: 10.5194/soil-7-399-2021

4 W. Zhang, J. Lin, S. Fang, C. Li, X. Yi, X. Hou, N. Chen, H. Zhang, Y. Xu, H. Dang, W. Wang, J. Xu Determination of ultra-trace level plutonium isotopes in soil samples by triple-quadrupole inductively coupled plasma-mass spectrometry with mass-shift mode combined with UTEVA chromatographic separation, Talanta, 2021, 234, 122652, DOI: 10.1016/j.talanta.2021.122652

5 C. Alewell, A. Pitois, K. Meusburger, M. Ketterer, L. Mabit, 239 + 240Pu from 'contaminant' to soil erosion tracer: Where do we stand?, Earth-Science Rev, 2017, 172, 107–123, DOI:10.1016/j.earscirev.2017.07.009

6 K. Meusburger, P. Porto, L. Mabit, C. La Spada, L. Arata, C. Alewell, Excess Lead-210 and Plutonium-239+240: Two suitable radiogenic soil erosion tracers for mountain grassland sites, Environ. Res, 2018, 160, 195–202, DOI:10.1016/j.envres.2017.09.020

7 X. Hou, W. Zhang, Y. Wang, Determination of Femtogram-Level Plutonium Isotopes in Environmental and Forensic Samples with High-Level Uranium Using Chemical Separation and ICP-MS/MS Measurement, Anal. Chem, 2019, 91, 11553–11561, DOI:10.1021/acs.analchem.9b01347

8 Y. Xu, C. Li, H. Yu, F. Fang, X. Hou, C. Zhang, X. Li, S. Xing, Rapid determination of plutonium isotopes in small samples using single anion exchange separation and ICP-MS/MS measurement in NH3–He mode for sediment dating, Talanta, 2022, 240, 123152, DOI: 10.1016/j.talanta.2021.123152

9 C. Shin, H. Choi, H. Kwon, H. Jo, H. Kim, H. Yoon, D. Kim, G. Kang, Determination of plutonium isotopes (238,239,240Pu) and strontium (90Sr) in seafood using alpha spectrometry and liquid scintillation spectrometry, J. Environ. Radioact, 2017, 177, 151–157, DOI:10.1016/j.jenvrad.2017.06.025

10 S. Xing, M. Luo, N. Yuan, D. Liu, Y. Yang, X. Dai, W. Zhang, N. Chen, Accurate determination of plutonium in soil by tandem quadrupole icp-ms with different sample preparation methods, At. Spectrosc, 2021, 42, 62–70, DOI:10.46770/AS.2021.011

11 J. Qiao, X. Hou, M. Miró, P. Roos, Determination of plutonium isotopes in waters and environmental solids: A review, Anal. Chim. Acta, 2009, 652, 66–84, DOI:10.1016/j.aca.2009.03.010

12 L. Cao, W. Bu, J. Zheng, S. Pan, Z. Wang, S. Uchida, Plutonium determination in seawater by inductively coupled plasma mass spectrometry: A review, Talanta, 2016, 151, 30–41, DOI: 10.1016/j.talanta.2016.01.010

13 CS. Kim, CK. Kim, P. Martin, U. Sansone, Determination of Pu isotope concentrations and isotope ratio by inductively coupled plasma mass spectrometry: a review of analytical methodology, J Anal At Spectrom, 2007, 22, 827–841, DOI: 10.1039/B617568F

14 SM. Dowell, OS. Humphrey, WH. Blake, O. Osano, S. Chenery, and MJ. Watts, Ultra-Trace Analysis of Fallout Plutonium Isotopes in Soil: Emerging Trends and Future Perspectives, Chemistry Africa, 2023, DOI: 10.1007/s42250-023-00659-7

15 S. Xing, W. Zhang, J. Qiao, X. Hou, Determination of ultra-low level plutonium isotopes (239Pu, 240Pu) in environmental samples with high uranium, Talanta, 2018, 187, 357–364, DOI: 10.1016/j.talanta.2018.05.051

16 SC. Metzger, KT. Rogers, DA. Bostock, EH. McBay, BW. Ticknor, BT. Manard, CR. Hexel, Optimization of uranium and plutonium separations using TEVA and UTEVA cartridges for MC-ICP-MS analysis of environmental swipe samples, Talanta, 2019, 198, 257–262, DOI: 10.1016/j.talanta.2019.02.034

17 Z. Varga, G. Surányi, N. Vajda, Z. Stefánka, Determination of plutonium and americium in environmental samples by inductively coupled plasma sector field mass spectrometry and alpha spectrometry, Microchem. J, 2007, 85, 39–45, DOI: 10.1016/j.microc.2006.02.006

18 A. Puzas, P. Genys, V. Remeikis, R. Druteikienė, Challenges in preparing soil samples and performing a reliable plutonium isotopic analysis by ICP-MS, J. Radioanal. Nucl. Chem, 2014, 303, 751–759, DOI: 10.1007/s10967-014-3411-8

19 U. Nygren, I. Rodushkin, C. Nilsson, DC. Baxter, Separation of plutonium from soil and sediment prior to determination by inductively coupled plasma mass spectrometry, J. Anal. At. Spectrom, 2003, 18, 1426–1434, DOI: 10.1039/B306357G

20 B. Liu, K. Shi, G. Ye, Z. Guo, W. Wu, Method development for plutonium analysis in environmental water samples using TEVA microextraction chromatography separation and low background liquid scintillation counter measurement, Microchemical Journal, 2016, 124, 824–830, DOI: 10.1016/J.MICROC.2015.10.007

21 EP. Horwitz, ML. Dietz, R. Chiarizia, H. Diamond, SL. Maxwell, MR. Nelson, Separation and preconcentration of actinides by extraction chromatography using

a supported liquid anion exchanger: application to the characterization of high-level nuclear waste solutions, Anal Chim Acta, 1995, 310, 63–78, DOI: 10.1016/0003-2670(95)00144-O

22 L. Cao, J. Zheng, H. Tsukada, S. Pan, Z. Wang, K. Tagami, S. Uchida, Simultaneous determination of radiocesium (135Cs, 137Cs) and plutonium (239Pu, 240Pu) isotopes in river suspended particles by ICP-MS/MS and SF-ICP-MS, Talanta, 2016, 159, 55–63, DOI: 10.1016/j.talanta.2016.06.008

23 W. Bu, M. Gu, X. Ding, Y. Ni, X. Shao, X. Liu, C. Yang, S. Hu, Exploring the ability of triple quadrupole inductively coupled plasma mass spectrometry for the determination of Pu isotopes in environmental samples, J. Anal. At. Spectrom, 2021, 36, 2330–2337, DOI: 10.1039/D1JA00288K

24 LYD. Tiong, S. Tan, In situ determination of 238Pu in the presence of uranium by triple quadrupole ICP-MS (ICP-QQQ-MS), J Radioanal Nucl Chem, 2019, 399–406, DOI: 10.1007/S10967-019-06695-3/TABLES/3

25 EM. Hamilton, RM. Lark, SD. Young, EH. Bailey, GM. Sakala, KK. Maseka, MJ. Watts, Reconnaissance sampling and determination of hexavalent chromium in potentially-contaminated agricultural soils in Copperbelt Province, Zambia, Chemosphere, 2020, 247, 125984, DOI: 10.1016/J.CHEMOSPHERE.2020.125984

26 ME. Ketterer, KM. Hafer, VJ. Jones, PG. Appleby, Rapid dating of recent sediments in Loch Ness: inductively coupled plasma mass spectrometric measurements of global fallout plutonium, Science of The Total Environment, 2004, 322, 221–229, DOI: 10.1016/J.SCITOTENV.2003.09.016

27 R. Portes, D. Dahms, D. Brandova, G. Raab, M. Christl, P. Kuhn, M. Ketterer, M. Egli, Evolution of soil erosion rates in alpine soils of the Central Rocky Mountains using fallout Pu and δ13C, Earth Planet. Sci. Lett, 2018, 496, 257–269, DOI: 10.1016/j.epsl.2018.06.002

28 F. Calitri, M. Sommer, K. Norton, A. Temme, D. Brandova, R. Portes, M. Christl, M. Ketterer, M. Egli, Tracing the temporal evolution of soil redistribution rates in an agricultural landscape using 239+240Pu and 10Be, Earth Surf. Process. Landforms, 2019, 44, 1783–1798 DOI: 10.1002/esp.4612

29 G. Raab, F. Scarciglia, K. Norton, D. Dahms, D. Brandova, R. Portes, M. Christl, M. Ketterer, A. Ruppli, M. Egli, Denudation variability of the Sila Massif upland (Italy) from decades to millennia using 10Be and 239+240Pu, L. Degrad. Dev, 2018, 29, 3736–3752 DOI: 10.1002/ldr.3120

30 C. Alewell, K. Meusburger, G. Juretzko, L. Mabit, ME. Ketterer, Suitability of 239+240Pu and 137Cs as tracers for soil erosion assessment in mountain

grasslands, Chemosphere, 2014, 103, 274–280, DOI: 10.1016/J.CHEMOSPHERE.2013.12.016

31 Y. Muramatsu, W. Rühm, S. Yoshida, K. Tagami, S. Uchida, E. Wirth, Concentrations of 239Pu and 240Pu and Their Isotopic Ratios Determined by ICP-MS in Soils Collected from the Chernobyl 30-km Zone, Environ Sci Technol, 2000, 34, 2913–2917, DOI: 10.1021/ES0008968

32 EP. Horwitz, ML. Dietz, R. Chiarizia, H. Diamond, SL. Maxwell, MR. Nelson, Separation and preconcentration of actinides by extraction chromatography using a supported liquid anion exchanger: application to the characterization of high-level nuclear waste solutions, Anal Chim Acta, 1995, 310, 63–78, DOI: 10.1016/0003-2670(95)00144-O

33 X. Hou, Radioanalysis of ultra-low level radionuclides for environmental tracer studies and decommissioning of nuclear facilities, J Radioanal Nucl Chem, 2019, 322, 1217–1245, DOI: 10.1007/s10967-019-06908-9

34 R. Lal, SG. Tims, LK. Fifield, RJ. Wasson, D. Howe, Applicability of 239Pu as a tracer for soil erosion in the wet-dry tropics of northern Australia, Nucl Instrum Methods Phys Res B, 2013, 294, 577–583, DOI: 10.1016/j.nimb.2012.07.041

35 Y. Xu, J. Qiao, X. Hou, S. Pan, Plutonium in Soils from Northeast China and Its Potential Application for Evaluation of Soil Erosion, Scientific Reports, 2013, 3, 1–8, DOI: 10.1038/srep03506

36 JM. Kelley, LA. Bond, TM. Beasley, Global distribution of Pu isotopes and 237Np, Science of The Total Environment, 1999, 237–238, 483–500, DOI: 10.1016/S0048-9697(99)00160-6

37 SE. Fick, RJ. Hijmans, WorldClim 2: new 1-km spatial resolution climate surfaces for global land areas, International Journal of Climatology, 2017, 37, 4302–4315, DOI: 10.1002/joc.5086

Chapter 4 – Suitability of $^{210}Pb_{ex}$, ^{137}Cs and $^{239+240}Pu$ as soil erosion tracers in western Kenya

.

This chapter has been published in *the journal of environmental radioactivity*

https://doi.org/10.1016/j.jenvrad.2023.107327

Author contributions:

Study conceived by SMD, OSH, WHB, OO, MJW

Experiments and analysis performed by SMD, TSB, CJBG and SRC

All figures produced by SMD

Construction of the paper by SMD

All authors were involved in the study and manuscript development

Dowell, S.M., Humphrey, O.S., Gowing, J.B., Barlow, T.S., Chenery, S.R., Isaboke, J., Blake, W.H., Osano, O., Watts, M.J. 2023. Suitability of $^{210}Pb_{ex}$, ^{137}Cs and $^{239+240}Pu$ as soil erosion tracers in western Kenya. J. Environ. Radioact. https://doi.org/10.1016/j.jenvrad.2023.107327

Supplimentary data associated with this chapter can be found in appendices section A4.

Suitability of $^{210}Pb_{ex}$, ^{137}Cs and $^{239+240}Pu$ as soil erosion tracers in western Kenya

Sophia M. Dowell [a,b], Olivier S. Humphrey [a], Charles J.B. Gowing [a], Thomas S. Barlow [a], Simon R. Chenery [a], Job Isaboke [c], William H. Blake [b], Odipo Osano [c], Michael J. Watts [a*]

[a] Inorganic Geochemistry, Centre for Environmental Geochemistry, British Geological Survey, Nottingham, NG12 5GG, UK
[b] School of Geography, Earth and Environmental Sciences, University of Plymouth, Plymouth, Devon, PL4 8AA, UK
[c] School of Environmental Sciences, University of Eldoret, Eldoret, Kenya

Highlights

- Applicability to large scale studies where selecting reference sites is a challenge
- Determination of Pu is possible to greater depth using ICP-MS/MS analysis
- Improved coefficient of variation at reference sites for Pu compared to Pb and Cs
- The allowable error criteria for reference sites was only met for Pu isotopes

Abstract

Land degradation resulting from soil erosion is a global concern, with the greatest risk in developing countries where food and land resources can be limited. The use of fallout radionuclides (FRNs) is a proven method for determining short and medium-term rates of soil erosion, to help improve our understanding of soil erosion processes. There has been limited use of these methods in tropical Africa due to the analytical challenges associated with ^{137}Cs, where inventories are an order of magnitude lower than in the Europe. This research aimed to demonstrate the usability of $^{239+240}Pu$ as a soil erosion tracer in western Kenya compared to conventional isotopes $^{210}Pb_{ex}$ and ^{137}Cs through the determination of FRN depth profiles at reference sites. Across six reference sites $^{239+240}Pu$ showed the greatest potential, with the lowest coefficient of variation and the greatest peak-to-detection limit ratio of 640 compared to 5 and 1 for $^{210}Pb_{ex}$ and ^{137}Cs respectively. Additionally, $^{239+240}Pu$ was the only radionuclide to meet the 'allowable error' threshold, demonstrating applicability to large scale studies in Western Kenya where the selection of suitable reference sites presents a significant challenge. The depth profile of $^{239+240}Pu$

followed a polynomial function, with the maximum areal activities found between depths 3 and 12 cm, where thereafter areal activities decreased exponentially. As a result, $^{239+240}$Pu is presented as a robust tracer to evaluate soil erosion patterns and amounts in western Kenya, providing a powerful tool to inform and validate mitigation strategies with improved understanding of land degradation.

Keywords

$^{239+240}$Pu, ^{210}Pb$_{ex}$, ^{137}Cs, Fallout radionuclides, Soil erosion, Kenya

1. Introduction

Accelerated soil erosion is a growing global concern, presenting the largest worldwide threat to land degradation and soil erosion may be intensified, particularly in developing countries resulting in a significant obstacle for the intensification of agriculture (Alewell et al., 2014; Deepak Lal, 2000; Lal, 2001; Lorenz et al., 2019; Pimentel, 2006). Inadequate land management techniques and vegetation clearance are major drivers of soil erosion, and with changes in precipitation as a result of climate change, soil erosion will be intensified to unsustainable levels (Borrelli et al., 2020; Negese, 2021). Quantitative data describing the amounts and patterns of soil erosion and sedimentation can be used to inform sustainable soil conservation practices. This data can also aid in the validation of predictive models for an improved understanding of factors influencing the acceleration of erosion processes (Boardman, 2006; Joint FAO/IAEA, 2014; Loba et al., 2022).

In Africa, traditional approaches such as erosion plots, surveying, and the use of aerial photography have been employed for decades to evaluate erosion process, however, they have several disadvantages, including poor representativeness and spatial resolution (Elwell, 1978; Whitlow, 1988). More recently, tracer methods using fallout radionuclides (FRNs) have been employed to determine long term rates of soil erosion over a period of >80 years. Without the need for costly long-term monitoring approaches, these strategies provide an alternative for quantifying soil erosion. In contrast to conventional methods, FRNs can quantify both erosion and deposition rates within a single sampling campaign, with the resulting erosional rates being representative of all redistribution processes (Alewell et al., 2017; Hou, 2019; Loba et al., 2022; Meusburger et al., 2018; Schimmack et al., 2004).

A critical requirement associated with the use of FRN to determine rates of soil erosion is the selection of suitable reference sites. A typical reference site will be a flat, well vegetated, and unploughed area, to limit any possible soil redistribution at that site. In addition, as the FRN inventory at the reference site is assumed to represent the baseline fallout, it is important that the fallout of the FRN was spatially uniform across the study site (Joint FAO/IAEA, 2014). The most frequently used FRNs for the assessment of long-term erosion studies were unsupported lead-210 ($^{210}Pb_{ex}$) and caesium-137 (^{137}Cs). However, plutonium ($^{239+240}Pu$) has gained recognition due to its long-term availability and advancements in detection using ICP-MS technology (Alewell et al., 2014; Dowell et al., 2023a; Gerd R. Ruecker et al., 2008; Meusburger et al., 2018).

Within tropical Africa, the limited application of these methods is likely due to the analytical challenges associated with ^{137}Cs analysis, as its inventories are an order of magnitude lower than in Europe. In Eastern Africa, studies utilising ^{137}Cs as a tracer for soil erosion have been reported in Uganda, Kenya, and Ethiopia with values ranging between 200 - 2064 Bq m^{-2} at reference sites (deGraffenried and Shepherd, 2009; Denboba AM, 2005; Gerd R. Ruecker et al., 2008). In Kenya, deGraffenried and Shepherd, 2009, reported that ^{137}Cs inventory was below the detection limit of 30 Bq m^{-2}, highlighting the challenges associated with the determination of ^{137}Cs activity in the tropics. Wilken et al., 2020, reported the application of $^{239+240}Pu$ as a soil erosion tracer with study sites in Democratic Republic of the Congo Uganda and Rwanda in three forest reference sites with mean $^{239+240}Pu$ inventories between 33 and 48 Bq m^{-2}. The aim of this paper was to demonstrate the utility of $^{239+240}Pu$ as a soil erosion tracer in western Kenya compared to $^{210}Pb_{ex}$ and ^{137}Cs with the objectives of 1) determining depth profiles of FRNs at six reference sites, 2) identifying the robustness of each FRN by calculating the

coefficient of variations and 3) assessing the improved applicability of $^{239+240}$Pu to large scale studies compared to other FRNs.

2. Materials and methods

2.1 Study area and soil sampling design

The study area was located within the Rift Valley, Nandi County, Kenya. The valley banks onto the Oroba river which drains into the Winam gulf of Lake Victoria. This valley was indicated to be at increased risk of erosion by Humphrey et al., 2022, with continuous land clearance over the past 80 years. According to the requirements of IAEA's 2014 guidelines, six suitable reference sites were identified (*Figure 1*) (Joint FAO/IAEA, 2014).

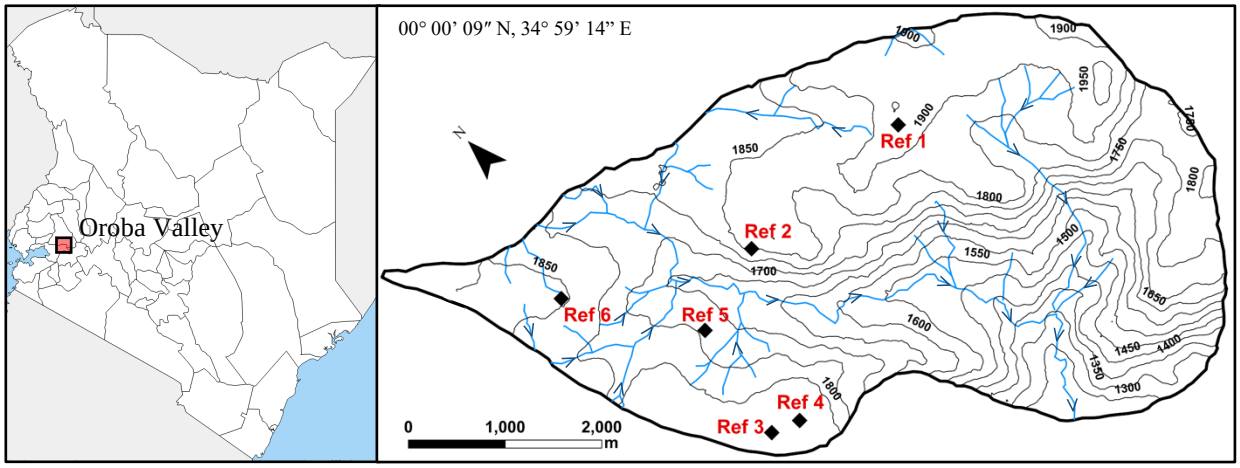

Figure 1 - Sample location of reference soil cores within the Oroba river catchment, Nandi County, Kenya. Map created using the GADM database.

At each reference site a 30 cm core with a 5 cm diameter was excavated and split into 10 sections to determine the inventories of $^{210}Pb_{ex}$, ^{137}Cs and $^{239+240}$Pu. The bulk density was determined following sample drying at 30°C for 24 hours or until the soils were fully dry, and then the sample was sieved to <2 mm before reweighing to determine the soil density (U.S. EPA. 1996, FAO, 2020).The average soil density calculated was 1.32 and values

ranged from 0.82 to 1.66 g cm^{-3}, with density increasing down the core. The depth profile data for $^{239+240}Pu$ at site 3 was previously published by Dowell et al., 2023b.

2.2 Sample preparation and analysis

2.3.1 Gamma spectroscopy – $^{210}Pb_{ex}$ and ^{137}Cs

Prior to analysis, the sieved soils (<2 mm) were placed into 147 mL polystyrene pots (base diameter 60 mm) with no headspace and sealed for 21 days to achieve equilibrium between ^{226}Ra and ^{222}Rn. After this time measurements of ^{137}Cs, ^{210}Pb and ^{226}Ra (via analysis of ^{214}Pb) activities were determined using a high resolution HPGe gamma detector at the British Geological Survey, Nottingham (Canberra Mirion, BE3825 with 71 mm active diameter and a carbon epoxy composite end cap, operated at a bias of +4 kV). Samples were counted between 24 and 48 hours (until the measured activity exceeded the Minimal Detectable Activity (MDA)). The measured spectrum was fitted using Genie 2000 software (Mirion technologies Inc, Atlanta, USA) and corrected for spectral background. Efficiency corrections were performed using LabSOCS calibration software (Mirion technologies Inc, Atlanta, USA) and spectral peaks were fitted against a library containing natural nuclide emission line energies from the ^{238}U, ^{235}U and ^{232}Th series. The Currie equation was used to calculate MDAs. Instrument QA was performed by analysis of ^{241}Am, ^{137}Cs and ^{60}Co spot sources. The unsupported ^{210}Pb ($^{210}Pb_{ex}$) activity was then calculated by the subtraction of supported ^{210}Pb (^{214}Pb equivalent) activity from the total ^{210}Pb activity in the sample.

2.3.2 ICP-MS/MS – $^{239+240}$Pu

The full analytical procedure for ICP-MS/MS analysis is outlined in Dowell et al., 2023b. Prior to analysis the soil samples were milled, and 50 g was weighed into a glass beaker. This sample was then ashed overnight. The ashed samples were placed into a PTFE beaker with a 50 pg of a ^{242}Pu spike to be leached using 100 ml concentrated HNO_3. The soil solution was then heated on a hotplate at 70°C for 24 hours, and then centrifuged. The supernatant was filtered through a 0.45 μm hydrophilic PTFE filter and collected. To adjust the Pu oxidation state to IV for the separation, 0.02 g $NaNO_2$ per 1 ml of solution was added. The Pu in the solution was then separated from interfering isotopes using a TEVA column separation. Within each dissolution process two silica sand column blanks (20 g) along with CRM sample IAEA 384 (0.5 g) were analysed to ensure validity of the analytical procedure and to determine the detection limits. The decontamination factor achieved for U isotopes after column separation was 200.

An ICP-MS/MS (Agilent 8900, Agilent Technologies, Japan) was used for the measurement of Pu isotopes in the soil samples with O_2 gas in the collision-reaction cell. The sample was introduced using an Agilent IaS micro-autosampler and a Cetac Aridus II desolvating nebuliser (Teledyne CETAC Technologies, Omaha, USA). The instrument was calibrated for sensitivity using a ^{238}U standard as no certified Pu standard was available (Dowell et al., 2023b). Average $^{239+240}$Pu dioxide counts for the samples were 604 counts per second with an average background of 3 counts per second. A concentration of 100 pg kg^{-1} is equivalent to 350 counts per second of $^{239+240}$Pu dioxide. The mean spike recoveries of the samples was 79%. The isotope ratio of ^{240}Pu/^{239}Pu was also measured alongside the $^{239+240}$Pu activities for each sample where all sampling sites had a ratio of 0.18 ± 0.02 which agrees with the stratospheric global fallout ratio of 0.18

± 0.014 (Kelley et al., 1999). Further details on the analytical methods performance have been published (open access) by Dowell et al., 2023b.

3. Results and discussion

The $^{210}Pb_{ex}$ areal activities for the six reference sites decreased exponentially with depth following a polynomial distribution, where the maximum areal activity was found within the first 3 cm of the soil core (*Figure 2*). This agrees with similar findings in the literature and is due to continual deposition of $^{210}Pb_{ex}$ into the soil as a result of rain-out (Meusburger et al., 2018). Although samples down to a depth of 30 cm were counted, it was not possible to detect $^{210}Pb_{ex}$ above the MDA beneath a depth of 21 cm. The depth distribution of both ^{137}Cs and $^{239+240}Pu$ at the reference sites follow a polynomial function with the maximum areal activities found between depths of 3 - 12 cm, where thereafter areal activities decreased exponentially. This has been shown to be a common depth distribution pattern and can be explained by the downward migration of isotopes in the time since the major bomb fallout events (Alewell et al., 2017, 2014; Lal et al., 2013; Zhang et al., 2019).

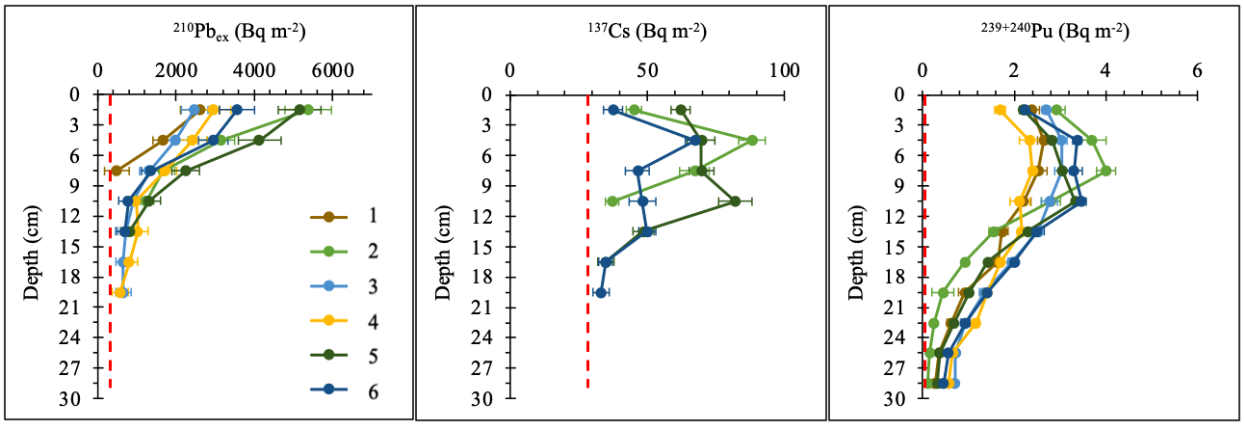

Figure 2 - Areal activity depth distribution patterns at the six reference sites for $^{210}Pb_{ex}$, ^{137}Cs and $^{239+240}Pu$ with detection limits (red dashed line).

Only three of the reference sites had measurable ^{137}Cs above the MDA and quantification was only possible to a maximum depth of 21 cm. The measurement of both $^{210}Pb_{ex}$ and ^{137}Cs is severely limited by the achievable MDAs using gamma spectroscopy, which

although requiring a much simpler sample preparation procedure, has much lower throughput than the ICP-MS/MS methodology due to long counting times, limiting applicability of the method (*Table 1*). On the other hand, $^{239+240}$Pu which was determined using ICP-MS/MS with O_2 reaction gas was quantified in all samples down to the total depth of 30 cm and with much greater peak to detection limit ratios.

Table 1 - Limits of detection and depth distribution patterns for $^{210}Pb_{ex}$, ^{137}Cs and $^{239+240}Pu$.

Isotope	Detection Limit (Bq m^{-2})	Max peak / Detection limit	Areal activity in top 3 cm (%)	Areal activity in top 12 cm (%)
$^{210}Pb_{ex}$	498 [a]	5	39	90
^{137}Cs	31 [a]	1	16	80
$^{239+240}Pu$	6 x 10^{-3} [b]	640	13	63

[a] *Gamma spectroscopy*
[b] *ICP-MS/MS using O_2 reaction gas*

Using the test proposed by Sutherland., 1996 the validity and accuracy of the reference values was verified by calculating the allowable error (AE) at the 90% confidence level where n' is the number of samples and t is the student's t-value for an $\alpha = 0.10$ (90% confidence level *(Equation 1).* The coefficients of variation (CV) for $^{210}Pb_{ex}$, ^{137}Cs ar $^{239+240}Pu$ were 31%, 21% and 11%, respectively (*Table 2*). Considering the number o samples, the AE was calculated as 25% for $^{210}Pb_{ex}$, 29% for ^{137}Cs and 9% for $^{239+240}$P Only Pu meets the requirement of having an AE ≤10% while the number of reference sites for ^{210}Pb and ^{137}Cs would need to be increased until the AE criteria was met (Mabit et al., 2012; Meusburger et al., 2018; Sutherland, 1996).

$$n' = \left[\frac{t_{(\alpha,n-1)}\, CV}{AE}\right]^2$$

Equation 1 – Equation for the calculation of allowable error (AE) (Sutherland, 1996).

The mean activity concentrations for ^{137}Cs was below previously reported vales for non-eroded sites in Kenya reported by deGraffenried and Shepherd, 2009 of 4.15 Bq kg^{-1} (Table S1). This is likely as a result of ^{137}Cs's short half-life and the 14 years between the studies. In Eastern Africa, studies utilising ^{137}Cs as a tracer for soil erosion reported inventories between 200 - 2064 Bq m^{-2} at reference sites in have been reported in Uganda and Ethiopia (Denboba, 2005; Gerd R. Ruecker et al., 2008; deGraffenried and Shepherd, 2009). The mean inventory of the six reference sites for $^{239+240}Pu$ of 18 Bq m^{-2} is consistent with the regional fallout estimations by Hardy et al., 1973 and Kelley et al., 1999 of 19.2 Bq m^{-2}, further supporting the validity of the reference site measurements. The results presented support the hypothesis that $^{239+240}Pu$ has the potential to be used as the preferred FRN tracer in western Kenya, with low achievable allowable error across the reference sites, allowing for greater applicability to study sites where the selection of appropriate reference sites is a challenge.

Table 2 - Total inventory of $^{210}Pb_{ex}$, ^{137}Cs and $^{239+240}Pu$ ($\pm 2\sigma$) and validity of reference site measurements to determine soil redistribution rates in the Oroba valley, Nandi County, Kenya.

Site	$^{210}Pb_{ex}$		^{137}Cs		$^{239+240}Pu$	
	Maximum depth (cm)	**inventory (Bq m^{-2})**	**Maximum depth (cm)**	**inventory (Bq m^{-2})**	**Maximum depth (cm)**	**inventory (Bq m^{-2})**
1	9	2385 ± 1178	-	-	30	15 ± 0.3
2	12	5721 ± 627	12	119 ± 8	30	17 ± 0.4
3	21	4360 ± 884	-	-	30	20 ± 0.5
4	21	5246 ± 817	-	-	30	16 ± 0.3
5	15	6840 ± 737	18	184 ± 11	30	18 ± 0.4
6	15	4681 ± 768	21	159 ± 10	30	20 ± 0.8
Mean	**4872 ± 2996**		**154 ± 66**		**18 ± 4.1**	
CV (%)	30.7		21.2		11.1	
AE (%)	25.3		28.8		9.2	

4. Conclusion

Here we assessed the suitability of $^{239+240}Pu$ as a soil erosion tracer in western Kenya compared to traditionally used FRNs $^{210}Pb_{ex}$ and ^{137}Cs. Reference sites to evaluate the potential of FRN were selected according to the guidelines set out by IAEA 2014 (Joint FAO/IAEA, 2014). Depth profiles of $^{210}Pb_{ex}$, ^{137}Cs, and $^{239+240}Pu$ were determined to establish the suitability of each radionuclide for the determination of soil erosion rates. Of the three elements, $^{239+240}Pu$ was the only one that met the requirements to be used as a reference set out by Sutherland., 1996, with an 'allowable error' of ≤10% across the six reference sites. This is likely a result of the advancements in analysis using ICP-MS/MS, where a much greater peak-to-detection limit ratio was achievable for $^{239+240}Pu$ compared to $^{210}Pb_{ex}$ and ^{137}Cs, allowing for greater precision and determination to greater depth. The low coefficient of variation and allowable error for $^{239+240}Pu$ across the reference sites indicates the applicability of Pu as a robust tracer of soil erosion in western Kenya with

applicable to large scale studies compared to other FRN tracers. The need for fewer reference sites, as a result of the low allowable error, lends well to study sites where the selection of appropriate reference sites is a challenge. The use of $^{239+240}$Pu as a robust soil erosion tracer will play a vital role in the determination of soil degradation amounts and patterns, providing a powerful tool to improve our understanding of the effectiveness of mitigation strategies.

Conflicts of interest

There are no conflicts to declare.

Acknowledgements

This work is published with the permission of the Executive Director, British Geological Survey. This work has originated from research conducted with the financial support of the following funders: BGS-NERC grant NE/R000069/1 entitled 'Geoscience for Sustainable Futures' and BGS Centre for Environmental Geochemistry programmes, the NERC National Capability International Geoscience programme entitled 'Geoscience to tackle global environmental challenges' (NE/X006255/1). Additionally financial support from The Royal Society international collaboration awards 2019 grant ICA/R1/191077 entitled 'Dynamics of environmental geochemistry and health in a lake wide basin', Natural Environment Research Councils ARIES Doctoral Training Partnership (grant number NE/S007334/1) and the British Geological Survey University Funding Initiative (GA/19S/017) was provided, alongside support provided from the British Academy Early Career Researchers Writing Skills Workshop (WW21100104).

References

Alewell, C., Meusburger, K., Juretzko, G., Mabit, L., Ketterer, M.E., 2014. Suitability of 239+240Pu and 137Cs as tracers for soil erosion assessment in mountain grasslands. Chemosphere 103, 274–280. https://doi.org/10.1016/J.CHEMOSPHERE.2013.12.016

Alewell, C., Pitois, A., Meusburger, K., Ketterer, M., Mabit, L., 2017. 239 + 240Pu from "contaminant" to soil erosion tracer: Where do we stand? Earth Sci Rev 172, 107–123. https://doi.org/10.1016/J.EARSCIREV.2017.07.009

Boardman, J., 2006. Soil erosion science: Reflections on the limitations of current approaches. Catena (Amst) 68, 73–86. https://doi.org/10.1016/j.catena.2006.03.007

Borrelli, P., Robinson, D.A., Panagos, P., Lugato, E., Yang, J.E., Alewell, C., Wuepper, D., Montanarella, L., Ballabio, C., 2020. Land use and climate change impacts on global soil erosion by water (2015-2070). Proceedings of the National Academy of Sciences 117, 21994–22001. https://doi.org/10.1073/pnas.2001403117

Deepak Lal, 2000. The Poverty of "development Economics", Second ed. The MIT Press, Massachusetts.

DeGraffenried, J.B., Shepherd, K.D., 2009. Rapid erosion modeling in a Western Kenya watershed using visible near infrared reflectance, classification tree analysis and 137Cesium. Geoderma 154, 93–100. https://doi.org/10.1016/j.geoderma.2009.10.001

Denboba AM, 2005. Forest conversion-soil degradation-farmers perception nexus: Implications for sustainable land use in the southwest of Ethiopia. Cuvillier Verlag 26.

Dowell, S.M., Humphrey, O.S., Blake, W.H., Osano, O., Chenery, S., Watts, M.J., 2023a. Ultra-Trace Analysis of Fallout Plutonium Isotopes in Soil: Emerging Trends and Future Perspectives. Chemistry Africa. https://doi.org/10.1007/s42250-023-00659-7

Dowell, S.M., Barlow, T.S., Chenery, S.R., Humphrey, O.S., Isaboke, J., Blake, W.H., Osano, O., Watts, M.J., 2023b. Optimisation of plutonium separations using TEVA cartridges and ICP-MS/MS analysis for applicability to large-scale studies in tropical soils. Analytical Methods. https://doi.org/10.1039/D3AY01030A

Elwell, H.A., 1978. Modelling soil losses in Southern Africa. Journal of Agricultural Engineering Research 23, 117–127. https://doi.org/10.1016/0021-8634(78)90043-4

FAO. 2020. Soil testing methods – Global Soil Doctors Programme - A farmer-to-farmer

training Programme. Rome. https://doi.org/10.4060/ca2796en

Gerd R. Ruecker, Soojin J. Park, Almut C. Brunner, Paul L. G. Vlek, 2008. Assessment of Soil Redistribution on Two Contrasting Hillslopes in Uganda Using Caesium-137 Modelling. Erdkunde 62, 259–272. https://www.jstor.org/stable/25648129

Hardy, E.P., Krey, P.W., Volchok, H.L., 1973. Global inventory and distribution of fallout plutonium [1]. Nature. https://doi.org/10.1038/241444a0

Hou, X., 2019. Radioanalysis of ultra-low level radionuclides for environmental tracer studies and decommissioning of nuclear facilities. J Radioanal Nucl Chem 322, 1217–1245. https://doi.org/10.1007/s10967-019-06908-9

Humphrey, O.S., Osano, O., Aura, C.M., Marriott, A.L., Dowell, S.M., Blake, W.H., Watts, M.J., 2022. Evaluating spatio-temporal soil erosion dynamics in the Winam Gulf catchment, Kenya for enhanced decision making in the land-lake interface. Science of The Total Environment 815, 151975. https://doi.org/10.1016/j.scitotenv.2021.151975

Joint FAO/IAEA Division of Nuclear Techniques in Food and Agriculture, Soil and Water Management and Crop Nutrition Section, Vienna (Austria) 2014. Guidelines for Using Fallout Radionuclides to Assess Erosion and Effectiveness of Soil Conservation Strategies (IAEA-TECDOC--1741). International Atomic Energy Agency (IAEA)

Kelley, J.M., Bond, L.A., Beasley, T.M., 1999. Global distribution of Pu isotopes and 237Np. Science of The Total Environment 237–238, 483–500. https://doi.org/10.1016/S0048-9697(99)00160-6

Lal, R., 2001. Soil degradation by erosion. Land Degrad Dev 12, 519–539. https://doi.org/10.1002/ldr.472

Lal, R., Tims, S.G., Fifield, L.K., Wasson, R.J., Howe, D., 2013. Applicability of 239Pu as a tracer for soil erosion in the wet-dry tropics of northern Australia. Nucl Instrum Methods Phys Res B 294, 577–583. https://doi.org/10.1016/j.nimb.2012.07.041

Loba, A., Waroszewski, J., Sykuła, M., Kabala, C., Egli, M., 2022. Meteoric 10Be, 137Cs and 239+240Pu as Tracers of Long- and Medium-Term Soil Erosion - A Review. Minerals 2022, Vol. 12, Page 359 12, 359. https://doi.org/10.3390/MIN12030359

Lorenz, K., Lal, R., Ehlers, K., 2019. Soil organic carbon stock as an indicator for

monitoring land and soil degradation in relation to United Nations' Sustainable Development Goals. Land Degrad Dev 30, 824–838. https://doi.org/10.1002/ldr.3270

Mabit, L., Chhem-Kieth, S., Toloza, A., Vanwalleghem, T., Bernard, C., Amate, J.I., González de Molina, M., Gómez, J.A., 2012. Radioisotopic and physicochemical background indicators to assess soil degradation affecting olive orchards in southern Spain. Agric Ecosyst Environ 159, 70–80. https://doi.org/10.1016/j.agee.2012.06.014

Meusburger, K., Porto, P., Mabit, L., La Spada, C., Arata, L., Alewell, C., 2018. Excess Lead-210 and Plutonium-239+240: Two suitable radiogenic soil erosion tracers for mountain grassland sites. Environ Res 160, 195–202. https://doi.org/10.1016/J.ENVRES.2017.09.020

Negese, A., 2021. Impacts of Land Use and Land Cover Change on Soil Erosion and Hydrological Responses in Ethiopia. Appl Environ Soil Sci 2021, 1–10. https://doi.org/10.1155/2021/6669438

Pimentel, D., 2006. Soil Erosion: A Food and Environmental Threat. Environ Dev Sustain 8, 119–137. https://doi.org/10.1007/s10668-005-1262-8

Schimmack, W., Auerswald, K., Bunzl, K., 2004. Estimation of soil erosion and deposition rates at an agricultural site in Bavaria, Germany, as derived from fallout radiocesium and plutonium as tracers. Naturwissenschaften 2001 89:1 89, 43–46. https://doi.org/10.1007/S00114-001-0281-Z

Sutherland, RA., 1996. Caesium-137 soil sampling and inventory variability in reference locations: A literature survey. Hydrol Process 10, 43–53. https://doi.org/10.1002/(SICI)1099-1085(199601)10:1<43::AID-HYP298>3.0.CO;2-X

U.S. EPA. 1996. "Method 3050B: Acid Digestion of Sediments, Sludges, and Soils," Revision 2. Washington, DC.

Whitlow, R., 1988. Land degradation in Zimbabwe: a geographical study. Harare: UZ/ Department of Natural Resources.

Wilken, F., Fiener, P., Ketterer, M., Meusburger, K., Muhindo, D.I., Van Oost, K., Doetterl, S., 2020. Assessing soil erosion of forest and cropland sites in wet tropical Africa using 239+240 Pu fallout radionuclides. Soil Discussions 2020, 1-22. https://doi.org/10.5194/soil-2020-95

Zhang, W., Xing, S., Hou, X., 2019. Evaluation of soil erosion and ecological

rehabilitation in Loess Plateau region in Northwest China using plutonium isotopes. Soil Tillage Res 191, 162–170. https://doi.org/10.1016/J.STILL.2019.04.004

Chapter 5 – Plutonium isotopes can be used to model soil erosion in Kenya

This chapter was submitted to *Environmental Geochemistry and Health* on 19th March 2024.

Author contributions:

Study conceived by SMD, OSH, WHB, OO, MJW

Experiments and analysis performed by SMD & TSB

All figures produced by SMD

Construction of the paper by SMD

All authors were involved in the study and manuscript development

Dowell, S.M., Humphrey, O.S., Isaboke, J., Barlow, T.B., Blake, W.H., Osano, O., Watts, M.J. 2023. Plutonium isotopes can be used to model soil erosion in Kenya. *Environmental Geochemistry and Health*.

Supplimentary data associated with this chapter can be found in appendices section A5.

Plutonium isotopes can be used to model soil erosion in Kenya

Sophia M. Dowell [a,b], Olivier S. Humphrey [a], Job Isaboke [c], Thomas S. Barlow [a], William H. Blake [b], Odipo Osano [c], Michael J. Watts [a*]

[a] Inorganic Geochemistry, Centre for Environmental Geochemistry, British Geological Survey, Nottingham, NG12 5GG, UK

[b] School of Geography, Earth and Environmental Sciences, University of Plymouth, Plymouth, Devon, PL4 8AA, UK

[c] School of Environmental Sciences, University of Eldoret, Eldoret, Kenya

Highlights

- Land degradation in tropical soils poses a significant risk to agricultural production
- Improved understanding of erosion can aid mitigation strategies
- Plutonium isotopes were used as a tool to determine soil erosion losses in tropical soils
- The lowest rates of soil erosion were a result of locally designed solutions
- Community engagement is vital for effective soil erosion mitigation

Graphical abstract

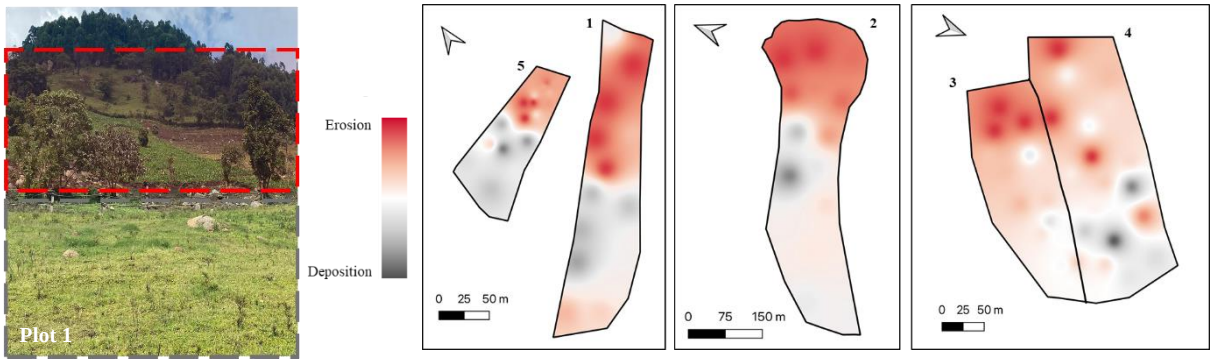

Modelling of soil erosion and deposition patterns using the MODERN model to calculate the depth of soil loss/gain.

Abstract

Climate change poses an immediate threat to tropical soils with changes in rainfall patterns resulting in accelerated land degradation processes. To ensure the future sustainability of arable land, it is essential to improve our understanding of the factors that influence soil erosion processes. This work aimed to evaluate patterns of soil erosion using the activity of plutonium isotopes (Pu) at sites with different land use and clearance scale in the Winam Gulf catchment of Lake Victoria in Kenya. Using previous work demonstrating the potential of $^{239+240}$Pu activity to trace soil erosion through the analysis of suitable reference sites, erosion rates were modelled at potential erosive sites using the MODERN model to understand small-scale erosion processes and the effect of different management practices. The lowest soil redistribution rates for arable land were 0.10 Mg ha^{-1} yr^{-1} showing overall deposition, resulting from community-led bottom-up mitigation practices. In contrast erosion rates of 8.93 Mg ha^{-1} yr^{-1} were found in areas where steep terraces have been formed; with the primary purpose of allowing farmers to use ox to plough fields resulting in an increase in soil redistribution rates. This demonstrates the significance of community-led participation in effectively managing land degradation processes. Another key factor identified in the acceleration of soil erosion rates was the clearance of land with an increased rate of erosion over three years reported (0.45 to 0.82 Mg ha^{-1} yr^{-1}) underlining the importance vegetation cover plays in limiting soil erosion processes. This novel application of fallout plutonium as a tracer, highlights the need to improve understanding of how soil erosion processes respond to land management, which will better support implementation of effective mitigation strategies. Data derived from plutonium activities in this way will aid the validation of predictive models to support future policies in translating community designed land degradation solutions.

Keywords

$^{239+240}$Pu, Soil Erosion, Kenya, MODERN model, Land Use Change, Tropical soils

1. Introduction

Accelerating soil erosion in tropical soils poses an immediate threat to land and water resources in developing nations. With the growing population in tropical Africa and with changes in weather patterns due to global warming, land degradation presents a significant obstacle to the sustainable development of agriculture (Borrelli et al., 2020; Kopittke et al., 2019). Therefore, increasing our knowledge of the processes and extent of soil erosion in tropical soils is crucial. Land cover changes and vegetation clearance are primary source of soil erosion, with a growing number of studies recognising soil erosion in tropical soils as a significant environmental concern (Flores et al., 2020; Labrière et al., 2015; Wilken et al., 2021). With the East African Rift valley's steep terrain, high rainfall erosivity, and often insufficient soil cover due to land management and increasingly changes in rainfall patterns, accelerating erosion rates are a major concern (Humphrey et al., 2022; Meshesha et al., 2012; Watene et al., 2021). As a consequence, nutrient deficiency as a result of land degradation in tropical soils poses a substantial hazard, reducing both crop yields, nutrients' uptake, and crop protection against disease. This could dramatically increase the risk of global food shortages, negatively impacting both human and animal nutrition (Hickey et al., 2012; Kogo et al., 2021). There has been limited research into the rates of soil erosion in tropical soils and consequently, there is an increasing demand for quantitative data characterising erosion amounts to enhance our understanding of erosion processes so effective mitigation strategies can be implemented. This data can also be utilised to validate prediction models, allowing for a clearer understanding of the factors that can influence erosion processes, which can also support the translation of Local Environmental Knowledge (LEK) at the community scale into national policy action (Castro et al., 2020).

Fallout radionuclides (FRNs) such as ^{137}Cs and $^{239+240}$Pu were deposited into the soil as a result of atmospheric nuclear weapons testing in the 1950's and 60's, provide an alternative to costly long-term monitoring approaches such as run off plots for soil erosion (Mabit et al., 2014; Parwada et al., 2023; Zapata, 2003). As a result of their capacity to bond strongly to soils, FRN are suited for use as soil erosion tracers and have been successfully utilised across the globe for over 20 years (Alewell et al., 2017; Schimmack et al., 2004, 2001). These techniques work by comparing the inventory (Bq per unit area) of a representative, undisturbed reference site to the inventory at a specific sampling site. By assuming that the loss of radionuclide at the reference site is only due to radioactive decay, soil erosion can be calculated from the loss of radionuclide within the sampling area (Joint FAO/IAEA, 2014). Detailing the subsequent redistribution of the FRN in the soil is a useful method for tracing erosion amounts and patterns within a landscape. Erosion is indicated by a lower FRN inventory than the reference inventory, whereas deposition is indicated by a larger FRN inventory than the reference inventory. In contrast to conventional methods, the FRN method can simultaneously analyse erosion and deposition rates during a single sampling campaign and can be used during a single sampling cycle (Alewell et al., 2017; Meusburger et al., 2018). Analysis of FRNs has proven to be an efficient and time saving way for calculating the redistribution of soil during the past 60 years, with due attention to sources of uncertainty (Parsons and Foster, 2011). These techniques have been utilised to enhance understanding of the resilience and state of agroecosystems worldwide (Alewell et al., 2014; Khodadadi et al., 2021; Lal et al., 2020; Meusburger et al., 2018; Portes et al., 2018; Wilken et al., 2021; Xu et al., 2015).

The environmental cycling behaviour of $^{239+240}$Pu is comparable to that of ^{137}Cs which has been more frequently utilised in the past, and given its advantages over ^{137}Cs, this

technique has the potential to replace the use of ^{137}Cs in tropical soils (Alewell et al., 2017; Xu et al., 2015). Due to the substantially longer half-lives of ^{239}Pu and ^{240}Pu (24110 and 6561 years, respectively), about 99% of the original activity is still present in soils, providing a significantly longer future availability than ^{137}Cs, which has a half-life of only 30 years (Muller et al., 1978; Schimmack et al., 2004). In addition, recent enhancements to analytical techniques for isotope atom counting, such as ICP-MS/MS, have boosted detection sensitivity (Dowell et al., 2023b; Zhang et al., 2021). Despite having significantly lower environmental activity, six times as many atoms of $^{239+240}$Pu were distributed from nuclear weapons testing compared to ^{137}Cs. Using alpha-particle spectroscopy and accelerator mass spectrometry (AMS), the measurement of plutonium in the environment was limited to a small number of laboratories worldwide (Esaka et al., 2017; Hrnecek et al., 2005; Varga et al., 2007). However, recent advancements in mass spectrometry techniques, such as ICP-MS, have increased the global availability of analysis, hence making the use of Pu isotopes for tracing soil erosion more appealing (Hou et al., 2019; Tiong and Tan, 2019; Xing et al., 2021; Yang et al., 2021; Dowell et al., 2023b).

Radionuclide inventory can be converted into estimated soil redistribution amounts using conversion models. Models which have been frequently used in the past include the Proportional Model (PM), Mass Balance Model (MBM), Profile Distribution Model (PDM) and Diffusion and Migration model (DDM) (Walling et al., 2011; Gharbi et al., 2020; He and Walling, 1997; Soto and Navas, 2008). Although these models are still frequently used the Modelling Deposition and Erosion rates with Radio-Nuclides (MODERN) approach proposed by Arata et al., (2016b) offers several advantages in the modelling of soil erosion by its ability to modify the depth profile of the reference location to simulate natural scenarios such as tillage, erosion, and deposition. This removes many

of the assumptions for the reference site to allow the conversion of isotope inventories into soil redistribution rates, independent of the type of land use (Arata et al., 2016a, 2016b).

Previous studies within tropical Africa have historically used ^{137}Cs and unsupported ^{210}Pb to determine soil erosion rates. In Uganda using ^{137}Cs, high soil erosion and deposition rates were reported between -21 to 25 Mg ha^{-1} yr^{-1} from using the mass balance model (Ruecker et al., 2008). In Zambia both ^{137}Cs and unsupported ^{210}Pb were used with much lower rates of soil erosion reported between -5.4 and – 0.3 Mg ha^{-1} yr^{-1} also using the mass balance model (Collins et al., 2001; Walling et al., 2003). Furthermore, Wilken et al., (2021) published work using $^{239+240}$Pu to determine soil erosion in DR Congo, Uganda, and Rwanda with rates between -51.4 and 20.2 Mg ha^{-1} yr^{-1} using the mass balance model. In this study, we aimed to determine soil erosion rates at plots with different land use and clearance scale in the Winam Gulf catchment of Lake Victoria in Kenya, with the following objectives: (1); determine the inventory of $^{239+240}$Pu isotopes at study sites in Western Kenya, (2); relate sample site inventory with reference sites to calculate rates of erosion and deposition using the MODERN model and (3); compare erosion scale according to different land use and management practices.

Accelerating soil erosion in tropical soils poses an immediate threat to land and water resources in developing nations. With the growing population in tropical Africa and with changes in weather patterns due to global warming, land degradation presents a significant obstacle to the sustainable development of agriculture (Borrelli et al., 2020; Kopittke et al., 2019). Therefore, increasing our knowledge of the processes and extent of soil erosion in tropical soils is crucial. Land cover changes and vegetation clearance are primary source of soil erosion, with a growing number of studies recognising soil

erosion in tropical soils as a significant environmental concern (Flores et al., 2020; Labrière et al., 2015; Wilken et al., 2021). With the East African Rift valley's steep terrain, high rainfall erosivity, and often insufficient soil cover due to land management and increasingly changes in rainfall patterns, accelerating erosion rates are a major concern (Humphrey et al., 2022; Meshesha et al., 2012; Watene et al., 2021). As a consequence, nutrient deficiency as a result of land degradation in tropical soils poses a substantial hazard, reducing both crop yields, nutrients' uptake, and crop protection against disease. This could dramatically increase the risk of global food shortages, negatively impacting both human and animal nutrition (Hickey et al., 2012; Kogo et al., 2021). There has been limited research into the rates of soil erosion in tropical soils and consequently, there is an increasing demand for quantitative data characterising erosion amounts to enhance our understanding of erosion processes so effective mitigation strategies can be implemented. This data can also be utilised to validate prediction models, allowing for a clearer understanding of the factors that can influence erosion processes, which can also support the translation of Local Environmental Knowledge (LEK) at the community scale into national policy action (Castro et al., 2020).

Fallout radionuclides (FRNs) such as ^{137}Cs and $^{239+240}$Pu were deposited into the soil as a result of atmospheric nuclear weapons testing in the 1950's and 60's, provide an alternative to costly long-term monitoring approaches such as run off plots for soil erosion (Mabit et al., 2014; Parwada et al., 2023; Zapata, 2003). As a result of their capacity to bond strongly to soils, FRN are suited for use as soil erosion tracers and have been successfully utilised across the globe for over 20 years (Alewell et al., 2017; Schimmack et al., 2004, 2001). These techniques work by comparing the inventory (Bq per unit area) of a representative, undisturbed reference site to the inventory at a specific sampling site. By assuming that the loss of radionuclide at the reference site is only due to radioactive

decay, soil erosion can be calculated from the loss of radionuclide within the sampling area (Joint FAO/IAEA, 2014). Detailing the subsequent redistribution of the FRN in the soil is a useful method for tracing erosion amounts and patterns within a landscape. Erosion is indicated by a lower FRN inventory than the reference inventory, whereas deposition is indicated by a larger FRN inventory than the reference inventory. In contrast to conventional methods, the FRN method can simultaneously analyse erosion and deposition rates during a single sampling campaign and can be used during a single sampling cycle (Alewell et al., 2017; Meusburger et al., 2018). Analysis of FRNs has proven to be an efficient and time saving way for calculating the redistribution of soil during the past 60 years, with due attention to sources of uncertainty (Parsons and Foster, 2011). These techniques have been utilised to enhance understanding of the resilience and state of agroecosystems worldwide (Alewell et al., 2014; Khodadadi et al., 2021; Lal et al., 2020; Meusburger et al., 2018; Portes et al., 2018; Wilken et al., 2021; Xu et al., 2015).

The environmental cycling behaviour of $^{239+240}$Pu is comparable to that of ^{137}Cs which has been more frequently utilised in the past, and given its advantages over ^{137}Cs, this technique has the potential to replace the use of ^{137}Cs in tropical soils (Alewell et al., 2017; Xu et al., 2015). Due to the substantially longer half-lives of ^{239}Pu and ^{240}Pu (24110 and 6561 years, respectively), about 99% of the original activity is still present in soils, providing a significantly longer future availability than ^{137}Cs, which has a half-life of only 30 years (Muller et al., 1978; Schimmack et al., 2004). In addition, recent enhancements to analytical techniques for isotope atom counting, such as ICP-MS/MS, have boosted detection sensitivity (Dowell et al., 2023b; Zhang et al., 2021). Despite having significantly lower environmental activity, six times as many atoms of $^{239+240}$Pu were distributed from nuclear weapons testing compared to ^{137}Cs. Using alpha-particle

spectroscopy and accelerator mass spectrometry (AMS), the measurement of Pu in the environment was limited to a small number of laboratories worldwide (Esaka et al., 2017; Hrnecek et al., 2005; Varga et al., 2007). However, recent advancements in mass spectrometry techniques, such as ICP-MS, have increased the global availability of analysis, hence making the use of Pu isotopes for tracing soil erosion more appealing (Hou et al., 2019; Tiong and Tan, 2019; Xing et al., 2021; Yang et al., 2021; Dowell et al., 2023b).

Radionuclide inventory can be converted into estimated soil redistribution amounts using conversion models. Models which have been frequently used in the past include the Proportional Model (PM), Mass Balance Model (MBM), Profile Distribution Model (PDM) and Diffusion and Migration model (DDM) (Walling et al., 2011; Gharbi et al., 2020; He and Walling, 1997; Soto and Navas, 2008). Although these models are still frequently used the Modelling Deposition and Erosion rates with Radio-Nuclides (MODERN) approach proposed by Arata et al., (2016b) offers several advantages in the modelling of soil erosion by its ability to modify the depth profile of the reference location to simulate natural scenarios such as tillage, erosion, and deposition. This removes many of the assumptions for the reference site to allow the conversion of isotope inventories into soil redistribution rates, independent of the type of land use (Arata et al., 2016a, 2016b).

Previous studies within tropical Africa have historically used ^{137}Cs and unsupported ^{210}Pb to determine soil erosion rates. In Uganda using ^{137}Cs, high soil erosion and deposition rates were reported between -21 to 25 Mg ha^{-1} yr^{-1} from using the mass balance model (Ruecker et al., 2008). In Zambia both ^{137}Cs and unsupported ^{210}Pb were used with much lower rates of soil erosion reported between -5.4 and – 0.3 Mg ha^{-1} yr^{-1} also using the

mass balance model (Collins et al., 2001; Walling et al., 2003). Furthermore, Wilken et al., (2021) published work using $^{239+240}$Pu to determine soil erosion in DR Congo, Uganda, and Rwanda with rates between -51.4 and 20.2 Mg ha^{-1} yr^{-1} using the mass balance model. In this study, we aimed to determine soil erosion rates at plots with different land use and clearance scale in the Winam Gulf catchment of Lake Victoria in Kenya, with the following objectives: (1); determine the inventory of $^{239+240}$Pu isotopes at study sites in Western Kenya, (2); relate sample site inventory with reference sites to calculate rates of erosion and deposition using the MODERN model and (3); compare erosion scale according to different land use and management practices.

2. Materials and methods

2.1 Study area

This study was carried out in the Oroba valley, located in the escarpment of the rift valley on the border of the Nandi and Kisumu Counties, Kenya (*Figure 1*). The valley banks onto the Oroba river which eventually drains into the Winam Gulf of Lake Victoria. The soils on the north westerly side of the valley are brown Acrisols which make up plots 1, 3, 4 and 5. The soils within plot 2 are red brown Cambisols. This valley was indicated to be at increased risk of erosion by Humphrey et al., (2022) and it has experienced a range of different management practices alongside continuous land clearance over the past 80 years so presented an ideal semi-natural laboratory to evaluate the Pu tracer in a tropical context. Along the valley, 6 suitable reference sites were selected according to the guidelines set out by Joint FAO/IAEA, (2014). The reference site data used in this study has been previously published by Dowell et al., *2024*. Samples which had undetectable $^{239+240}$Pu or had inventories which exceeded the MODERN confidence limits were excluded from the modelling process (*Supplementary Table 1*).

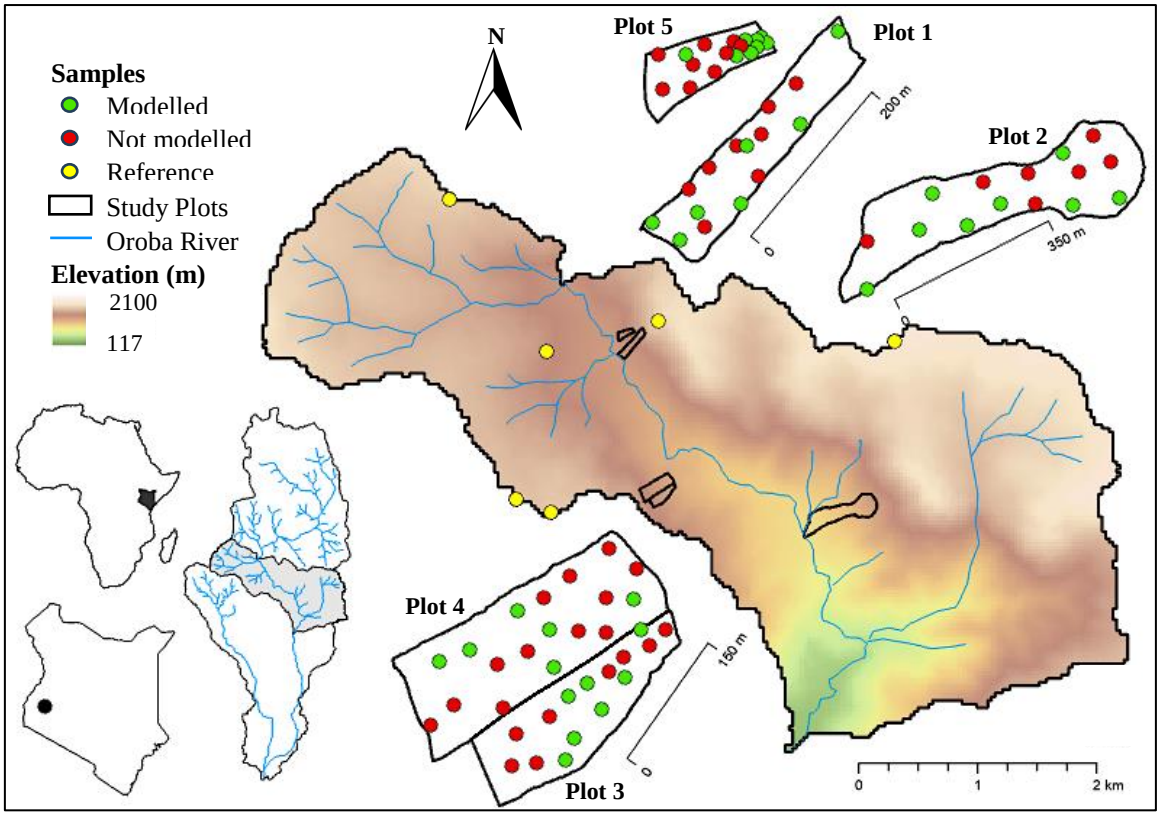

Figure 1 - Elevation map of sample location within the upper Oroba river catchment, Nandi County, Kenya. "Not modelled" samples either had undetectable 239+240Pu activity concentrations or inventories which exceeded the MODERN confidence limits (Supplementary Table 1).

.

The Oroba valley has experienced land use change and significant clearance over the past 100 years to create many smallholdings which support the people living in and around the valley. This valley is characteristic of agricultural soils in the Rift Valley escarpment and provides a representative view of erosion processes in the area. Many of the originally cleared plots have seen significant erosion events leading to further clearance of the valley to sustain the local people; a perpetual cycle often seen in the tropics. With the valley's steep slopes, increasing rainfall, and changes in land cover, these sites are at high risk of erosion, posing a substantial challenge to the 'sustainable intensification' of agriculture in the area (Borrelli et al., 2020, 2017). For this reason, the valley was selected as an ideal study location to demonstrate the applicability of the plutonium erosion model with MODERN in tropical environments and to predict erosion extent according to different land use within the Winam Gulf catchment of Victoria.

Through evaluating erosion patterns and differences across land management practice within the valley, this cycle of clearance and subsequent degradation of the soils can be further understood and communicated to local stakeholders, to improve our understanding of the effectiveness of mitigation strategies and break the cycle. Within the valley, five study sites were selected according to differing land use, management, and clearance scale (Figure 2).

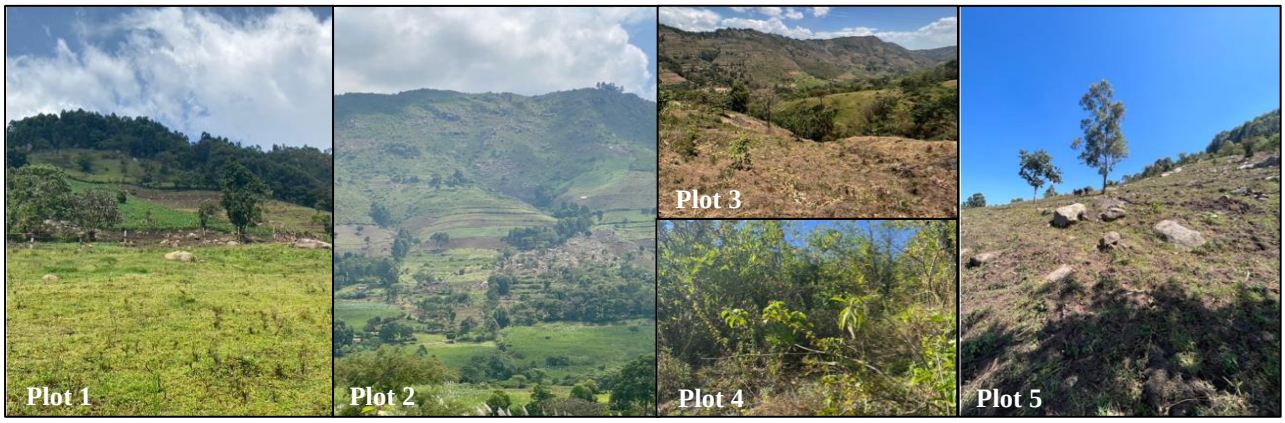

Figure 8 - Images detailing the land use, slope, and condition of the five study plots.

The first four plots were sampled in October 2021 while plot 5 was sampled in January 2023. The first of the four plots was cleared of natural vegetation over 80 years and during the past decades farmers have been continually adapting their mitigation strategies based on observational evidence and peer-to-paper Local Environmental Knowledge (LEK) exchange to avoid soil erosion. This includes the use of drainage ditches, cover and companion crops, and crop rotation. The land is hand ploughed using a hoe with a plough depth of approximately 6 cm. The average slope of the plot is 23° with the greatest slopes towards the top of the plot at 33° (*Table 1 & Figure 3).* The slope has a flat top with a sheer drop at the edge. The top of plot 1 is an example of a suitable reference location (Dowell et al., 2024).

Plot 2 which was cleared at the same time as plot 1, is utilising terraces that were fabricated primarily to allow farmers to use ox to plough the fields. This was done by creating strips through the movement of soil into dips in the landscape which were created using large boulders. The overall slope of the top half of plot two was very steep with slopes up to 38°. While terracing as a practice implies erosion control, in this case the terraces remained relatively steep with slopes up to 33° and delineated using large rocks, noting the primary purpose was to create units that were amenable to plough by oxen rather than by hand in site 1. The site features areas of rocky outcrops where significant erosion events have occurred in the past. Towards the bottom of the slope the area is dominated by sugar cane crop (Saccharum officinarum) and slopes are a lot shallower with an average slope of 14°.

Table 2 - Descriptions of study plots selected to demonstrate soil erosion according to differing land use and clearance scale

	Plot 1	**Plot 2**	**Plot 3**	**Plot 4**	**Plot 5**
Year of first cultivation	1940	1940	2019	N/A	2003
Sampling year	2021	2021	2021	2021	2023
Mitigation practices	Community led adaptation of mitigation based on observational evidence including drainage ditches, cover/companion crops & crop rotation	Terraces formed through the movement of soil into dips with large boulders for the purpose of creating a flat surface to be plough by oxen rather than by hand	Since clearance there has been no mitigation measures implemented	Remains uncleared for the most part	Since clearance the land was not used for cultivation until 2022 and there have been no mitigation measures implemented
Plough technique	Hand ploughed using a hoe	Oxen plough	Hand ploughed using a hoe	N/A	Hand ploughed using a hoe
Section 1					
Slope	33.4°	37.8°	27.2°	27.9°	35.6°
Land use	Grazing	Terrace planting	Maize/Beans crop	Uncleared	Maize/Beans crop
Section 2					
Slope	28.1°	32.2°	20.9°	26.2°	33.4°
Land use	Maize/Beans crop	Terrace planting	Maize/Beans crop	Uncleared	Maize/Beans crop
Section 3					
Slope	25.6°	20.5°	17.6°	20.2°	28.1°
Land use	Maize/Beans crop	Leafy vegetables	Maize/Beans crop	Grazing	Maize/Beans crop
Section 4					
Slope	15.5°	13.8°	13.2°	18.1°	25.6°
Land use	Grazing	Grazing	Maize/Beans crop	Uncleared	Maize/Beans crop
Section 5					
Slope	14.0°	9.8°	9.8°	10.6°	15.5°
Land use	Grazing	Sugar cane	Maize/Beans crop	Uncleared	Maize/Beans crop

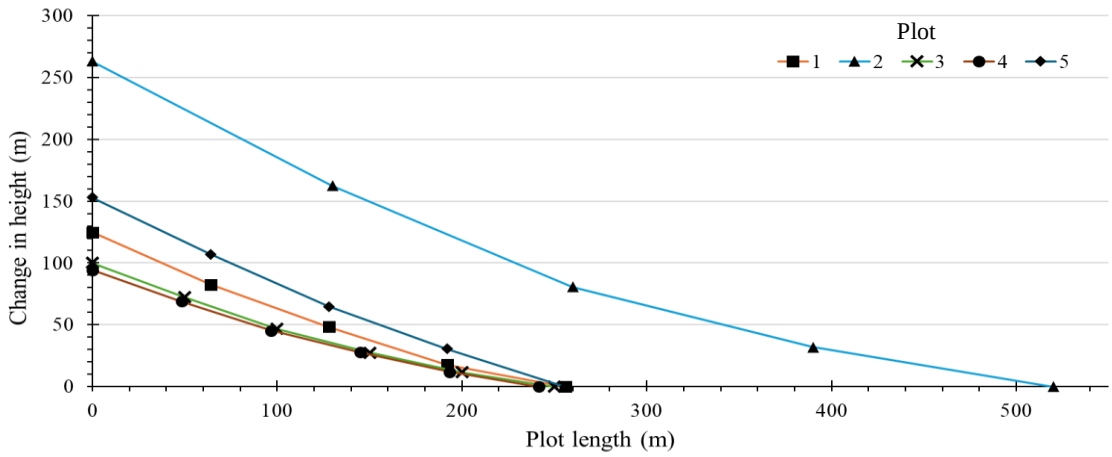

Figure 3 - Slope gradients across the 5 study sites

Plots 3 and 4 are located on the opposite side of the valley and adjoin each other. Plot 3 was cleared to be used for various crops, including maize (Zea mays) and beans (Phaseolus vulgaris L.) in 2019. Since this clearance there has been no mitigation measures implemented. Plot 3 was re-sampled in January 2023 to assess the temporal changes in soil erosion due to land clearance. On the other hand, plot 4 remains uncleared for the most part and is dominated by native shrubs and grass. The average slope of the two plots is 20°.

Plot 5 had similar topography to plot 1 and is farmed by the same family with the most major difference being the management practices in place. Plot 5 was cleared for cultivation in 2003, however, the land was then not farmed again until 2022 and during this time no land management practices were put in place. The steepest section of the plot was towards the top with slopes up to 36°, whereafter the slope levels off to give slopes similar to plot 1 towards the bottom of 16°.

2.2 Soil sampling design

At each reference site a 30 cm core with a 5 cm diameter was excavated using a bulk density tin by digging a pit and inserting the bulk density tin with a diameter of 5 cm and

a height of 3 cm into the pit wall. The reference core comprised of 10 individual stacked samples to determine the $^{239+240}$Pu depth profile at the reference site where the sampling depth exceeded the depth to which fallout Pu had reached (Dowell et al., *2024*). To collect the soils at the sample sites, three cores were collected down to a depth of 60 cm (split into 20 cm increments) using a bucket auger where the depth ensured the entire inventory of Pu had been captured. At each site, the cores were combined and homogenised to create one composite sample representative of each depth increment at that site. The bulk density was determined following sample drying at 30°C and then the sample was sieved to <2 mm before reweighing to determine the soil density using the known volume of the bulk density tin. In addition, detailed depth profiles were determined at one erosion site and one deposition site within plot 1 using the same method as for the reference sites collected.

2.3 Analysis of plutonium isotope activity in soil samples

A detailed description of the analytical procedure used for ICP-MS/MS analysis is provided elsewhere (Dowell et al., 2023a). In brief, before analysis, the soils were milled to a fine powder with 50 g of each sample being weighed into a glass beaker and then ashed overnight in a furnace at 550°C. The ashed samples were then placed into a PTFE beaker and spiked with 50 pg of a ^{242}Pu spike. To the soil mixture 100 ml of concentrated HNO_3 was added to leach the Pu isotopes. The soil solution was then heated on a hotplate for 24 hours at 70°C. Subsequently the solution was centrifuged at 3000 rpm for 15 minutes and the resultant supernatant was then collected and filtered through a 0.45 μm hydrophilic PTFE filter. To the residual soil pellet in the centrifuge tube, 100 ml of water was added and then the pellet was redistributed into the water before being centrifuged again. The additional supernatant was then filtered and added to the sample, adjusting the concentration of HNO_3 to 8 M. To convert the oxidation state of Pu to IV for separation,

4 g of $NaNO_2$ was added to the leachate solution. The Pu isotopes were then separated from the matrix and interfering isotopes using a column containing TEVA resin. Within each analytical batch two silica sand column blanks (20 g) and CRM sample IAEA 384 (0.5 g) were also prepared to determine detection limits for the method (0.108 ± 0.105 pg kg^{-1} $^{239+240}Pu$; n = 32) and assess the accuracy and precision of the separation (114 ± 12 Bq kg^{-1} measured; n=36 versus certified value of 108 ± 13 Bq kg^{-1}).

The $^{239+240}Pu$ isotope concentrations in the soil were then analysed using ICP-MS/MS with O_2 gas in the collision-reaction cell to mass shift Pu isotopes away from any $^{238}U^{1}H^{+}$ interferences (Agilent 8900, Agilent Technologies, Japan). The sample was introduced using an Agilent IaS micro-autosampler and a Cetac Aridus II desolvating nebuliser (Teledyne CETAC Technologies, Omaha, USA). The instrument was auto-tuned using the Agilent Masshunter software using a 1 μg kg^{-1} tune solution (SPEX CertiPrep #CL-TUNE-1) for general performance (Dowell et al., 2023a). For samples which had $^{239+240}Pu$ below the detection limit the reported values were calculated according to the limit of detection divided by 2 (0.09 pg Kg^{-1}). Concentrations of Pu (pg kg^{-1}) were then converted to mass activity using the specific activity for each Pu isotope.

2.4 Quantitative model for estimating soil erosion rates

The mass activities (Bq kg^{-1}) of the FRNs were first converted into areal activities (Bq m^{-2}) using the measured mass depth of the <2mm soil fraction (kg m^{-2}). Total inventories at each of the sites were then calculated from the sum of total $^{239+240}Pu$ areal activities down the depth profile. Total inventories determined at the sampling sites were then converted into estimated rates of erosion by using the Modelling Deposition and Erosion rates with Radio-Nuclides (MODERN) model (Arata et al., 2016a, 2016b). Soil erosion and deposition derived from the MODERN model are expressed as rates in terms of the thickness of the soil layer impacted by soil redistribution processes. This is achieved by

matching the complete inventory of the sample site with the depth profile of the reference site to calculate the depth of soil loss or gain. The point of intersection of the sample on the depth profile of the reference site indicates the model's solution which can then be converted to erosion or deposition. The MODERN model offers advantages over other modelling techniques as it allows for the simulation of different agricultural activities by modelling erosion, and deposition at the reference site, to ensure the reference and sampling sites are comparable to one another (Arata et al., 2016a, 2016b).

In this study, two different adaptations were applied to the reference site depth profile of $^{239+240}$Pu inventory to account for both erosion and deposition scenarios of the studied sites. For eroded sites 10 additional smoothed layers were added to the reference profile to where an exponential smoothing of FRN inventories is simulated to a new depth of 60 cm. This allows the MODERN model to find a solution when the sample site has a FRN inventory less than the FRN inventory of the last layer of the reference profile (Arata et al., 2016b). The second adaptation simulates an additional six depositional layers added to the top of the depth profile to model deposition at the sites. These additional layers were created using of an average of the top two reference site layers, equivalent to the plough depth of 6 cm. Where the inventory of $^{239+240}$Pu exceeded the modelled reference inventory with additional layers, the sample was not modelled as the total inventory exceeded the MODERN confidence limits (*Supplementary table 1*). This technique is based on the following assumptions: (1) the plutonium isotopes in the research region originate from global nuclear weapon fallout; (2) the reference site has the same depth distribution of $^{239+240}$Pu; and (3) deposition at sample sites originates from the plough depth of the reference sites.

The MODERN model provides results in terms of cm of soil losses/gains (*x*'). These results can then be converted to soil erosion/deposition rates as Mg ha^{-1} yr^{-1} (Y) using the following equation:

$$Y = 10 \times \frac{x' \times xm}{d(t_1 - t_0)}$$

Where *x*m is the mass depth of the soil at the sample site (kg m^{-2}), d is the entire depth increment measured at the sampling site, t_1 is the year of sampling (yr), and t_0 (yr) is the year of the main radionuclide fallout; typically, 1963 for $^{239+240}$Pu (Arata et al., 2016a, 2016b).

3. Results and discussion

3.1 Depth distribution of $^{239+240}$Pu in soils

The coefficient of variation and allowable error (as proposed by Sutherland, (1996)), for the $^{239+240}$Pu reference sites was 11%, and 9%, respectively, meeting the requirement to be used as a suitable reference inventory for the site (Dowell et al., 2024). *Figure 4* shows the average depth distribution of $^{239+240}$Pu at the reference sites as well as an example depth profile of an erosional and depositional site collected within plot 1. The reference sites follow a polynomial function with the maximum areal activities found between a depth of 6 - 9 cm. Thereafter the areal activities at the reference site decreased exponentially. This has been demonstrated previously as a common pattern of depth distribution, which can be explained by the downward migration of $^{239+240}$Pu isotopes in the soil subsequently to the main fallout from nuclear tests in the 1950/60s (Alewell et al., 2017, 2014; Lal et al., 2013; Zhang and Hou, 2019). The $^{239+240}$Pu areal activities in the reference sites' surface soils (0 – 6 cm) of the reference sites range from 3.82 to 5.75 Bq m^{-2} with total inventories ranging from 13.76 to 21.01 Bq m^{-2}. The mean inventory of the six reference sites was 18 Bq m^{-2} which is consistent with the fallout estimations by

Hardy et al., (1973) and Kelley et al., (1999) for the study region of 19.2 Bq m^{-2}, further supporting the validity of the reference site measurements.

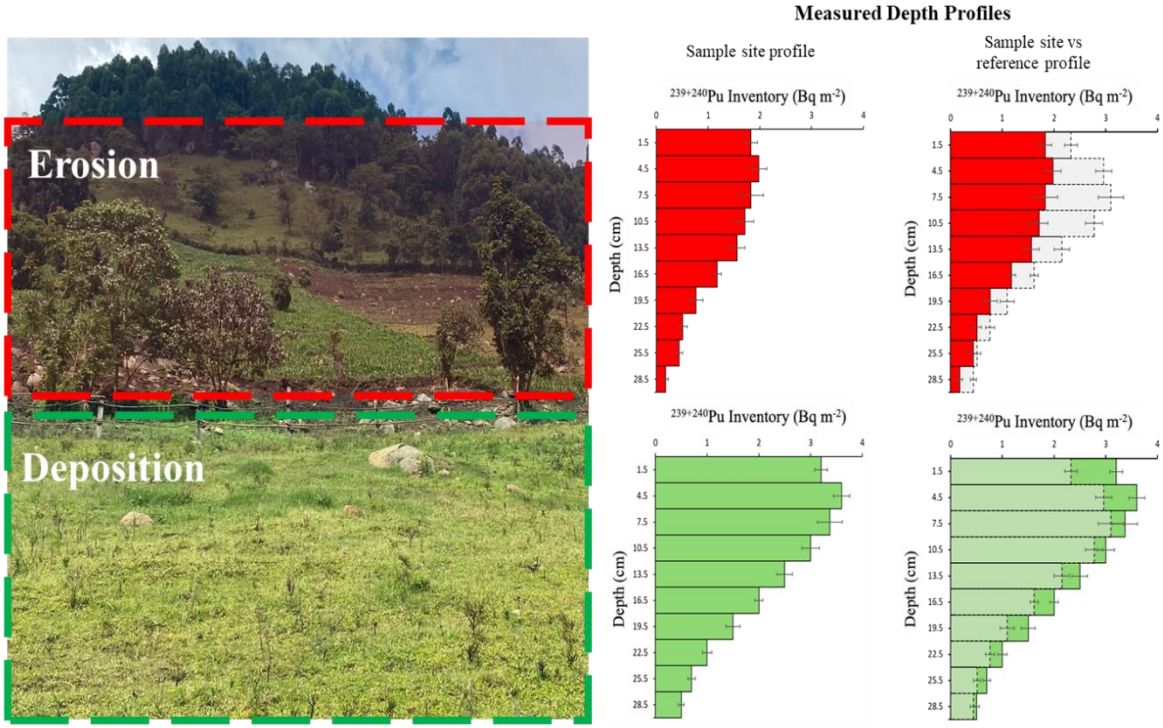

Figure 4 - Depth profiles of eroded and deposited soil patterns compared to the depth profile of the reference sites within plot 1

Depth profiles at the erosion and deposition sites within plot 1 showed similar patterns with maximum areal activities found between 3 – 6 cm. The top three layers of the depth profile show a similar areal activity relating to the plough depth of 6 cm which has resulted in mixing of the soil layers overtime. Thereafter the depth profiles of $^{239+240}$Pu at the sampling sites decreased exponentially. The increase in total inventory at the deposition site and the increased areal activity at 30 cm shows the addition of soil layers to the top of the profile. Similarly, this can also be seen for the erosional site where the areal activity at 30 cm suggests that soil layers have been lost towards the top of the profile. The total inventories for the erosion and deposition sites collected within plot 1 were 11.98 Bq m^{-2} and 22.37 Bq m^{-2} respectively. The isotope ratio of ^{240}Pu/^{239}Pu was also measured alongside the $^{239+240}$Pu activities for each sample where all sampling sites

had a ratio of 0.18 ± 0.02 which agrees with the stratospheric global fallout ratio of 0.18 ± 0.014 (Kelley et al., 1999).

3.2 Inventory and distribution of plutonium in soils

Within plot 1 the difference between inventory and reference site ranged from -33% to 30% with three sites showing a negative change in inventory indicating erosion with total inventories of 11.98 - 15.13 Bq m^{-2} and two sites showing a positive change in inventory indicating deposition with total inventories of 21.58 – 23.49 Bq m^{-2} (*Figure 5&6*). Plot 2 which was cleared at the same time as plot 1 but with engineering of terraces to create units for ox ploughing saw a much greater range of inventory difference to reference from -76% to 26%. Within the plot, a total of seven sites showed a negative change in inventory (4.23 – 17.89 Bq m^{-2}) and two showed a positive change (21.28 – 24.46 Bq m^{-2}). Most of the eroded sites (71%) were found within the terraces towards the top of the plot where the steepest topography is found with the depositional sites being found towards the bottom of the plot where sugar cane is grown, which was less steep.

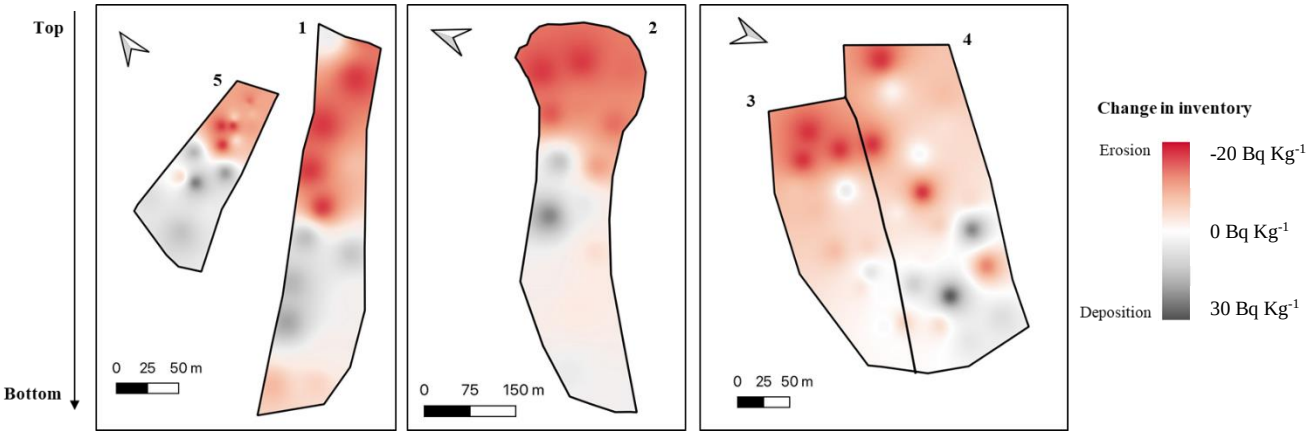

Figure 5 - Erosion sensitivity map of study sites within the Oroba Valley, Nandi County, Kenya.

Within plot 5 the difference in inventory ranged from -63% to 5% with total inventories between 6.67 and 18.82 Bq m^{-2}. The lowest inventories were found towards the top of the plot with a gradual increase towards the bottom of the plot.

Plots 3 and 4, located adjacent to each other, showed similar soil redistribution patterns of soil redistribution but plot 3 had notably greater amounts compared to plot 4. Plot 3 had inventory changes between -22% and 9% with five sites showing a negative change in inventory (14.01 – 17.14 Bq m^{-2}) and two sites showing a positive change in inventory (18.63 – 19.55 Bq m^{-2}). Plot 4 had a similar range of inventory changes from -22% to 16% with two sites showing erosion (14.10 – 16.27), one with a similar inventory as the reference site (17.93 Bq m^{-2}) and three sites showing deposition (18.40 – 20.81 Bq m^{-2}). With these two sites being historically very similar, the main variation being that plot 3 was cleared in 2019 while plot 4 remains uncleared, demonstrating the increase in erosion as a result of clearance and land use change.

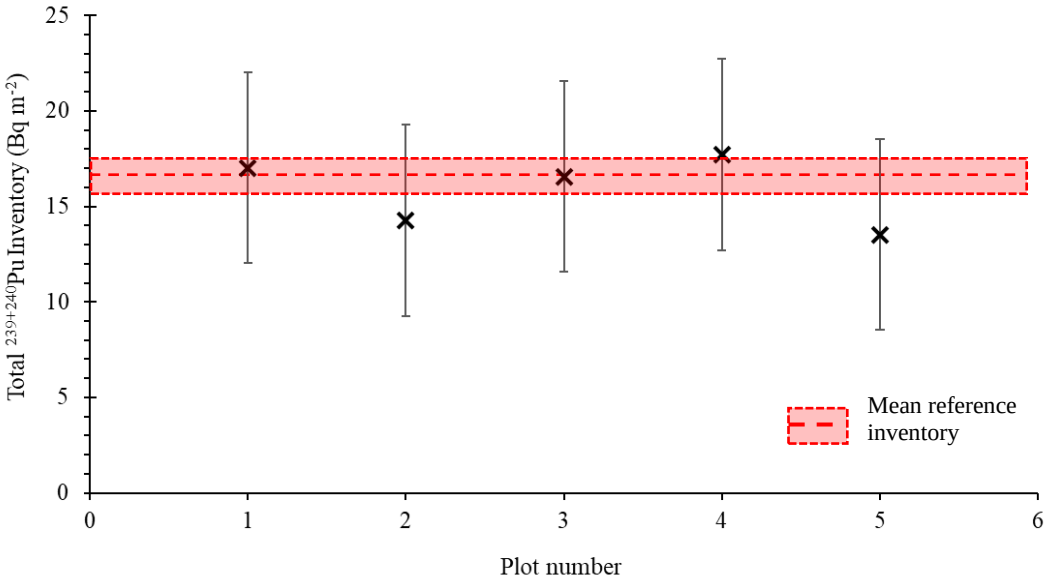

Figure 6 - 239+240Pu mean inventory, where uncertainty is standard deviation, of sample sites compared to the reference site.

3.3 Comparison of soil erosion rate estimates

The soil redistribution rates, determined using the MODERN model, for each plot are shown in *Table 2.* The highest soil erosion rate was found within the terraced area of plot 2 where estimates of erosion were between 5.44 and 9.41 Mg ha^{-1} yr^{-1}. This area had the

steepest hill slopes and towards the bottom of plot 2 where slopes were much more moderate redistribution rates were between -5.44 and 8.07 Mg ha^{-1} yr^{-1}. In contrast plot 1 which was cleared at the same time showed redistribution rates between -4.41 and 6.52 Mg ha^{-1} yr^{-1}. Within plot 5 soil redistribution rates were between -11.20 and 6.46 Mg ha^{-1} yr^{-1}.

Plots 3 and 4 showed varying rates of soil erosion with plot 3 showing a greater overall extent of erosion compared to plot 4. Plot 3 saw redistribution rates between -2.12 to 2.76 Mg ha^{-1} yr^{-1} while plot 4 had rates between -2.06 to 4.02 Mg ha^{-1} yr^{-1}. This likely a result of deposition occurring within the dense native shrubs within the area due to higher infiltration capacity and reduced overland flow energy. The re-sampling of plot 3 shows the increasing rates of soil erosion as a result of land clearance. Erosion rates had increased up to 4.55 Mg ha^{-1} yr^{-1} in 2023 from 2.12 Mg ha^{-1} yr^{-1} in 2021 in some areas and towards the bottom of the plot deposition had increased to 5.47 Mg ha^{-1} yr^{-1} from 2.76 Mg ha^{-1} yr^{-1}. Overall, within the plot the rates of erosion were 0.37 Mg ha^{-1} yr^{-1} higher which is equivalent to an additional half a tonne of soil loss within the area of plot 3 every year.

The rates of erosion determined within the valley are comparable with reported values using ^{137}Cs and unsupported ^{210}Pb in Zambia, with erosion rates between -5.4 and -0.3 Mg ha^{-1} yr^{-1} (Collins et al., 2001; Walling et al., 2003). The only other study using $^{239+240}Pu$ in tropical African soils found rates found much greater values for both erosion and deposition with rates between -51.4 and 20.2 Mg ha^{-1} yr^{-1}.

Table 2 - Net contribution of soil redistribution rates at sample sites within the Oroba valley, western Kenya (± σ)

	Plot 1	**Plot 2**	**Plot 3**	**Plot 4**	**Plot 5**
Year of first cultivation	1940	1940	2019	N/A	2003
Sampling year	2021	2021	2021	2021	2023
Mitigation practices	Community led	Terraces	None	N/A	None
Number of sampling sites	7	9	7	6	8
Soil redistribution depth (cm)	0.60 ± 8.30	-2.89 ± 11.31	-0.77 ± 3.40	1.26 ± 3.91	-4.29 ± 7.06
Soil redistribution rates (Mg ha^{-1} yr^{-1})	0.30 ± 4.82	-1.66 ± 6.50	-0.45 ± 1.96	0.72 ± 2.25	-3.58 ± 5.89

Rates of soil erosion within the Winam Gulf have previously been estimated using the RUSLE (Revised Universal Soil Loss Equation) model by Humphrey et al., (2022) with estimated erosion rates between 0 and 14.50 Mg ha^{-1} $year^{-1}$ within the Oroba valley. The overall erosion rates determined using $^{239+240}$Pu and the MODERN model were 2 – 3 times lower than the rates calculated using the RUSLE model. However, RUSLE does not take into consideration deposition within the site which skews the results in favour of erosion processes. Furthermore, the RUSLE prediction calculated by Humphrey et al., (2022) did not include the P factor (support practice layer), which could lead to the model overestimating the loss rates as seen. *Figure 7* shows the relationship between rates predicted using the RUSLE model and the $^{239+240}$Pu with MODERN model. Additionally, the RUSLE model demonstrated the potential to be reliable to aid with the selection of appropriate reference sites. Overall, the predicted rates of erosion at the selected reference sites were 0.5 Mg ha^{-1} yr^{-1} with 4 out of the 6 reference sites having a predicted rate of 0 Mg ha^{-1} yr^{-1}.

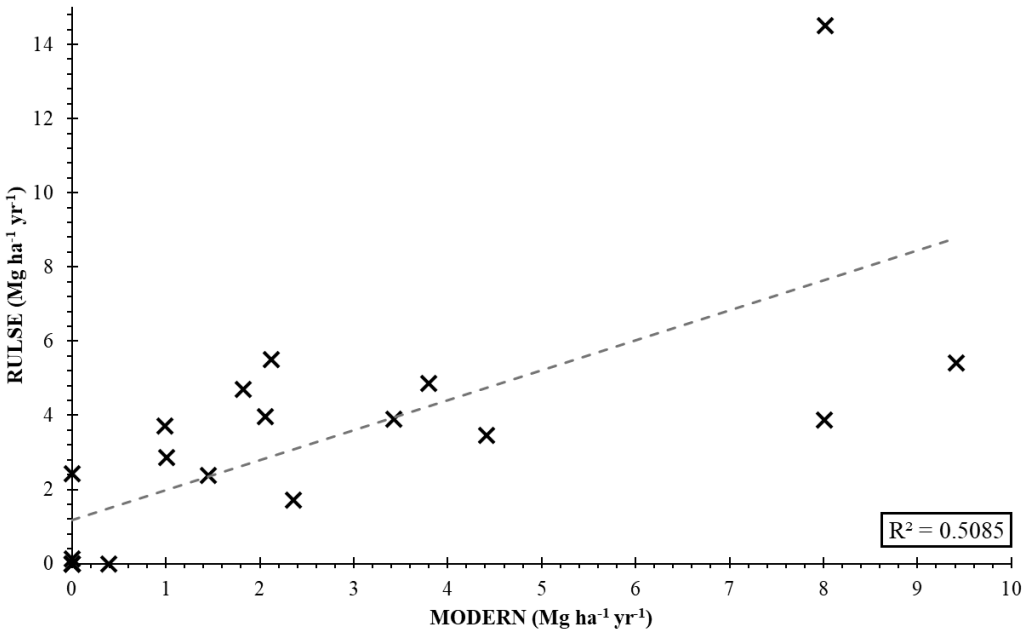

Figure 7 - Comparison of predicted soil erosion rates calculated using the RUSLE and MODERN ($^{239+240}$Pu) models within the Oroba valley.

3.4 Land use and management effect on soil erosion rates

Due to the relatively small sampling area (40 km^2) the plots have experienced historically similar rainfall and weather patterns. Across the different plots, the greatest rates of erosion were observed within plot 2 in the areas where the land had been terraced to support ploughing of larger scale land parcels. These terraces are primarily formed by moving large boulders that demark the land parcels but still have slopes up to 33°. Soil movement within these plots may be related to the movement of soil to create the terraces, however, while movement of soil could over time lead to formation of more level terrace surfaces in line with slow forming terrace principles, the net loss of trace inventory from these slopes implies material is still being transferred downslope. This has implications for soil health in the long term possibly resulting from the effects of tillage erosion (Kagabo et al., 2012; Kraemer et al., 2019). This is also demonstrated by the large areas of the land have been denuded and are no longer productive where there is a visible exposure of the bedrock.

In comparison, Plot 1 which was cleared around the same time with similar slopes of 33° saw much lower rates of soil erosion. The main difference between the two plots is that in plot 1 the farmers have implemented mitigation strategies around their farming practices including the use of drainage ditches to channel run off water away from the crop beds and rotation of crops with mixed pastoral farming adding to soil resilience through addition of organic matter (Joshi et al., 2021; Kimaro et al., 2012). The farmers are very active in preserving the land which is reflected by the low rates of erosion, despite the severe weather conditions and steep slopes. Additionally, the relatively higher rates of soil erosion seen within plot 5 where no land management practices are in place reiterates the import role soil mitigation practices play in the limitation of land degradation. The effectiveness of community engagement within plot 1 shows the importance it has on implementing successful change. The low overall rates of erosion suggest that the area could be potentially sustainable for agriculture with the correct management of the land.

Plots 3 and 4 show how land clearance affects the acceleration of soil erosion rates within the valley. With plot 3 being cleared in 2019 and plot 4 remaining uncleared the two plots model the change in soil redistribution as a result of erosion. The farmers managing plot 3 are not using any mitigation practices and reported in 2023 that the soil is progressively becoming less productive. This observation is supported by the increased rates of erosion determined in 2023 of 0.82 Mg ha^{-1} yr^{-1}, with rates in some areas reaching 5.47 Mg ha^{-1} yr^{-1} (*Table 3*). Overall, the soil is more eroded than plot 4 which generally showed deposition processes dominated. This is likely from soil redistribution from runoff of both plot 3 and cleared land above the uncleared area, demonstrating the ability of intact vegetation cover in preventing the extent of redistribution processes. The data indicates the importance of strengthening the resilience of complex soil erosion challenges to

achieve change towards a more sustainable future for tropical soils which are at risk as a result of changing weather conditions and growing pressure on land resources. Empirical estimates of soil erosion rates, especially comparison of relative amounts between management practice, support evaluation of land degradation risk and agricultural sustainability.

Table 3 - Changes in the rate of soil erosion within plot 3 between 2021 and 2023

Sampling year	**2021**	**2023**
Soil redistribution depth (cm)	-0.77 ± 3.40	-0.99 ± 5.25
Soil redistribution rates (Mg ha^{-1} yr^{-1})	-0.45 ± 1.96	-0.82 ± 4.37

4. Conclusion

Using variation in $^{239+240}$Pu activities, this work provides the first insight into soil redistribution patterns in Kenya according to different land management and clearance scale. This work supports previous work modelling rates of soil erosion and provides a clearer image of small-scale erosion processes. The MODERN model returned rates of soil redistribution ranging from -8.93 to 7.14 Mg ha^{-1} yr^{-1} with the greatest rates of redistribution likely related to soil movement as a result of the formation of terracing and steep slopes of up to 38°. The lowest overall rates of soil erosion for arable land resulted from small-scale bottom-up mitigation practices indicating the important role that community led engagement plays in the effective control of land degradation processes. The low net contribution of erosion within the sites suggest that the area could be potentially sustainable for agriculture with effective management of the land. The accelerated erosion rates presented relating to the recent clearance of vegetation for arable farming show the important role that intact vegetation cover plays in ensuring the future resilience of tropical soils. To ensure the future sustainability of arable land and aquaculture downstream, it is necessary to address the complex mix of issues that influence the degradation of tropical soils. This work benefits our understanding of the

factors which influence soil erosion and is the first step towards supporting the integration of locally designed solutions into policy.

CRediT authorship contribution statement

Sophia M. Dowell: Conceptualisation, Methodology, Investigation, Writing – original draft. **Olivier S. Humphrey**: Conceptualisation, Validation, Methodology, Writing – review & editing. **Job Isaboke**: Methodology, Writing – review & editing. **Thomas S. Barlow:** Methodology, Writing – review & editing. **William H. Blake**: Conceptualisation, Funding acquisition, Writing – review & editing. **Odipo Osano**: Conceptualisation, Funding acquisition, Writing – review & editing. **Michael J. Watts**: Conceptualisation, Funding acquisition, Writing – review & editing.

Declaration of competing interest

The authors declare that they have no known competing financial interests or personal relationships that could have appeared to influence the work reported in this paper.

Acknowledgements

Special thanks to Thomas Barlow and Simon Chenery for ICP-MS/MS analysis of Pu in soils. This work is published with the permission of the Executive Director, British Geological Survey. The work represents contribution to the joint UN FAO/IAEA Coordinated Research Projects (CRP) "D15017: Nuclear Techniques for a Better Understanding of the Impact of Climate Change on Soil Erosion in Upland agro-ecosystems" and "D1.50.18: 'Multiple Isotope Fingerprints to Identify Sources and Transport of agro-Contaminants". This work was financially supported by the Natural Environment Research Council [grant number NE/R000069/1, NE/X006255/1,

NE/S007334/1, GA/19S/017]; the Royal Society [grant number ICA/R1/191077]; and the British Academy [grant number WW21100104].

References

Alewell, C., Meusburger, K., Juretzko, G., Mabit, L., Ketterer, ME., (2014) Suitability of 239+240Pu and 137Cs as tracers for soil erosion assessment in mountain grasslands. Chemosphere 103:274–280 https://doi.org/10.1016/j.chemosphere.2013.12.016

Alewell, C., Pitois, A., Meusburger, K., Ketterer, M., Mabit, L., (2017) 239 + 240Pu from 'contaminant' to soil erosion tracer: Where do we stand?. Earth-Science Rev 172:107–123 https://doi.org/10.1016/j.earscirev.2017.07.009

Arata, L., Alewell, C., Frenkel, E., A'Campo-Neuen, A., Iurian, A.-R., Ketterer, ME., Mabit, L., Meusburger, K., (2016a). Modelling Deposition and Erosion rates with RadioNuclides (MODERN) – Part 2: A comparison of different models to convert 239+240 Pu inventories into soil redistribution rates at unploughed sites. J Environ Radioact 162–163, 97–106. https://doi.org/10.1016/j.jenvrad.2016.05.009

Arata, L., Meusburger, K., Frenkel, E., A'Campo-Neuen, A., Iurian, AR., Ketterer, ME., Mabit, L., Alewell, C., (2016b). Modelling Deposition and Erosion rates with RadioNuclides (MODERN) – Part 1: A new conversion model to derive soil redistribution rates from inventories of fallout radionuclides. J Environ Radioact 162–163, 45–55. https://doi.org/10.1016/j.jenvrad.2016.05.008

Borrelli, P., Robinson, DA., Fleischer, LR., Lugato, E., Ballabio, C., Alewell, C., Meusburger, K., Modugno, S., Schütt, B., Ferro, V., Bagarello, V., Oost, K. Van, Montanarella, L., Panagos, P., (2017). An assessment of the global impact of 21st century land use change on soil erosion. Nat Commun 8, 2013. https://doi.org/10.1038/s41467-017-02142-7

Borrelli, P., Robinson, DA., Panagos, P., Lugato, E., Yang, JE., Alewell, C., Wuepper, D., Montanarella, L., Ballabio, C., (2020). Land use and climate change impacts on global soil erosion by water (2015-2070). Proceedings of the National Academy of Sciences 117, 21994–22001. https://doi.org/10.1073/pnas.2001403117

Castro, RB., Fabré, NN., Oliveira, AS., Oliveira Júnior, JGC., Batista, VS., (2020). Local Ecological Knowledge Networks in Tropical Artisanal Shrimp Fisheries. Res Sq. PREPRINT https://doi.org/10.21203/rs.3.rs-125962/v1

Collins, AL., Walling, DE., Sichingabula, HM., Leeks, GJL., (2001). Using 137Cs measurements to quantify soil erosion and redistribution rates for areas under different land use in the Upper Kaleya River basin, southern Zambia. Geoderma 104, 299–323. https://doi.org/10.1016/S0016-7061(01)00087-8

Dowell, SM., Humphrey, OS., Blake, WH., Osano, O., Chenery, S., Watts, MJ., (2023a). Ultra-Trace Analysis of Fallout Plutonium Isotopes in Soil: Emerging Trends and

Future Perspectives. Chemistry Africa 6, 2429–2444. https://doi.org/10.1007/s42250-023-00659-7

Dowell, SM., Barlow, TS., Chenery, SR., Humphrey, OS., Isaboke, J., Blake, WH., Osano, O., Watts, MJ., (2023b). Optimisation of plutonium separations using TEVA cartridges and ICP-MS/MS analysis for applicability to large-scale studies in tropical soils. Analytical Methods 15, 4226-4235. https://doi.org/10.1039/D3AY01030A

Dowell, SM., Humphrey, OS., Gowing, CJB., Barlow, TS., Chenery, SR., Isaboke, J., Blake, WH., Osano, O., Watts, MJ., (*2024*). Suitability of 210Pbex, 137Cs and 239+240Pu as soil erosion tracers in western Kenya. J Environ Radioact 270. https://doi.org/10.1016/j.jenvrad.2023.107327

Esaka, F., Yasuda, K., Suzuki, D., Miyamoto, Y., Magara, M., (2017). Analysis of plutonium isotope ratios including 238Pu/239Pu in individual U–Pu mixed oxide particles by means of a combination of alpha spectrometry and ICP-MS. Talanta 165, 122–127. https://doi.org/10.1016/J.TALANTA.2016.12.041

Flores, BM., Staal, A., Jakovac, CC., Hirota, M., Holmgren, M., Oliveira, RS., (2020). Soil erosion as a resilience drain in disturbed tropical forests. Plant Soil 450, 11–25. https://doi.org/10.1007/s11104-019-04097-8

Gharbi, F., AlSheddi, TH., Ammar, RB., El-Naggar, MA., (2020). Combination of 137Cs and 210Pb Radioactive Atmospheric Fallouts to Estimate Soil Erosion for the Same Time Scale. Int J Environ Res Public Health 17, 8292. https://doi.org/10.3390/ijerph17228292

Hardy, EP., Krey, PW., Volchok, HL., (1973) Global inventory and distribution of fallout plutonium. Nature 241:444–445 https://doi.org/10.1038/241444a0

He, Q., Walling, DE., (1997). The distribution of fallout 137Cs and 210Pb in undisturbed and cultivated soils. Applied Radiation and Isotopes 48, 677–690. https://doi.org/10.1016/S0969-8043(96)00302-8

Hickey, GM., Pelletier, B., Brownhill, L., Kamau, GM., Maina, IN., (2012). Preface: Challenges and opportunities for enhancing food security in Kenya. Food Secur 4, 333–340. https://doi.org/10.1007/s12571-012-0203-2

Hou, X., Zhang, W., Wang, Y., (2019) Determination of Femtogram-Level Plutonium Isotopes in Environmental and Forensic Samples with High-Level Uranium Using Chemical Separation and ICP-MS/MS Measurement. Anal. Chem 91:11553–11561 https://doi.org/10.1021/acs.analchem.9b01347

Hrnecek, E., Steier, P., Wallner, A., (2005) Determination of plutonium in environmental samples by AMS and alpha spectrometry. Appl. Radiat. Isot 63:633–638 https://doi.org/10.1016/j.apradiso.2005.05.012

Humphrey, OS., Osano, O., Aura, CM., Marriott, AL., Dowell, SM., Blake, WH., Watts, MJ., (2022). Evaluating spatio-temporal soil erosion dynamics in the Winam Gulf catchment, Kenya for enhanced decision making in the land-lake interface. Science of The Total Environment 815, 151975. https://doi.org/10.1016/j.scitotenv.2021.151975

Joint FAO/IAEA Division of Nuclear Techniques in Food and Agriculture, Soil and Water Management and Crop Nutrition Section, Vienna (Austria) 2014. Guidelines for Using Fallout Radionuclides to Assess Erosion and Effectiveness of Soil Conservation Strategies (IAEA-TECDOC--1741). International Atomic Energy Agency (IAEA)

Joshi, DR., Ghimire, R., Kharel, T., Mishra, U., Clay, SA., (2021). Conservation agriculture for food security and climate resilience in Nepal. Agron J 113, 4484–4493. https://doi.org/10.1002/agj2.20830

Kagabo, DM., Stroosnijder, L., Visser, SM., Moore, D., (2013). Soil erosion, soil fertility and crop yield on slow-forming terraces in the highlands of Buberuka, Rwanda. Soil Tillage Res 128, 23–29. https://doi.org/10.1016/j.still.2012.11.002

Kelley, JM., Bond, LA., Beasley, TM., (1999) Global distribution of Pu isotopes and 237Np. Sci. Total Environ 237–238:483–500 https://doi.org/10.1016/s0048-9697(99)00160-6

Khodadadi, M., Alewell, C., Mirzaei, M., Ehssan-Malahat, EE., Asadzadeh, F., Strauss, P., Meusburger, K., (2021) Deforestation effects on soil erosion rates and soil physicochemical properties in Iran: a case study of using fallout radionuclides in a Chernobyl contaminated area. SoilD (Preprint) https://doi.org/10.5194/soil-2021-2

Kimaro, AA., Weldesemayat, SG., Mpanda, M., Swai, E., Kayeye, H., Nyoka, BI., Majule, AE., Perfect, J., Kundhlande, G., (2012). Evidence-based scaling-up of evergreen agriculture for increasing crop productivity, fodder supply and resilience of the maize-mixed and agro-pastoral farming systems in Tanzania and Malawi. Nairobi, Kenya. https://hdl.handle.net/10568/69125

Kogo, BK., Kumar, L., Koech, R., (2021). Climate change and variability in Kenya: a review of impacts on agriculture and food security. Environ Dev Sustain 23, 23–43. https://doi.org/10.1007/s10668-020-00589-1

Kopittke, PM., Menzies, NW., Wang, P., McKenna, BA., Lombi, E., (2019). Soil and the intensification of agriculture for global food security. Environ Int 132, 105078. https://doi.org/10.1016/j.envint.2019.105078

Kraemer, N., Dercon, G., Cisneros, P., Lopez, FA., Wellstein, C., (2019). Adding another dimension: Temporal development of the spatial distribution of soil and crop

properties in slow-forming terrace systems. Agric Ecosyst Environ 283, 106543. https://doi.org/10.1016/j.agee.2019.05.002

Labrière, N., Locatelli, B., Laumonier, Y., Freycon, V., Bernoux, M., (2015). Soil erosion in the humid tropics: A systematic quantitative review. Agric Ecosyst Environ 203, 127–139. https://doi.org/10.1016/j.agee.2015.01.027

Lal R, Tims SG, Fifield LK, Wasson RJ, Howe D (2013) Applicability of 239Pu as a tracer for soil erosion in the wet-dry tropics of northern Australia. Nucl. Instruments Methods Phys. Res. Sect. B Beam Interact. with Mater. Atoms 294:577–583 https://doi.org/10.1016/j.nimb.2012.07.041

Lal R, Fifield LK, Tims SG, Wasson RJ, Howe D (2020) A study of soil erosion rates using 239Pu, in the wet-dry tropics of northern Australia. J. Environ. Radioact 211:106085 https://doi.org/10.1016/j.jenvrad.2019.106085

Mabit, L., Benmansour, M., Abril, JM., Walling, DE., Meusburger, K., Iurian, AR., Bernard, C., Tarján, S., Owens, PN., Blake, WH., Alewell, C., (2014). Fallout 210Pb as a soil and sediment tracer in catchment sediment budget investigations: A review. Earth Sci Rev 138, 335–351. https://doi.org/10.1016/j.earscirev.2014.06.007

Meshesha, DT., Tsunekawa, A., Tsubo, M., Haregeweyn, N., (2012). Dynamics and hotspots of soil erosion and management scenarios of the Central Rift Valley of Ethiopia. International Journal of Sediment Research 27, 84–99. https://doi.org/10.1016/S1001-6279(12)60018-3

Meusburger, K., Porto, P., Mabit, L., La Spada, C., Arata, L., Alewell, C., (2018) Excess Lead-210 and Plutonium-239+240: Two suitable radiogenic soil erosion tracers for mountain grassland sites, Environ. Res, 160, 195–202, https://doi.org/10.1016/j.envres.2017.09.020

Muller, RN., Sprugel, DG., Kohn, B., (1978) Erosional Transport and Deposition of Plutonium and Cesium in Two Small Midwestern Watersheds. J. Environ. Qual 7:171–174 https://doi.org/10.2134/jeq1978.00472425000700020003x

Parsons, AJ., Foster, IDL., (2011). What can we learn about soil erosion from the use of 137Cs? Earth Sci Rev 108, 101–113. https://doi.org/10.1016/j.earscirev.2011.06.004

Parwada, C., Chipomho, J., Tibugari, H., (2023). Comparison of conventional and artificial fallout radionuclide (FRNs) methods in assessing soil erosion. Sustainable Environment 9. https://doi.org/10.1080/27658511.2023.2236406

Portes, R., Dahms, D., Brandova, D., Raab, G., Christl, M., Kuhn, P., Ketterer, M., Egli, M., (2018) Evolution of soil erosion rates in alpine soils of the Central Rocky Mountains using fallout Pu and δ13C. Earth Planet. Sci. Lett 496:257–269 https://doi.org/10.1016/j.epsl.2018.06.002

Ruecker, GR., Park, SJ., Brunner, AC., Vlek, PLG., (2008). Assessment of Soil Redistribution on Two Contrasting Hillslopes in Uganda Using Caesium-137 Modelling. Erdkunde 62, 259–272. https://www.jstor.org/stable/25648129

Schimmack, W., Auerswald, K., Bunzl, K., (2002) Estimation of soil erosion and deposition rates at an agricultural site in Bavaria, Germany, as derived from fallout radiocesium and plutonium as tracers. Naturwissenschaften 89:43–46 https://doi.org/10.1007/s00114-001-0281-z

Schimmack, W., Auerswald, K., Bunzl, K., (2001) Can 239+240Pu replace 137Cs as an erosion tracer in agricultural landscapes contaminated with Chernobyl fallout?. J. Environ. Radioact 53:41–57 https://doi.org/10.1016/s0265-931x(00)00117-x

Soto, J., Navas, A., (2008). A simple model of Cs-137 profile to estimate soil redistribution in cultivated stony soils. Radiat Meas 43, 1285–1293. https://doi.org/10.1016/j.radmeas.2008.02.024

Sutherland, RA., (1996). Caesium-137 soil sampling and inventory variability in reference locations: A literature survey. Hydrol Process 10, 43–53. https://doi.org/10.1002/(SICI)1099-1085(199601)10:1<43::AID-HYP298>3.0.CO;2-X

Tiong, LYD., Tan, S., (2019) In situ determination of 238Pu in the presence of uranium by triple quadrupole ICP-MS (ICP-QQQ-MS). J. Radioanal. Nucl. Chem 322:399–406 https://doi.org/10.1007/s10967-019-06695-3

Varga, Z., Surányi, G., Vajda, N., Stefánka, Z., (2007) Determination of plutonium and americium in environmental samples by inductively coupled plasma sector field mass spectrometry and alpha spectrometry. Microchem. J 85:39–45 https://doi.org/10.1016/j.microc.2006.02.006

Walling, DE., Collins, AL., Sichingabula, HM., (2003). Using unsupported lead-210 measurements to investigate soil erosion and sediment delivery in a small Zambian catchment. Geomorphology 52, 193–213. https://doi.org/10.1016/S0169-555X(02)00244-1

Walling, DE., Zhang, Y., He, Q. (2011). Models for Deriving Estimates of Erosion and Deposition Rates from Fallout Radionuclide (Caesium-137, Excess Lead-210, and Beryllium-7) Measurements and the Development of User-Friendly Software for Model Implementation (IAEA-TECDOC--1665). International Atomic Energy Agency (IAEA)

Watene, G., Yu, L., Nie, Y., Zhu, J., Ngigi, T., Nambajimana, J. de D., Kenduiywo, B., (2021). Water Erosion Risk Assessment in the Kenya Great Rift Valley Region. Sustainability 13, 844. https://doi.org/10.3390/su13020844

Wilken, F., Fiener, P., Ketterer, M., Meusburger, K., Muhindo, DI., van Oost, K., Doetterl, S., (2021) Assessing soil erosion of forest and cropland sites in wet

tropical Africa using 239+240 Pu fallout radionuclides. SOIL., 7:399-414 https://doi.org/10.5194/soil-7-399-2021

Xing, S., Luo, M., Yuan, N., Liu, D., Yang, Y., Dai, X., Zhang, W., Chen, N., (2021) Accurate determination of plutonium in soil by tandem quadrupole icp-ms with different sample preparation methods. At. Spectrosc., 42:62–70 https://doi.org/10.46770/AS.2021.011

Xu, Y., Qiao, J., Pan, S., Hou, X., Roos, P., Cao, L., (2015) Plutonium as a tracer for soil erosion assessment in northeast China. Sci. Total Environ 511:176–185 https://doi.org/10.1016/j.scitotenv.2014.12.006

Yang, G., Zheng, J., Kim, E., Zhang, S., Seno, H., Kowatri, M., Aono, T., Kurihara, O., (2021) Rapid analysis of 237Np and Pu isotopes in small volume urine by SF-ICP-MS and ICP-MS/MS. Anal. Chim. Acta 1158:338431 https://doi.org/10.1016/j.aca.2021.338431

Zapata, F., (2003). The use of environmental radionuclides as tracers in soil erosion and sedimentation investigations: recent advances and future developments. Soil Tillage Res 69, 3–13. https://doi.org/10.1016/S0167-1987(02)00124-1

Zhang, W., Hou, X., (2019). Level, distribution and sources of plutonium in the coastal areas of China. Chemosphere 230, 587–595. https://doi.org/10.1016/j.chemosphere.2019.05.094

Zhang, W., Lin, J., Fang, S., Li, C., Yi, X., Hou, X., Chen, N., Zhang, H., Xu, Y., Dang, H., Wang, W., Xu, J., (2021) Determination of ultra-trace level plutonium isotopes in soil samples by triple-quadrupole inductively coupled plasma-mass spectrometry with mass-shift mode combined with UTEVA chromatographic separation. Talanta 234:122652 https://doi.org/10.1016/j.talanta.2021.122652

Chapter 6 – General discussion and conclusions

Supplementary data associated with this chapter can be found in appendices section A6.

The aim of this work was to advance capability using the fallout plutonium (Pu) tracer methodology as a novel tool in tropical soils to determine small scale soil redistribution patterns under a range of land use histories and management practices. Research was conducted in Kenya where in addition to challenges with traditional fallout radionuclide approaches, e.g. low levels of fallout ^{137}Cs, the sustainability of tropical agri-systems, depends on new data-led innovation for the sustainable use of one of the most important resources on Earth: soil. In recent years, it has become more crucial to understand and mitigate soil erosion in Sub-Saharan agri-systems, since it presents a risk to food security with effects on both land and in aquatic ecosystems. Established techniques for measuring soil erosion by conventional means often do not provide representativeness at scale due to work effort and consequently cost required to undertaken monitoring, hence the need to seek alternative methodologies to better understand the complex dynamics of soil erosion and deposition. One of these methodologies is the use of Fallout Radionuclides (FRN) to trace the redistribution of soil within an area. Conventional isotopes such as ^{137}Cs and ^{210}Pb$_{ex}$ have some major geographical limitations; and as a result, $^{239+240}$Pu is emerging as an excellent alternative tracer. For this reason, this thesis focusses on the optimisation of the $^{239+240}$Pu tracer method for the determination of soil erosion rates in tropical African soils to address implications of land use management on the extent of soil erosion.

The results of this work offer to improve our understanding of the driving factors for soil erosion at the escarpment of the Rift Valley region and Winam Gulf catchment of Lake Victoria in western Kenya. This can help facilitate further research into the effectiveness of mitigation strategies which can be translated into policy action. The aim of this thesis was achieved through a series of analytical experiments and method developments to compliment the application of Pu as a tracer to determine soil redistribution rates in tropical soils. The major results, in conjunction with their potential impact, recommendations for further work and conclusions, are summarised in this chapter.

Optimisation of plutonium separations for applicability to studies in tropical soils

The first objective of the study was to develop an analytical method to accurately determine low levels of fallout Pu activity concentration in tropical soils with improved separation and analysis of ultra-trace Pu isotopes. While pioneering work has suggested that global acceleration of soil erosion processes can be better understood using $^{239+240}$Pu as a soil redistribution tracer, there are specific challenges concerning the analysis of Pu in tropical soils which must first be addressed (Alewell et al., 2017). A limitation of using $^{239+240}$Pu in tropical African soils is that only 10% of atmospheric nuclear weapons tests are carried out in the southern hemisphere, resulting in Pu isotope activity being two to three times lower than in European soils where the application of $^{239+240}$Pu is much greater (Wilken et al., 2021; Zhang et al., 2021). The developed method highlights the potential of using $^{239+240}$Pu as a soil erosion tracer in areas where fallout is low due to lower atmospheric nuclear weapons tests as highlighted in *Figure 1*. Furthermore, with the concentration of U in the soils being several orders of magnitude higher than that of ^{239}Pu, polyatomic interferences, most notably uranium hydrides (UH^+), can significantly affect

ICP-MS analysis of Pu in soils. For this reason, an analytical method that ensures maximum sensitivity is essential (Xing et al., 2018).

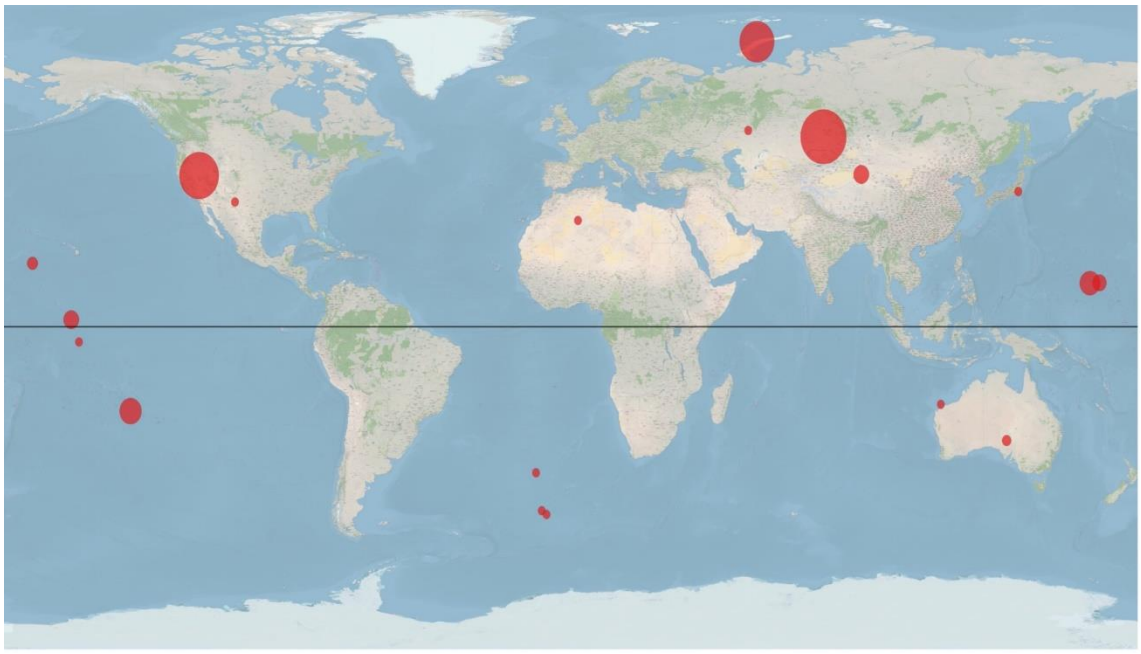

Figure 1 – Map showing the locations and number of atmospheric nuclear weapons tests and releases globally (Source - www.johnstonsarchive.net/nuclear/tests/)

Due to their low abundance in environmental samples, trace Pu isotopes must be accurately determined through a high level of enrichment before analysis. This study has shown that it is possible to optimise the extraction the Pu isotopes from the matrix and other interfering substances using specialised separation techniques. This allows for pre-concentration, which ensures maximum sensitivity (Xing et al., 2018). TEVA was selected as the resin of choice for the analytical method development as it is reported to have the maximum separation efficiency of Pu isotopes from soils. (Nygren et al., 2003; Horwitz et al., 1995). An alternative analysis method for determining Pu is ICP-MS/MS analysis using reaction cell technology, which ensures maximum sensitivity and minimises the impact of any residual U in the samples (Cao et al., 2016). By using different reaction gases in the collision-reaction cell, the major interference of $^{238}UH^{+}$ on ^{239}Pu can be eliminated. In addition, the analysis method offers enhanced abundance sensitivity, which can effectively eliminate the interference caused by ^{238}U peak tailing

on the measurement of ^{239}Pu and ^{240}Pu (Hou et al., 2019; Xu et al., 2022; Xing et al., 2021; Bu et al., 2021).

In order to ensure that the separation method is applicable to laboratories with limited resources, the research reported in Chapter 3 developed a method for the analysis of Pu isotopes using TEVA columns and ICP-MS/MS with O_2 reaction gas presenting a simple, cost-effective, robust sequence with considerations for the reduction of laboratory waste disposal. The separation method expands on earlier research employing TEVA columns, demonstrating their value in reducing the effects of U interference. Here, several processes were optimised to improve Pu recovery, including lowering the method blank concentration, ensuring a low environmental impact, and optimising the separation procedure by determining the U and Pu elution profiles. Furthermore, the investigation of $^{239+240}$Pu down a depth profile in a tropical African soil showed that the developed method could be applied to detect Pu at depths of 30 cm, where activities are exponentially lower than those in the topsoil. This indicated the potential to apply $^{239+240}$Pu as a soil erosion tracer in tropical African soils with the support of this improved analytical method.

In comparison to conventional methods of analysis such as alpha spectroscopy and AMS, analysis by ICP-MS/MS using O_2 as a reaction gas provides a reliable method with high throughput, which makes it suitable for field and survey-scale soil erosion assessment. This method proved useful for the detection of ultra-trace fallout Pu in African soils due to its low achievable detection limits of 0.18 pg kg^{-1} $^{239+240}$Pu which are comparable to those of alternative but less abundant mass spectrometric methods (e.g. AMS). The optimised separation method using TEVA cartridges reduced waste and increased throughput whilst ensuring maximum sensitivity for Pu isotopes. The specialist analysis

of $^{239+240}$Pu isotopes presents a challenge, especially to low-income countries where access to specialised instrumentation is limited, however, the method was designed with the intention that the separations could be completed in the country of sampling and then samples could be transported to specialised laboratories for analysis. Alternative methods of analysis such as alpha spectroscopy require a longer and more challenging separation process prior to analysis and the availability of specialised laboratories is limited in a similar way to ICP-MS/MS. With the limitations of using alternative fallout radionuclides such as ^{137}Cs and $^{210}Pb_{ex}$ making the isotopes unviable to large scale erosion studies, the presented method demonstrates the potential to determine soil erosion across agriculturally critical regions. Chapter 3 demonstrated a robust analytical sequence for the determination of ultra-trace level Pu isotopes with sufficient sensitivity for tropical African soil samples, which could be utilised globally in areas where $^{239+240}$Pu fallout is lower.

Suitability of $^{239+240}$Pu as a soil erosion tracer in western Kenya

Lack of effective land management practices and vegetation clearance are two of the main drivers of soil erosion, which causes escalating to land degradation every year (Borrelli et al., 2020). These concerns are even greater in tropical soils, where soil erosion could reach unsustainable levels in the future due to poor land management practices and changes in precipitation patterns influenced by climate change (Lorenz et al., 2019; Negese, 2021). Climate projections by Borrelli et al., (2020) predict that water erosion could increase globally by 30 to 66% as a result of the changing hydrological cycle and the overall increase of soil erosion by water in tropical Africa is estimated to be 4.3 Pg yr^{-1}, due to substantial clearance of land for agriculture (Borrelli et al., 2017). For many years, traditional methods have been used in Africa to assess erosion process, such as erosion plots, surveying, and aerial photography. However, these methods have several drawbacks, including poor representativeness and spatial resolution (Elwell, 1978;

Whitlow, 1988). In recent times, soil erosion rates that were indicative of all soil redistribution processes were measured using FRN tracer techniques (Alewell et al., 2017; Loba et al., 2022; Meusburger et al., 2018). The limited application of these techniques in tropical Africa is likely a result of the analytical difficulties involved in the analysis of ^{137}Cs (de Graffenried and Shepherd, 2009; Denboba, 2005; Ruecker et al., 2008). More recently, $^{239+240}$Pu has become a popular alternative tracer due to ^{239}Pu and ^{240}Pu's much longer half-lives (24100 and 6562 years respectively vs 30 years for ^{137}Cs) and improvements in ICP-MS detection of Pu in soils enabling the Pu method to be used as a tracer with applicability to tropical soils, however, until this study, this potential had yet to be fully tested and realised (Alewell et al., 2014; Schimmack et al., 2004; Wilken et al., 2021).

The second objective of the thesis deployed the Pu method in chapter 3 to demonstrate the utility of $^{239+240}$Pu as a soil erosion tracer for the evaluation of soil redistribution patterns in Kenya; overcoming regional challenges in existing FRN tracer-based approaches such as the low environmental activity of ^{137}Cs and the high spatial variability of $^{210}Pb_{ex}$. Through the determination of FRN depth profiles at reference sites, Chapter 4 illustrated the benefits of using $^{239+240}$Pu as a soil erosion tracer in western Kenya in comparison to conventional isotopes $^{210}Pb_{ex}$ and ^{137}Cs. The improved applicability of $^{239+240}$Pu compared to other FRNs could be demonstrated by identifying the robustness of each FRN. The analysis of $^{210}Pb_{ex}$ and ^{137}Cs in the samples was performed using gamma spectroscopy, and the analysis of $^{239+240}$Pu was performed using the ICP-MS/MS method described in Chapter 3. With the lowest coefficient of variation and the largest peak-to-detection limit ratio of 640, $^{239+240}$Pu demonstrated the greatest potential as an effective FRN tracer among the six reference sites. The validity and accuracy of the reference values was verified by calculating the allowable error (AE) at the 90% confidence level

as proposed by Sutherland, (1996). The only isotope to meet the allowable error criteria was $^{239+240}$Pu indicating its applicability to large-scale studies such as Western Kenya, where finding appropriate reference sites is a major challenge due to environmental constraints and the extent of land clearance (Sutherland, 1996). This success in method development can be attributed, at least in part, to the developments in ICP-MS/MS analysis developed by this study, providing greater sensitivity to enable detection to greater depths and more accurate determinations of $^{239+240}$Pu activities than for ^{137}Cs and $^{210}Pb_{ex}$.

The mean inventory of the six reference sites for $^{239+240}$Pu of 18 Bq m^{-2}, is consistent with the regional fallout estimates of 19.2 Bq m^{-2} by Hardy et al., (1973) and Kelley et al., (1999) further confirming the accuracy of the reference site measurements. The depth profile of $^{239+240}$Pu followed a polynomial function with the maximum areal activities observed between 3 and 12 cm, after which there was an exponential decrease in areal activities. In comparison to other FRN tracers, the low coefficient of variation and allowable error across the reference sites present $^{239+240}$Pu as a reliable tracer of soil erosion in western Kenya that can be applied to large-scale studies. Using $^{239+240}$Pu lowers the requirement for the number of reference sites as a result of the low allowable error, which is advantageous for study sites where choosing relevant reference sites can be difficult.

Compared to traditional methods such as sediment traps and erosion plots which do not require such specialised methods, the Pu method offers the advantage of being able to describe patterns of erosion, such as areas of deposition and erosion down a slope profile, but it also gives an insight into historical erosion rates which represent erosion which has occurred over the past 60 years. Additionally, the re-sampling of sites can facilitate the

assessment of how changes in land management and clearance effect the overall rates of erosion occurring over a shorter time frame. The fallout radionuclide methods ability to distinguish areas within a plot at increased risk of erosion can allow for the implementation of targeted mitigation which would not be possible using only the total overall erosion rate of the plot. With the need for a better understanding of land degradation rates and patterns, $^{239+240}$Pu has been shown to be a reliable tracer to assess soil erosion patterns and amounts in western Kenya. Thus, it can serve as a powerful tool to inform and validate the effectiveness of mitigation strategies by determining long term soil erosion patterns which can inform the extent of land degradation.

Modelling of soil erosion patterns in Kenya using $^{239+240}$Pu

The final objective to achieve the aim of the thesis was, to evaluate erosion dynamics, according to different land uses and recent land clearance within a typical small-scale agricultural plot of the Winam Gulf catchment of Lake Victoria using $^{239+240}$Pu. As a result of the steep terrain, high rainfall erosivity, and often insufficient soil cover, coupled with poor cultivation practices, accelerating erosion rates are becoming a major concern and implications for the long-term sustainability of soil in the East African Rift valley region of Western Kenya (Humphrey et al., 2022; Meshesha et al., 2012; Watene et al., 2021; Borrelli et al., 2020). Chapter 5 assessed the patterns of soil erosion in the Winam Gulf catchment of Lake Victoria in Kenya, using the activity of Pu isotopes at sites with varying land use and clearance scale. Within the valley, five plots were chosen, each with specific management and clearance scales. These sites were challenging due to terrain, however, provide useful examples of land management practices within the area, owing to different clearing periods for cultivation of the land. Images depicting the study plots can be found in Supplementary Figure 1.

There has been limited research into the rates of soil erosion in tropical soils and as a result, there is a growing need for quantitative data characterising the amounts of erosion to improve our understanding of the processes involved to enable the implementation of effective mitigation strategies (Wilken et al., 2021). Utilising conversion models, radionuclide inventories found within a site can be translated into estimated rates of soil redistribution by comparing them to measurements made at reference sites. The MODERN approach, by Arata et al. (2016a), has the capacity to alter the reference location's depth profile to replicate events such as tillage, erosion, and deposition; thereby eliminating assumptions regarding the reference site and providing a number of benefits for soil erosion modelling (Arata et al., 2016a; 2016b). Prior to this research the MODERN model had yet to be tested in a Sub-Saharan African context.

Across the five study sites, the MODERN model yielded rates of soil redistribution ranging from -8.93 to 7.14 Mg ha^{-1} yr^{-1}. The highest rates of redistribution were likely caused by soil movement as a result of terracing formation which have steep slopes of up to 33°. However, according to the net loss of trace inventory across the site, the movement of soil to create terraces is not completely responsible for the redistribution of soil and material is still moving downslope (-1.66 Mg ha^{-1} yr^{-1}). Plot 1 which utilised community-led bottom-up mitigation practices, such as the use of drainage ditches to channel runoff water away from the crop beds using weeds growth to stabilise the soil and the selective placement of stumps/boulders as well as crop rotation with mixed pastoral farming adding to soil resilience through the addition of organic matter (*Supplementary Figure 1*). Additionally, the farmers have been using minimal tillage since 2019. These measures resulted in the lowest rates of soil redistribution for arable land of 0.10 Mg ha^{-1} yr^{-1} showing overall deposition and indicating the efficacy of such measures in soil conservation. This illustrates how important community-led involvement is to efficiently

manage soil resources. Effective land management has the potential to make the area sustainable for agriculture, as indicated by the relatively low net contribution of erosion within the sites with a worst-case scenario of erosion rates reported at 9.41 Mg ha^{-1} yr^{-1}.

Conversely, the accelerated erosion rates observed in plot 3 following shrub clearance underscore the importance of vegetation cover in erosion prevention. The increase in soil erosion within plot 3 is equivalent to an additional half a tonne of soil is lost annually due to increased soil erosion brought on by clearance of the native shrubs and a lack of land management practices. These findings suggest that community-led involvement and practices such as minimal tillage and organic matter addition play a significant role in soil resource management and erosion control. However, it is notable that these strategies may not necessarily align with those promoted by agricultural extension representatives, who might prioritise different approaches or lack awareness of the effectiveness of community-led initiatives. Further evaluation and collaboration between local communities and agricultural extension services are essential to align strategies with local needs and enhance overall soil conservation efforts.

The rates of erosion across the sites were similar to other studies conducted using FRN in tropical Africa. Overall erosion rates estimated with the MODERN model and $^{239+240}Pu$ were two to three times lower than those estimated by Humphrey et al. (2022) using the RUSLE model. RUSLE, however, ignores deposition within the site, which biases the findings in favour of erosion processes and operates at a much larger basin wide scale. The plots in this study are much more detailed as fine precision and accuracy can only be achieved at small scale. However, the RUSLE model can assess erosion patterns quickly and cheaply at large scale. Furthermore, the RUSLE model showed promise to be used as a reliable tool to help select relevant reference sites for potential study areas to

complement local knowledge and the geographical features of the area. Overall, the predicted rates of erosion at the selected reference sites were 0.5 Mg ha^{-1} yr^{-1} with 4 out of the 6 reference sites having a predicted rate of 0 Mg ha^{-1} yr^{-1}. With the selection of reference sites being a significant challenge in the application of FRN tracer methods the RUSLE model has the potential to make the process of choosing reference sites easier in the future.

This novel use of fallout Pu as a tracer has emphasised the need to better understand how land management affects soil erosion processes to support the development of successful mitigation strategies and targeting of limited resources. In this way, data from Pu activities can validate predictive models that will support future policies communicating the effectiveness of community-designed solutions to reduce land degradation for sustainable agriculture. This work demonstrates small-scale erosion patterns associated with different land management regimes and supports earlier work modelling soil erosion rates within Western Kenya. In order to guarantee the sustainability of arable land in the future, it is imperative to tackle the multifaceted problems that contribute to the deterioration of tropical soils. This work advances our knowledge of the variables influencing soil erosion and serves as a foundation for the incorporation of Local Environmental Knowledge (LEK) and solutions into national policy initiatives (Castro et al., 2020). Furthermore, this study demonstrates the novel application of $^{239+240}Pu$ as a soil erosion tracer in tropical African soils, offering a comprehensive tool to enhance our understanding of soil erosion mechanisms and reinforce the successful execution of future mitigation approaches.

Summary

The multi-disciplinary outcomes of this thesis deepen our understanding of soil erosion dynamics in Tropical East African agri-systems, providing a useful tool to support

effective mitigation strategies aimed at preserving the fertile soils. Food security, which can be defined as "improved health through food sufficiency, quality and safety", is key to Kenya's economic and social development; yet approximately 10 million people in Kenya currently suffer from some kind of food insecurity (Mutie et al., 2020). Ultimately, this research stands as a vital step toward securing the sustainable future of this agriculturally crucial region and works towards addressing several of the United Nations Sustainable development goals, including: 1. no poverty; 14. life below water and 15. life on land.

Whilst a significant amount of work is still required to demonstrate this method at a larger scale, this study has enabled some important conclusions to be drawn:

- separations using TEVA cartridges reduced the environmental impact of Pu isotope analysis while increasing throughput, lowering cost, and ensuring maximum sensitivity of soils with low $^{239+240}$Pu atmospheric fallout;

- analysis by ICP-MS/MS using O_2 as a reaction gas provided a sensitive and reliable method with high throughput, suitable for field and survey-scale soil erosion assessment due to lower unit cost;

- in tropical soils, $^{239+240}$Pu was presented as a reliable tracer of soil erosion that can be applied to large-scale studies, overcoming the challenges associated with ^{137}Cs;

- intact vegetation cover plays an important role in ensuring the future resilience of tropical soils and mitigating against soil erosion processes;

- the importance of community-led involvement was demonstrated for the effective control of land degradation to protect the future sustainability of tropical agri-systems;

- the benefits of the Pu method can assist our understanding of the factors which influence soil erosion through a method that can provide greater data collection over traditional methods and could therefore facilitate the integration of locally designed solutions into policy in the future.

Future work

The completion of additional investigation and experimentation is required to further develop our understanding of soil erosion processes and to effectively communicate the results presented in this thesis to develop future pathways to impact. Based on the results presented in this thesis there is a need to further understand the erosion dynamics within the Winam Gulf region through conducting further temporal studies to understand the acceleration of soil erosion as a result of clearance of land for agricultural use. This includes investigating the possible deceleration of soil erosion through the implementation of successful mitigation strategies to understand the impact they have on the sustainability of agri-systems in the area. This may include the re-sampling of the erosion plots presented within this thesis using the developed Pu method after the implementation of mitigation on recently cleared plots. This has the potential to demonstrate the real-time effectiveness of different strategies so that the results can be clearly communicated to implement change. The collaboration of social scientists and local stakeholders within the region is critical for the integration of local knowledge and solutions into policy.

Additionally, the effect of land degradation due to soil erosion processes on the nutritional status of soil for agriculture is critical to better understand the ultimate impact on human and animal health in the region. Through understanding the loss of micronutrients as a result of soil erosion processes the correct management of the land through fertilisers can be better advised. Ultimately, the impact that soil erosion on land in the Winam Gulf is

having on the security of aquaculture further downstream in the Winam Gulf of Lake Victoria should be investigated to understand the relative contributions of sediment load from different land use and management practices within the catchment. Through linking the Pu method with other monitoring techniques such as source apportionment within the waterways and the RUSLE model on land, the Pu model has the potential to optimise future studies, targeting areas with the highest sediment input into the lake to implement successful change ensuring the sustainability of soils and lakes in the area. This will also help to define the most critical areas where mitigation strategies could be implemented, optimising the use of vital scarce resources.

Beyond the Winam Gulf region, the Pu method has the potential to be used across a range of diverse settings, including the Lake Victoria basin, Africa and globally in other tropical soils where 239+240Pu fallout is low, using the analytical method developed in Chapter 3. Within Western Kenya specifically its utility extends to comparing steep slopes, such as the Rift Valley region in this study, with environments with flat terrains such as the Kisumu basin to understand their relative contributions of sediment load and effects of land degradation in different landscapes such as grasslands and arid regions. By doing so, the method can become a versatile tool with global applications, aiding researchers and in assessing soil erosion processes across varied scenarios.

References

Alewell, C., Meusburger, K., Juretzko, G., Mabit, L., Ketterer, M.E., (2014). Suitability of 239+240Pu and 137Cs as tracers for soil erosion assessment in mountain grasslands. Chemosphere 103, 274–280. https://doi.org/10.1016/J.CHEMOSPHERE.2013.12.016

Alewell, C., Pitois, A., Meusburger, K., Ketterer, M., Mabit, L., (2017). 239 + 240Pu from "contaminant" to soil erosion tracer: Where do we stand? Earth Sci Rev 172, 107–123. https://doi.org/10.1016/J.EARSCIREV.2017.07.009

Arata, L., Meusburger, K., Frenkel, E., A'Campo-Neuen, A., Iurian, AR., Ketterer, ME., Mabit, L., Alewell, C., (2016a). Modelling Deposition and Erosion rates with RadioNuclides (MODERN) – Part 1: A new conversion model to derive soil redistribution rates from inventories of fallout radionuclides. J Environ Radioact 162–163, 45–55. https://doi.org/10.1016/j.jenvrad.2016.05.008

Arata, L., Alewell, C., Frenkel, E., A'Campo-Neuen, A., Iurian, A.-R., Ketterer, ME., Mabit, L., Meusburger, K., (2016b). Modelling Deposition and Erosion rates with RadioNuclides (MODERN) – Part 2: A comparison of different models to convert 239+240 Pu inventories into soil redistribution rates at unploughed sites. J Environ Radioact 162–163, 97–106. https://doi.org/10.1016/j.jenvrad.2016.05.009

Borrelli, P., Robinson, D.A., Panagos, P., Lugato, E., Yang, J.E., Alewell, C., Wuepper, D., Montanarella, L., Ballabio, C., (2020). Land use and climate change impacts on global soil erosion by water (2015-2070). Proceedings of the National Academy of Sciences 117, 21994–22001. https://doi.org/10.1073/pnas.2001403117

Bu, W., Gu, M., Ding, X., Ni, Y., Shao, X., Liu, X., Yang, C., Hu, S. (2021) Exploring the ability of triple quadrupole inductively coupled plasma mass spectrometry for the determination of Pu isotopes in environmental samples, J. Anal. At. Spectrom, 36, 2330–2337, https://doi.org/10.1039/D1JA00288K

Cao, L., Zheng, J., Tsukada, H., Pan, S., Wang, Z., Tagami, K., Uchida, S., (2016) Simultaneous determination of radiocesium (135Cs, 137Cs) and plutonium (239Pu, 240Pu) isotopes in river suspended particles by ICP-MS/MS and SF-ICP-MS, Talanta, 159, 55–63, https://doi.org/10.1016/j.talanta.2016.06.008

Castro, RB., Fabré, NN., Oliveira, AS., Oliveira Júnior, JGC., Batista, VS., (2020). Local Ecological Knowledge Networks in Tropical Artisanal Shrimp Fisheries. Res Sq. PREPRINT https://doi.org/10.21203/rs.3.rs-125962/v1

DeGraffenried, J.B., Shepherd, K.D., (2009). Rapid erosion modeling in a Western Kenya watershed using visible near infrared reflectance, classification tree analysis and 137Cesium. Geoderma 154, 93–100. https://doi.org/10.1016/j.geoderma.2009.10.001

Denboba A.M, (2005). Forest conversion-soil degradation-farmers perception nexus: Implications for sustainable land use in the southwest of Ethiopia. Cuvillier Verlag 26.

Elwell, H.A., (1978). Modelling soil losses in Southern Africa. Journal of Agricultural Engineering Research 23, 117–127. https://doi.org/10.1016/0021-8634(78)90043-4

Horwitz, EP., Dietz, ML., Chiarizia, R., Diamond, H., Maxwell, SL., Nelson, MR. (1995) Separation and preconcentration of actinides by extraction chromatography using a supported liquid anion exchanger: application to the characterization of high-level nuclear waste solutions, Anal Chim Acta, 310, 63–78, https://doi.org/10.1016/0003-2670(95)00144-O

Hou, X., Zhang, W., Wang, Y., (2019) Determination of Femtogram-Level Plutonium Isotopes in Environmental and Forensic Samples with High-Level Uranium Using Chemical Separation and ICP-MS/MS Measurement, Anal. Chem, 91, 11553–11561, https://doi.org/10.1021/acs.analchem.9b01347

Humphrey, OS., Osano, O., Aura, CM., Marriott, AL., Dowell, SM., Blake, WH., Watts, MJ., (2022). Evaluating spatio-temporal soil erosion dynamics in the Winam Gulf catchment, Kenya for enhanced decision making in the land-lake interface. Science of The Total Environment 815, 151975. https://doi.org/10.1016/j.scitotenv.2021.151975

Joint FAO/IAEA Division of Nuclear Techniques in Food and Agriculture, Soil and Water Management and Crop Nutrition Section, Vienna (Austria) (2014). Guidelines for Using Fallout Radionuclides to Assess Erosion and Effectiveness of Soil Conservation Strategies (IAEA-TECDOC--1741). International Atomic Energy Agency (IAEA)

Loba, A., Waroszewski, J., Sykuła, M., Kabala, C., Egli, M., (2022). Meteoric 10Be, 137Cs and 239+240Pu as Tracers of Long- and Medium-Term Soil Erosion - A Review. Minerals, 12, 359. https://doi.org/10.3390/MIN12030359

Lorenz, K., Lal, R., Ehlers, K., (2019). Soil organic carbon stock as an indicator for monitoring land and soil degradation in relation to United Nations' Sustainable Development Goals. Land Degrad Dev 30, 824–838. https://doi.org/10.1002/ldr.3270

Meshesha, DT., Tsunekawa, A., Tsubo, M., Haregeweyn, N., (2012). Dynamics and hotspots of soil erosion and management scenarios of the Central Rift Valley of Ethiopia. International Journal of Sediment Research 27, 84–99. https://doi.org/10.1016/S1001-6279(12)60018-3

Meusburger, K., Porto, P., Mabit, L., La Spada, C., Arata, L., Alewell, C., (2018). Excess Lead-210 and Plutonium-239+240: Two suitable radiogenic soil erosion tracers for mountain grassland sites. Environ Res 160, 195–202. https://doi.org/10.1016/J.ENVRES.2017.09.020

Mutie, F. M., Rono, P. C., Kathambi, V., Hu, G. W., & Wang, Q. F. (2020). Conservation of Wild Food Plants and Their Potential for Combatting Food Insecurity in Kenya as Exemplified by the Drylands of Kitui County. Plants, 9(8), 1017. https://doi.org/10.3390/plants9081017

Negese, A., (2021). Impacts of Land Use and Land Cover Change on Soil Erosion and Hydrological Responses in Ethiopia. Appl Environ Soil Sci, 1–10. https://doi.org/10.1155/2021/6669438

Nygren, U., Rodushkin, I., Nilsson, C., Baxter, DC. (2003) Separation of plutonium from soil and sediment prior to determination by inductively coupled plasma mass spectrometry, J. Anal. At. Spectrom, 18, 1426–1434, https://doi.org/10.1039/B306357G

Ruecker G.R., Park, S.J., Brunner, A.C., Vlek P.l.G., (2008). Assessment of Soil Redistribution on Two Contrasting Hillslopes in Uganda Using Caesium-137 Modelling. Erdkunde 62, 259–272. https://www.jstor.org/stable/25648129

Schimmack, W., Auerswald, K., Bunzl, K., (2004). Estimation of soil erosion and deposition rates at an agricultural site in Bavaria, Germany, as derived from fallout radiocesium and plutonium as tracers. Naturwissenschaften 2001 89:1 89, 43–46. https://doi.org/10.1007/S00114-001-0281-Z

Sutherland, RA., (1996). Caesium-137 soil sampling and inventory variability in reference locations: A literature survey. Hydrol Process 10, 43–53. https://doi.org/10.1002/(SICI)1099-1085(199601)10:1<43::AID-HYP298>3.0.CO;2-X

Watene, G., Yu, L., Nie, Y., Zhu, J., Ngigi, T., Nambajimana, J. de D., Kenduiywo, B., (2021). Water Erosion Risk Assessment in the Kenya Great Rift Valley Region. Sustainability 13, 844. https://doi.org/10.3390/su13020844

Whitlow, R., (1988). Land degradation in Zimbabwe: a geographical study. Harare: UZ/ Department of Natural Resources.

Wilken, F., Fiener, P., Ketterer, M., Meusburger, K., Muhindo, DI., van Oost, K., Doetterl, S. (2021). Assessing soil erosion of forest and cropland sites in wet tropical Africa using 239+240 Pu fallout radionuclides, SOIL, 7, 399-414, https://doi.org/10.5194/soil-7-399-2021

Xing, S., Zhang, W., Qiao, J., Hou, X. (2018) Determination of ultra-low level plutonium isotopes (239Pu, 240Pu) in environmental samples with high uranium, Talanta, 187, 357–364, https://doi.org/10.1016/j.talanta.2018.05.051

Xing, S., Luo, M., Yuan, N., Liu, D., Yang, Y., Dai, X., Zhang, W., Chen, N. (2021) Accurate determination of plutonium in soil by tandem quadrupole icp-ms with different sample preparation methods, At. Spectrosc, 42, 62–70, https://doi.org/10.46770/AS.2021.011

Xu, Y., Li, C., Yu, H., Fang, F., Hou, X., Zhang, C., Li, X., Xing, S. (2022) Rapid determination of plutonium isotopes in small samples using single anion exchange separation and ICP-MS/MS measurement in NH3–He mode for sediment dating, Talanta, 240, 123152, https://doi.org/10.1016/j.talanta.2021.123152

Zhang, W., Lin, J., Fang, S., Li, C., Yi, X., Hou, X., Chen, N., Zhang, H., Xu, Y., Dang, H., Wang, W., Xu, J., (2021) Determination of ultra-trace level plutonium isotopes in soil samples by triple-quadrupole inductively coupled plasma-mass spectrometry with mass-shift mode combined with UTEVA chromatographic separation, Talanta, 234, 122652, https://doi.org/10.1016/j.talanta.2021.122652

Appendices

A0 – Associated Publications and reports

Humphrey, OS., Middleton, DRS., Ahmad, S., Cocerva, T., **Dowell, SM.,** et al., (2021). The Society for Environmental Geochemistry and Health (SEGH): building for the future of early career researchers. Environ Geochem Health 43, 2455–2458. https://doi.org/10.1007/s10653-020-00620-4

Humphrey, OS., Osano, O., Aura, CM., Marriott, AL., **Dowell, SM**., Blake, WH., Watts, MJ., (2022). Evaluating spatio-temporal soil erosion dynamics in the Winam Gulf catchment, Kenya for enhanced decision making in the land-lake interface. Science of The Total Environment 815, 151975. https://doi.org/10.1016/j.scitotenv.2021.151975

Humphrey, OS.; Marriott, AL.; **Dowell, SM.**; King, D.; Watts, MJ.. (2023) Dynamics of environmental geochemistry and health in a lake-wide basin : stakeholder engagement meeting. Nottingham, UK, British Geological Survey, 20pp. (OR/23/010) (Unpublished) https://nora.nerc.ac.uk/id/eprint/534235

Isaboke, J., Osano, O., Humphrey, OS., **Dowell, SM.,** Watts, MJ., (2023). The nutritional quality of forage grass changes due to changing soil chemistry resulting from different land-use management in the Oroba Valley, Kenya. AJOL 7(3), 40-54. https://www.ajol.info/index.php/ajedscitech/article/view/254387

A3 - Chapter 3

Supplementary table 1 – Typical operating condition of Agilent 8900 ICP-MS/MS for the analysis of Pu isotopes using O_2 gas

Parameter	Typical operating conditions
Forward power	1550 W
Reflected power	<20 W
Plasma gas	15 l min^{-1}
Auxiliary gas flow	0.9 l min^{-1}
Nebuliser carrier gas flow	1.0 l min^{-1}
Nebuliser make up gas flow	0.25 l min^{-1}
Cooling water temperature	15-40 °C
Cooling water minimum flow rate	5.0 l min^{-1}
Cooling water inlet pressure	230-400 kPa
Exhaust duct extraction flow rate	4-6 m^3 min^{-1}
O_2 gas	0.3 ml min^{-1} (30%)
Environment Temperature	15-30ºC <2ºC Change in 1 hr
Acquisition time	149 s
Integration time	0.05 secs for ^{193}Ir (on mass), $^{209}IrO^+$ (mass sift), $^{225}IrO^+$ (mass sift) and 0.2 secs for $^{270}UO^+$, $^{271}PuO^+$, $^{272}PuO^+$, $^{273}PuO^+$ and $^{274}PuO^+$
Nebuliser	Glass Expansion concentric
Spray chamber	Double pass
Spray chamber temperature	2°C
Spray chamber drain pump tubing	PharMed tubing yellow/blue 1.52 mm
Mass range	6 – 275 amu
Mode of acquisition	Time Resolved Analysis
Type of detector	Simultaneous
Detector mode	Pulse counting
Total acquisition time	149 s
Sampling period	1.18 s
Quaternary Pump stop time	120 s
Quaternary Pump post time	120 s

Supplementary table 2 - Sensitivity of measurement for isotopes ^{238}U, ^{239}Pu and ^{242}Pu using ICP-MS/MS

Isotope	^{238}U	^{239}Pu	^{242}Pu
Sensitivity (cps / pg kg^{-1})	1089	974	1197

A4 – Chapter 4

Table S1 - Activity concentration and Inventory calculations for reference site samples

Depth (cm)	$^{210}Pb_{ex}$		^{137}Cs		$^{239+240}Pu$	
	Activity concentration (Bq kg^{-1})	Inventory (Bq m^{-2})	Activity concentration (Bq kg^{-1})	Inventory (Bq m^{-2})	Activity concentration (Bq kg^{-1})	Inventory (Bq m^{-2})
REF 1						
3	148.74	2613.31	-	-	0.098	2.92
6	120.56	1669.99	-	-	0.101	3.70
9	100.78	486.18	-	-	0.109	4.01
12	-	-	-	-	0.074	2.79
15	-	-	-	-	0.040	1.56
18	-	-	-	-	0.021	0.93
21	-	-	-	-	0.012	0.44
24	-	-	-	-	0.006	0.25
27	-	-	-	-	0.004	0.15
30	-	-	-	-	0.003	0.12
REF 2						
3	153.28	5375.46	1.02	45.17	0.062	2.70
6	100.07	3148.56	2.03	88.09	0.067	3.03
9	66.57	1676.33	1.62	67.27	0.070	3.04
12	54.69	1242.40	0.92	37.28	0.065	2.77
15	-	-	-	-	0.052	2.53
18	-	-	-	-	0.043	1.95
21	-	-	-	-	0.029	1.35
24	-	-	-	-	0.021	0.93
27	-	-	-	-	0.016	0.72
30	-	-	-	-	0.014	0.70
REF 3						
3	108.55	2470.04	-	-	0.043	1.69
6	84.67	1980.01	-	-	0.046	2.34
9	67.15	1322.61	-	-	0.047	2.40
12	50.15	920.38	-	-	0.047	2.12
15	47.62	714.91	-	-	0.041	2.16
18	42.30	655.09	-	-	0.037	1.70
21	47.55	657.66	-	-	0.030	1.41
24	-	-	-	-	0.025	1.17
27	-	-	-	-	0.014	0.65
30	-	-	-	-	0.012	0.57

Depth (cm)	$^{210}Pb_{ex}$		^{137}Cs		$^{239+240}Pu$	
	Activity concentration (Bq kg^{-1})	Inventory (Bq m^{-2})	Activity concentration (Bq kg^{-1})	Inventory (Bq m^{-2})	Activity concentration (Bq kg^{-1})	Inventory (Bq m^{-2})
REF 4						
3	93.97	2967.73	-	-	0.078	2.20
6	77.63	2427.86	-	-	0.079	2.83
9	67.42	1717.79	-	-	0.088	3.05
12	53.18	977.62	-	-	0.087	3.33
15	48.12	1022.09	-	-	0.059	2.30
18	43.54	804.96	-	-	0.036	1.42
21	40.67	573.77	-	-	0.026	1.02
24	-	-	-	-	0.020	0.68
27	-	-	-	-	0.015	0.37
30	-	-	-	-	0.011	0.32
REF 5						
3	168.99	5163.30	1.68	62.26	0.083	2.24
6	110.27	4129.70	1.45	69.66	0.090	3.37
9	67.92	2247.75	1.45	69.74	0.104	3.30
12	56.67	1322.50	1.87	82.09	0.094	3.47
15	40.61	816.89	0.97	48.54	0.083	2.49
18	-	-	0.76	34.82	0.059	2.00
21	-	-	-	-	0.045	1.41
24	-	-	-	-	0.029	0.94
27	-	-	-	-	0.018	0.56
30	-	-	-	-	0.016	0.45
REF 6						
3	179.42	3562.43	1.32	37.42	0.050	2.39
6	130.36	2949.98	1.87	67.37	0.059	2.65
9	82.42	1366.94	1.34	46.41	0.056	2.53
12	72.99	784.34	1.26	48.20	0.052	2.20
15	70.78	698.03	1.28	49.94	0.043	1.73
18	-	-	0.89	34.91	0.034	1.65
21	-	-	0.85	33.19	0.019	0.92
24	-	-	-	-	0.012	0.62
27	-	-	-	-	0.008	0.36
30	-	-	-	-	0.006	0.27

A5 – Chapter 5

Supplementary Table 1 – Associated sample data (Sample locations, $^{239+240}$Pu activity and modelling decision)

Sample ID	Latitude	Longitude	Activity (Bq kg^{-1})	Inventory (Bq m^{-2})	MODERN
P1_S1_1	0.008706	34.988239	0.10	23.49	Modelled
P1_S2_1	0.008209	34.987842	< LOD	-	Not Modelled
P1_S2_2	0.007996	34.987582	< LOD	-	Not Modelled
P1_S2_3	0.007829	34.987878	0.05	12.61	Modelled
P1_S3_1	0.007727	34.987505	0.11	27.89	Not Modelled
P1_S3_2	0.007614	34.987274	0.13	30.36	Not Modelled
P1_S3_3	0.007330	34.987482	0.12	29.27	Not Modelled
P1_S3_4	0.007610	34.987377	0.05	11.98	Modelled
P1_S4_1	0.007408	34.987004	0.13	31.41	Not Modelled
P1_S4_2	0.007062	34.987313	0.09	21.58	Modelled
P1_S4_3	0.007200	34.986821	0.14	33.71	Not Modelled
P1_S4_4	0.006974	34.986893	0.09	22.37	Modelled
P1_S5_1	0.006885	34.986473	0.05	12.04	Modelled
P1_S5_2	0.006710	34.986735	0.06	15.13	Modelled
P1_S5_3	0.006839	34.986973	0.09	20.64	Not Modelled
P2_S1_1	-0.004453	35.005352	< LOD	-	Not Modelled
P2_S1_2	-0.003961	35.005022	< LOD	-	Not Modelled
P2_S1_3	-0.005112	35.005496	0.02	5.77	Modelled
P2_S2_1	-0.005222	35.004650	0.02	5.79	Modelled
P2_S2_2	-0.004629	35.004773	0.03	7.17	Not Modelled
P2_S2_3	-0.004291	35.004478	0.02	4.23	Modelled
P2_S3_1	-0.004662	35.003826	0.12	29.73	Not Modelled
P2_S3_2	-0.005220	35.003974	0.04	9.64	Not Modelled
P2_S3_3	-0.005204	35.003343	0.10	24.46	Modelled
P2_S4_1	-0.004805	35.003019	0.15	36.42	Not Modelled
P2_S4_2	-0.005034	35.002102	0.09	21.28	Modelled
P2_S4_3	-0.005615	35.002737	0.07	16.57	Modelled
P2_S5_1	-0.005682	35.001862	0.07	17.89	Modelled
P2_S5_2	-0.005886	35.000923	0.10	23.98	Not Modelled
P2_S5_3	-0.006769	35.000908	0.09	22.73	Modelled
P3_S1_1	-0.004365	34.989138	< LOD	-	Not Modelled
P3_S1_2	-0.004066	34.989185	< LOD	-	Not Modelled
P3_S1_3	-0.004338	34.989370	< LOD	-	Not Modelled
P3_S2_1	-0.004309	34.989656	0.06	15.12	Modelled
P3_S2_2	-0.003903	34.989493	0.11	26.68	Not Modelled
P3_S2_3	-0.004110	34.989728	0.06	14.46	Modelled
P3_S3_1	-0.003707	34.989684	0.08	18.63	Modelled
P3_S3_2	-0.003834	34.990001	0.00	14.01	Modelled
P3_S3_3	-0.003580	34.989864	0.07	17.14	Modelled
P3_S4_1	-0.003476	34.990068	0.11	27.77	Not Modelled
P3_S4_2	-0.003524	34.990219	0.08	19.55	Modelled
P3_S4_3	-0.003328	34.990205	0.10	23.60	Not Modelled
P3_S5_1	-0.003067	34.990372	0.07	17.12	Modelled

Sample ID	Latitude	Longitude	Activity (Bq kg^{-1})	Inventory (Bq m^{-2})	MODERN
P3_S5_2	-0.003216	34.990455	0.10	24.05	Not Modelled
P3_S5_3	-0.003065	34.990599	0.09	22.95	Not Modelled
P4_S1_1	-0.003977	34.988360	< LOD	-	Not Modelled
P4_S1_2	-0.003793	34.988582	0.09	21.60	Not Modelled
P4_S1_3	-0.003376	34.988445	0.06	14.10	Modelled
P4_S2_1	-0.003815	34.989057	0.14	33.95	Not Modelled
P4_S2_2	-0.003264	34.988734	0.08	18.77	Modelled
P4_S2_3	-0.003403	34.989000	0.10	24.40	Not Modelled
P4_S3_1	-0.003274	34.989293	0.15	36.06	Not Modelled
P4_S3_2	-0.003427	34.989537	0.09	20.81	Modelled
P4_S3_3	-0.002884	34.989194	0.07	17.93	Modelled
P4_S4_1	-0.002770	34.989448	0.17	40.77	Not Modelled
P4_S4_2	-0.003070	34.989494	0.07	16.27	Modelled
P4_S4_3	-0.003078	34.989774	0.09	21.43	Not Modelled
P4_S5_1	-0.003090	34.990042	0.13	31.57	Not Modelled
P4_S5_2	-0.002766	34.990035	0.19	45.22	Not Modelled
P4_S5_3	-0.002550	34.989694	0.03	8.37	Not Modelled
P4_S6_1	-0.002287	34.990062	0.12	28.97	Not Modelled
P4_S6_2	-0.002488	34.990334	0.11	27.44	Not Modelled
P4_S6_3	-0.002778	34.990297	0.08	18.40	Modelled
P5_S1_1	0.008652	34.987511	0.03	6.67	Modelled
P5_S1_2	0.008605	34.987566	0.05	11.57	Modelled
P5_S1_3	0.008632	34.987468	0.05	12.02	Modelled
P5_S2_1	0.008562	34.987472	0.06	13.55	Modelled
P5_S2_2	0.008496	34.987412	0.04	10.81	Modelled
P5_S2_3	0.008621	34.987356	0.07	16.80	Modelled
P5_S3_1	0.008620	34.987242	< LOD	-	Not Modelled
P5_S3_2	0.008574	34.987309	< LOD	-	Not Modelled
P5_S3_3	0.008470	34.987271	0.08	18.82	Modelled
P5_S4_1	0.008505	34.987170	< LOD	-	Not Modelled
P5_S4_2	0.008327	34.987069	0.16	38.45	Not Modelled
P5_S4_3	0.008580	34.986969	0.15	35.30	Not Modelled
P5_S5_1	0.008394	34.986854	0.17	41.79	Not Modelled
P5_S5_2	0.008165	34.986830	0.11	26.43	Not Modelled
P5_S5_3	0.008492	34.986787	0.07	18.01	Modelled
P5_S6_2	0.008489	34.986519	0.12	29.02	Not Modelled
P5_S6_3	0.008160	34.986563	0.14	33.66	Not Modelled

A6 – Chapter 6

Supplementary Figure 1 – Sample location images

Plot 1 – Cultivated 1940 with Community led mitigation. Mixed pastoral farming and formation of drainage ditches using boulders moved within the landscape.

Plot 2 – Cultivated 1940 with terracing mitigation. Steep terraces formed using the movement of soil into dips in the landscape which were created using large boulders with some rocky outcrops.

Plot 3&4. Plot 3 - Cultivated 2019 with no current mitigation.
Plot 4 – Uncultivated with prominent shrub growth since 1940.

Plot 5 – Cultivated 2003 with no current mitigation and method of ploughing the land using hoes.